Bicolored tilings and the totally non-negative Grassmannian

Joel Costa da Rocha

June 2023

Submitted in accordance with the requirements for the degree of Doctor of Philosophy.

The University of Leeds, School of mathematics

The candidate confirms that the work submitted is his own and that appropriate credit has been given where reference has been made to the work of others.

Acknowledgements

This research has been supervised by Karin Baur and João Faria Martins. The author was supported by Royal Society Wolfson Fellowship 180004.

The author would like to thank Karin Baur and João Faria Martins for their help, and insightful comments during the writing of this thesis and the work that preceded it.

The author would also like to thank the Isaac Newton Institute for Mathematical Sciences, Cambridge, for support and hospitality during the programme *Cluster algebras and representation theory* where work on this paper was undertaken. This work was supported by EPSRC grant no EP/K032208/1.

Abstract

Bicolored tilings are a generalization of triangulations of a surface. These tilings naturally map to a variety of combinatorial objects, namely Postnikov diagrams, plabic graphs, quivers, and positroid cells.

We will first generalize the notion of *edges* to *hyperedges* to allow them to connect any number n of vertices ($n > 1$), and define tilings as a surface equipped with a collection of compatible hyperedges. Bicolored tilings are considered up to isotopy, and will also be subject to two equivalences that preserve some of the combinatorial properties of the tiling. We will also define a *flip/mutation* on the hyperedges of a tiling, which will correspond to equivalent local transformations in other combinatorial objects.

We then define the Scott map and the stellar-replacement map, drawing inspiration from their definitions in [16, p.14-15] and [4, 2.1], where these maps have already been defined for triangulations and monocolored tilings. These will allow us to map bicolored tilings onto Postnikov diagrams and plabic graphs. In particular, we establish a bijection between reduced tilings and reduced Postnikov diagrams.

We will dedicate a section of this paper to discuss different classes of tilings, as well as how to construct a tiling for any given permutation.

Finally, we use bicolored tiling to parametrize positroid cells in the totally non-negative Grassmannian. The construction will resemble the parametrization of these cells found in [15, 12.7] and [21, 2.17], now using bicolored tilings. This will establish a bijection between the reduction-flip-equivalence classes of tilings and the positroid cells that stratify the totally non-negative Grassmannian. *Degenerations* of tilings will then allow us to find tilings associated to lower-dimensional positroid cells in the same Grassmannian, which also gives us a partial ordering on bicolored tilings.

Table of contents

0 Introduction

In [15, 14.1], Postnikov introduced Postnikov diagrams (Definition 1.5), which are a collection of strands in a closed disk with endpoints on the disk, satisfying some conditions. In the same paper, Postnikov relates Postnikov diagrams to plabic graphs, graphs embedded in a disk with black and white internal vertices and boundary vertices on the disk, (Definition 1.11), as well as positroid cells (Definition 1.21), cells that decompose the totally non-negative Grassmannian $Gr_{k,n}^{\geq 0}$ of k-subspaces in $\mathbb{R}^n$ (Definition 1.19).

In particular, plabic graphs can be used to parametrize corresponding positroid cells, as described with different approaches in [15, 3.2] by Postnikov, in [18, 1.1] by Talaska, and in [21, 2.17] by Williams.

In [16, Thm.3 p.24], Scott used Postnikov diagrams to show that the homogeneous coordinate ring of the Grassmannian $Gr_{k,n}$ is a cluster algebra of geometric type. Cluster algebras are a class of commutative rings introduced in [9] by Fomin and Zelevinsky, and expanded upon in [10] and [5]. In [17] Serhiyenko, Sherman-Bennett, and Williams generalise this result to Schubert cells, and finally in [11] Galashin and Lam generalise the result to open positroid varities, proving that the coordinate ring of an open positroid variety coincides with the cluster algebra associated to a Postnikov diagram.

Each Postnikov diagram of permutation $i \longmapsto i+k$ (p.13) gives rise to a cluster, with each alternating region corresponding to a different cluster variable in the cluster [16, Thm.2 p.24]. Mutations of cluster variables can be achieved through a local transformation of the corresponding region in the Postnikov diagram.

Scott also introduces the *Scott map* in [16, p.14-15], which maps triangulations of a regular n-gon to $\Gamma_{2,n}$-diagrams (Postnikov diagrams with decorated permutation $i \longmapsto i+2 \mod n$).

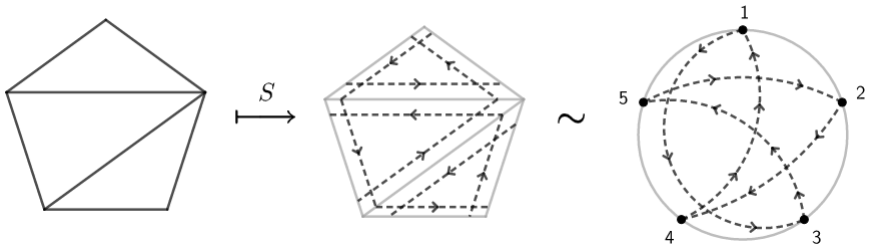

Figure 1

The mutable cluster variables are the diagonals of the triangulation, and flipping the diagonal corresponds to a mutation of the corresponding cluster variable, as described in [16, p.6-7] and [2, p.4-5]. Consequently, every triangulation of the n-gon corresponds to a different cluster for the corresponding cluster algebra. Scott furthermore introduces *quadrilateral arrangements* in [16, p.18-21], giving us a recursive way to generate $\Gamma_{k,n}$-diagrams for any $1 < k < n$.

In [4, 2.1], Baur and Martin generalize the Scott map to tilings of polygons, giving a construction for more Postnikov diagrams that aren't $\Gamma_{k,n}$-diagrams. Naturally, we ask ourselves the question if this construction can be further generalized to allow us to generate more Postnikov diagrams.

One can naturally extend this mapping to a larger class of Postnikov diagrams [4, 2.1], by applying the Scott map to a general tiling of a polygon, which can be defined similarly to a triangulation, e.g. by removing the requirement that the collection of non-crossing chords in the polygon is maximal, or by allowing for internal vertices in the polygon. Two examples of such tilings and their corresponding diagram are as follows.

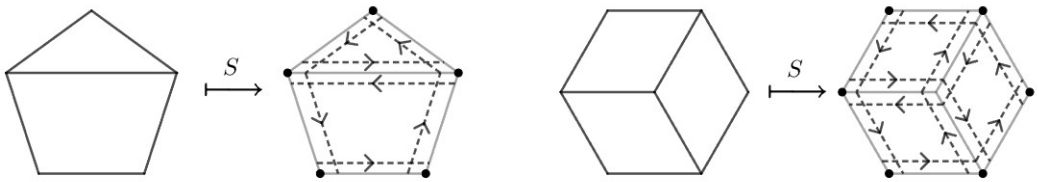

Figure 2

The first tiling maps to a Postnikov diagram of type permutation $\pi = (143)(25)$, while the second tiling has an internal vertex and maps to a $\Gamma_{4,6}$-diagram. However, there is no canonical way to flip diagonals in these tilings. This setup also does not generate all Postnikov diagrams. Moreover, we may encounter tilings that do not map to Postnikov diagrams, such as the example below.

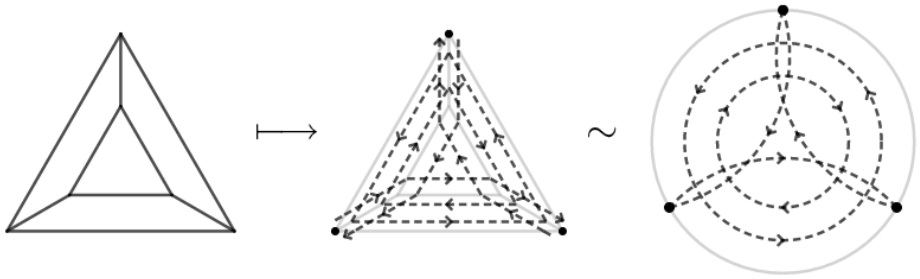

Figure 3

This motivates the introduction of bicolored tilings, which help us construct similar correspondences with Postnikov diagrams and positroid cells for any given decorated permutation, which is reflected in our first main result.

Theorem A (Theorem 3.24)**.** For any decorated permutation π, there is a tiling T whose permutation is π. Alternatively, any Postnikov diagram can be obtained as the image of a bicolored tiling by the Scott map.

Furthermore, these bicolored tilings naturally map to plabic graphs via the *stellar-replacement map* Φ and can be used to parametrize corresponding positroid cells (drawing inspiration from the method described in [21, 2.17]), allowing for a more explicit description of the bijections between the different combinatorial objects. That correspondence is given by the second main result of this paper.

Theorem B (Theorem 5.22)**.** Reduced (bicolored) tilings of type (k, n) up to tiling equivalence are in bijection with positroid cells of the totally non-negative Grassmannian $Gr_{k,n}^{\geq 0}$.

Bicolored tilings also allow us to read off some important information geometrically, such as what type (k, n) of Grassmannian the corresponding diagram/plabic graph/positroid cell belongs to, and what dimension the corresponding positroid cell has.

There are more approaches to describing bijections between combinatorial objects related to the Grassmannian. In [20], Thurston defines triple crossing diagrams, which map onto a subset of Postnikov diagrams as described in [15, p.56]. Similarly

to Postnikov diagrams, triple crossing diagrams induce a permutation of $[n]$, but describe it as a matching of $2n$ points $1, 1', \ldots, n, n'$. In that setup, [20, Theorem 3] proves an analogous result to Theorem 3.24.

In [13] Mohammadi and Zaffalon construct another representation of positroids in the form of graphs defined in [13, 3.2], which allow for easy computation of the dimension of the positroid, (which is related to the dimension of the positroid cells as described in Definition 2.12), as well as the boundary and intersection of positroids.

While the plabic cycles described in [1, p.15] by Baltisky and Wellman visually resemble the bicolored tilings the most, and while plabic cycles are related to plabic graphs and triple crossing diagrams, the connection to plabic cycles remains unexplored, and is, therefore, a source for more research.

Chapter 1 contains the necessary background. Chapter 2 and 3 are submitted for publication [7] and introduce bicolored tilings and how they map to Postnikov diagrams and plabic graphs. Chapter 4 introduces some examples of bicolored tilings and is a work in progress [6]. Chapter 5 is submitted for publication [8] and analyzes the connection between bicolored tilings and the totally non-negative Grassmannian.

Chapters 4 and 5 may be read in any order. Chapter 4 uses some propositions proven in Chapter 5 and thus follows it in terms of mathematical consistency. However, it is advised to read Chapter 4 before Chapter 5, as it shows some examples of tilings, which may facilitate the understanding of propositions proven in Chapter 5.

1 Background

We will start by recalling cluster algebras that arise from finite quivers, and how to geometrically interpret a class of such cluster algebras using triangulations of a polygon. Then we recall Postnikov diagrams and describe their relation to triangulations. This will motivate our search for a generalization of triangulations, namely bicolored tilings, that extend the correspondence to Postnikov diagrams.

Definition 1.1. [9] [12, 2.1.1-2.1.2] A *quiver* Q is a directed graph without 2-cycles and loops. Let V be the vertex set of Q. We define the *mutation* $\mu_v(Q)$ of Q with respect to the vertex $v \in V$ to be the quiver Q' obtained by the following steps:

(i) we reverse the orientation of all arrows in Q adjacent to v.

(ii) for each path $u \longrightarrow v \longrightarrow w$ in Q, we add an arrow $u \longrightarrow w$.

(iii) we remove all 2-cycles that appear in the resulting graph.

The final graph is $Q' = \mu_v(Q)$.

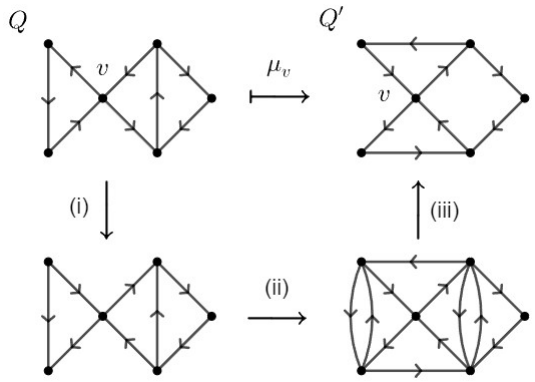

Figure 4

The mutation of a quiver with respect to a given vertex is an involution, that is $\mu_v \circ \mu_v(Q) = Q$.

The mutation class of a quiver Q is the class of all quivers obtained by a sequence of finite mutations of Q. A quiver is said to be of *finite mutation type* if its mutation class has finitely many quivers.

Definition 1.2. A *seed* is a pair (Q, u), where Q is a quiver with vertices $v_1, \ldots, v_n$, and $u = (u_1, \ldots, u_n)$ is a set of rational functions in variables $x_1, \ldots, x_n$. We denote $\mu_i = \mu_{v_i}$. Then we define the *seed mutation* μ_i of (Q, u) to be the seed $(\mu_i(Q), \mu_i(u))$, where $\mu(u) = (u_1, \ldots, u_i', \ldots, u_n)$, with the exchange relation

$$u_i' \cdot u_i = \prod_{u_j \longrightarrow v} u_j + \prod_{v \longrightarrow u_j} u_j$$

The set u is called a *cluster*, and any function u_i in a seed is called a *cluster variables*. The mutation class of (Q, u) is the class of all seeds (Q', u') obtained by a finite sequence of mutations of (Q, u).

We choose an *initial seed* (Q, x), with $x = (x_1, \ldots, x_n)$. Then a cluster algebra $\mathcal{A}(Q)$ is the $\mathbb{Q}$-subalgebra of $\mathbb{Q}(x_1, \ldots, x_n)$ generated by all cluster variables in the mutation class of (Q, x). A cluster algebra is of *finite type* if it contains finitely many cluster variables.

Remark 1.3. In Definition 1.2 we do not set restrictions on which vertices can and cannot be mutated. However, we may select a subset of vertices of the quiver and decide that they cannot be mutated. In that case, we call those vertices *frozen*, and the corresponding cluster variables *coefficients*. When we do that, we find that the arrows between frozen vertices do not affect the mutated vertices and their relations, and thus we simply omit them for simplicity.

An example of finite-type cluster algebras can be described via triangulations.

Definition 1.4. [16, p.6-7] [2, p.4-5] Let X be a regular n-gon (regular polygon with n sides) with its vertices labeled $1, \ldots, n$ in clockwise order. A *chord* in X is a straight line segment $[ij]$ between any two distinct vertices i and j. Two chords are said to be *crossing* if they cross in the interior of X. Then a *triangulation* T of X is a maximal collection of non-crossing chords in X.

Figure 5

Any two edge-adjacent triangles in T form a quadrilateral with a diagonal d between two oppositve vertices. A *(quadrilateral) flip* of T is obtained by removing such a diagonal and replacing it with the other diagonal in the same quadrilateral.

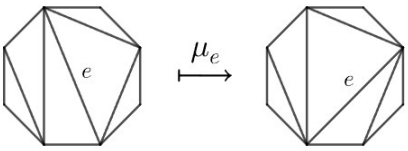

Figure 6

Then we can map any triangulation T to a quiver Q with frozen boundary vertices, by mapping each edge in T to a vertex in Q, and by adding an arrow to any two consecutive edges of a triangle in counter-clockwise order. The frozen vertices of Q are those that map from boundary vertices of T. As noted in Remark 1.3, arrows

between frozen vertices can be omitted, which in this case corresponds to arrows between boundary edges.

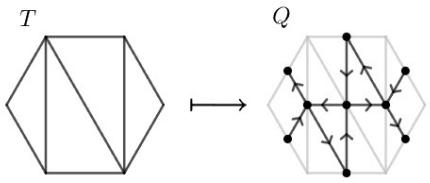

Figure 7

Then mutating a vertex in Q is equivalent to flipping the corresponding edge in T. In other words, each triangulation is a cluster, and each edge of a triangulation is a cluster variable. Moreover, the exchange relation of the cluster variable can described as a Ptolemy relation in the quadrilateral [2, 1.11]. Let's consider the following quadrilateral.

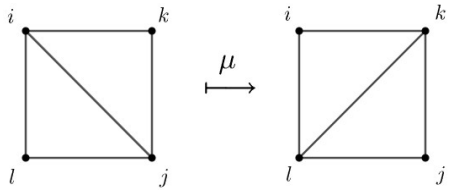

Figure 8

If we label each edge in the triangulation by its endpoints, the Ptolemy relation gives us the following exchange relation:

$$[ij] \cdot [kl] = [ik] \cdot [jl] + [il] \cdot [jk]$$

And if the cluster variable corresponding to an edge $[ij]$ is denote Δ_{ij}, this gives rise to the exchange relation

$$\Delta_{ij} \cdot \Delta_{kl} = \Delta_{ik} \cdot \Delta_{jl} + \Delta_{il} \cdot \Delta_{jk}$$

in the corresponding cluster algebra $\mathcal{A}_T = \mathcal{A}(Q)$, where $\mathcal{A}(Q)$ is the quiver of the triangulation T. Every mutation gives rise to another triangulation, and thus all clusters are given by a triangulation of the same polygon and the above relations.

Definition 1.5. [3, 2.1] Consider a disk with n vertices drawn on its boundary, labeled by the elements in $\{1, \ldots, n\}$, in clockwise order. A *Postnikov diagram*, or *alternating strand diagram*, consists of a collection of n oriented curves called strands, such that each curve has boundary vertices as endpoints, with every boundary vertex having exactly one incoming and outgoing strand, and satisfying the following conditions:

(i) A curve does not cross itself in the interior of the disk.

(ii) No three curve cross in one single point.

(iii) All crossings are transversal, i.e. the curves have different tangents on their intersection (left figure as opposed to right figure).

Figure 9

(iv) There are finitely many crossings between strands.

(v) Following any curve in one direction, the strands that intersect it must alternate in orientation.

Figure 10

(vi) If two strands cross at two points A and B, then one strand is oriented from A to B, and the other from B to A (left figure as opposed to right figure). In other words, no two strands create unoriented lenses, or more informally, there are no *bad double crossings*.

Figure 11

We define alternating strand diagrams up to equivalence of two local transformations, namely twisting and untwisting oriented lenses inside the disk or on the boundary.

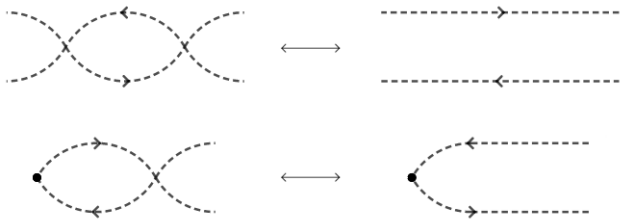

Figure 12

We call the transformations from left to right a *reduction*, and diagrams to which no further reduction can be applied *reduced diagrams*. If two Postnikov diagrams D_1, D_2 are equivalent up to these transformations, we write $D_1 \equiv D_2$. The set of Postnikov diagrams in a disk with n boundary vertices up to equivalence is denoted $\mathbf{Diag_n}$. The set of all Postnikov diagrams is denoted $\mathbf{Diag} = \bigcup \mathbf{Diag_n}$. Furthermore, we treat every diagram up to isotopy with the boundary vertices fixed. When necessary, we denote this equivalence $\sim$. For any $i \in \{1, \ldots, n\}$, the strand that starts at the boundary vertex i is denoted γ_i.

A *decorated permutation* $\overline{\pi}$ of $\{1, \ldots, n\}$ is a pair (π, c) consisting of a permutation π of $\{1, \ldots, n\}$ and a coloring map c that maps any fixed point of π to an element in $\{-1, 1\}$ (or $\{\text{black}, \text{white}\}$) . Any Postnikov diagram defines a permutation π of $\{1, \ldots, n\}$ where $\pi(i) = j$ when γ_i ends at the boundary vertex j. For any fixed point i where γ_i is oriented clockwise, $c(i) = 1$ (white). Otherwise $c(i) = -1$ (black). We call i the *source (vertex)* and $\pi(i) = j$ the *target (vertex)* of γ_i.

Example 1.6. The following Postnikov diagram in a disk with 6 boundary vertices.

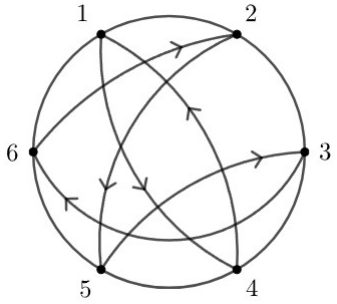

Figure 13

Every strand in a Postnikov diagram divides the disk into two parts, one to its left and one to its right (with respect to the orientation of the strand). Furthermore, every Postnikov diagram subdivides the disk into alternating and oriented regions. We label each alternating region of the diagram with a subset $I \subset [n] := \{1, \ldots, n\}$, such that $i \in I$ if the corresponding region is to the left of the strand γ_i. Then, every label is a k-subset of $[n]$ ([16, Prop. 5]), for a fixed $1 < k < n$.

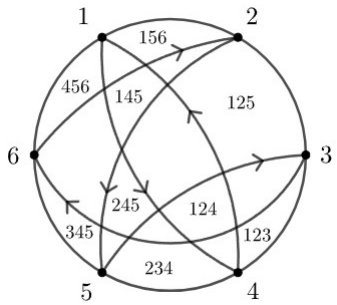

Figure 14

If a Postnikov diagram has n boundary vertices and each of its alternating regions is labeled with k-subset I of $[n]$, we say that the diagram has *rank* k and is of *type* (k, n). Any diagram with decorated permutation $i \longmapsto i + k$ for all i is a (k, n)-diagram, and denoted a $\Gamma_{k,n}$-diagram.

Definition 1.7. Let D be a Postnikov diagram, and Δ an internal quadrilateral alternating region of D. We define the *geometric exchange* of D with respect to Δ as the local transformation on the diagram illustrated as follows

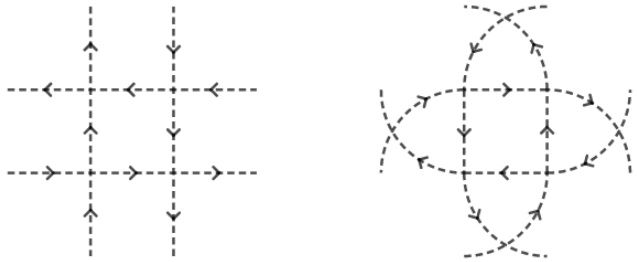

Figure 15

We denote the resulting diagram $\mu_\Delta(D)$. It is easy to check that the geometric exchange does not change the type or permutation of a diagram.

Proposition 1.8. *Let D be a Postnikov diagram of type (k, n). Let π be the a decorated permutation of D, written as $\pi : i \longmapsto i + s(i)$, where $s(i) \in \{0, \ldots, n\}$, such that $s(i) = n$ exactly then when $col(i) = 1$, i.e. γ_i is a clockwise loop starting and ending at i. Then the rank of D is also given by*

$$k = \frac{1}{n} \sum_{i=1}^{n} s(i)$$

Proof. Every alternating region of D has k labels, and there are n such regions on the boundary. Thus the following statement is true for exactly nk couples of (Δ, γ) where Δ is an alternating boundary region and γ is a strand:

"Δ is to the left of γ"

The number of such couples can also be counted by counting over strands and looking at boundary regions to the left of them, i.e.

$$nk = \sum_{i=1}^{n} \#\text{ of boundary regions to the left of } \gamma_i$$

The number of regions to the left of a strand γ_i is just $s(i)$, and thus

$$nk = \sum_{i=1}^{n} s(i) \Longleftrightarrow k = \frac{1}{n} \sum_{i=1}^{n} c(i)$$

Which concludes the proof. □

In other words, the rank of a diagram can be viewed as the average number of boundary points $s(i)$ a strand γ_i *"shifts"* in the diagram between its source vertex i and its target vertex $\pi(i)$. This gives us an alternative way of defining the rank and type of a Postnikov diagram. This also gives us the following definition.

Definition 1.9. Let π be the a decorated permutation of $[n]$, written as $\pi : i \longmapsto i + s(i)$, where $s(i) \in \{0, \ldots, n\}$, such that $s(i) = n$ exactly then when $col(i) = 1$. Then the *rank* of π defined as

$$k = \frac{1}{n} \sum_{i=1}^{n} s(i)$$

The *type* of π is defined as the pair (k, n). The set of (k, n)-permutations is denoted $\mathbb{S}_{k,n}$.

We can map a triangulation T of an n-gon to a $\Gamma_{2,n}$-diagram by mapping every triangle t in T to a collection of three strand segments on the inside of t, following along the edges of t in a counterclockwise order

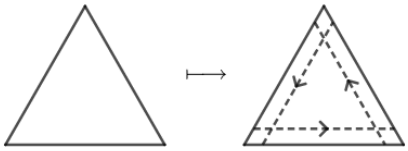

Figure 16

Then if two triangles are edge-adjacent, we join the pairs of oriented strand segments along their shared boundary. The oriented strands obtained from concatenating all strand segments make up the full diagram.

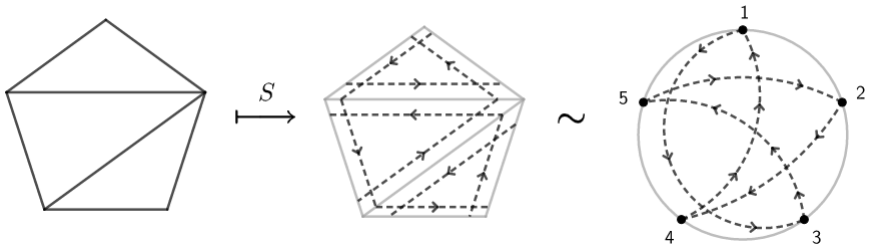

Figure 17

We call this map S the *Scott map*, as it was first described in [16, p.14-15]. The Scott map maps every chord of a triangulation T to a quadrilateral alternating region of $S(T)$. If T_1 and T_2 are two triangulations related by a flip, then $D_1 = S(T_1)$ and $D_2 = S(T_2)$ are related by a geometric exchange. More precisely, we obtain D_2 from D_1 by mutating the quadrilateral region in D_1 that corresponds to the edge in T_1 that is flipped to obtain T_2. This is visualized by the following figure (which we will recall in Proposition 3.8).

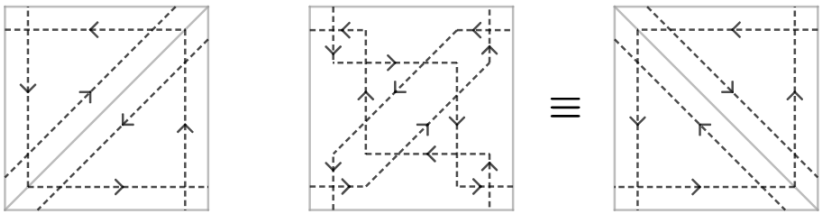

Figure 18

If $D = S(T)$, we also notice that if the labels of the alternating regions of D are the same as the labels of the corresponding chord in T, that is if a region in D is labeled with the 2-subset $\{i, j\}$, it is mapped from the chord $[ij]$ in T.

We will later extend this map to bicolored tilings (Definition 3.1). We will also use bicolored tilings to parametrize positroid cells in the Grassmannian (Definition 5.8). In order to facilitate that, we want to recall a method used in [21, Ch. 2.2] using plabic graphs.

Definition 1.10. A *graph* G is a triple (V, E, ϕ), where V is a finite set of vertices, E a finite set of edges, and $\phi : E \longrightarrow V \times V$ a function called the *incidence function* that maps every edge in E to a pair of vertices in V.

Definition 1.11. [21, 2.11] A *plabic graph* G is a planar graph embedded into a closed disk with n boundary vertices labeled $1, \ldots, n$ in clockwise order for $n > 0$, such that

(i) every boundary vertex is incident to a single edge.

(ii) every vertex is connected by a path to some boundary vertex.

(iii) every internal vertex is colored black or white.

(iv) if an internal vertex v of G is a leaf, the second endpoint of its incident edge is a boundary vertex.

We consider three local transformations, called *moves* on plabic graphs:

(M1) Square move: if four vertices form a square such that each vertex is trivalent and their colors alternate, we may switch the colors of the vertices

Figure 19

(M2) Edge (de)contraction: if two adjacent vertices u and v are of the same color, we may replace them with one single vertex w whose incident edges are those of u and v combined. Conversely, we may replace any vertex w with two adjacent vertices u and v of the same color such that the edge set of w is the union of the edge sets of u and v.

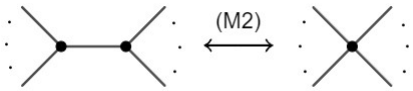

Figure 20

(M3) Vertex removal: if a vertex v is 2-valent, we may replace v and its incident edges with one single edge. Conversely, we may replace a single edge with two edges incident on a single vertex v.

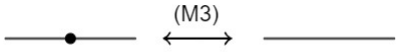

Figure 21

Furthermore, we define a (parallel edge) reduction on plabic graphs

(R) If two adjacent vertices are connected by more than one edge, we may remove an edge.

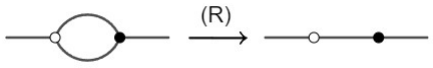

Figure 22

We say that two plabic graphs G and G' are *move-equivalent*, and denote $G \equiv G'$, if one can be obtained by the other by a finite sequence of moves (M1)-(M3). We say that a plabic graph is *reduced* if no graph in its move-equivalence class can be reduced by (R).

We further note that G is a bipartite graph if and only if its internal vertices can be colored in an alternating pattern. Thus, when referring to a bipartite plabic graph, its internal vertices are assumed to be colored in an alternating pattern.

Definition 1.12. [15, p.47] [21, 2.13] Let G be a reduced bipartite plabic graph. A *trip* is an oriented path in G that starts at a boundary vertex i, such that the path turns maximally right at every black vertex, maximally left at every white vertex, and stops at the second boundary vertex it meets.

A graph with n boundary vertices has n trips. Every trip starts at a boundary vertex i and ends in a boundary vertex j. This defines a permutation $\pi(i) = j$.

We define a coloring c on the fixed points of π. If i is a fixed point, the boundary vertex i is vertex-adjacent to an internal leaf v. Then $c(i) = -1$ if v is black, and $c(i) = 1$ if v is white. This assigns a decorated permutation to any reduced plabic graph.

Example 1.13. Here is an example of a reduced bipartite plabic graph G with 6 boundary vertices, and a trip of G mapping $1 \longmapsto 5$.

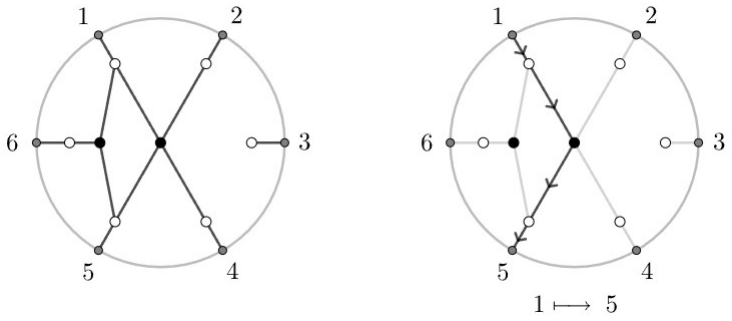

Figure 23

Completing the remaining trips, we obtain the trip permutation $\pi = (15)(264)$ with the coloring on the fixed point $c(3) = 1$.

Proposition 1.14. *[15, 13.1] Let G and G' be reduced plabic graphs with decorated permutations π and π'. If G' can be obtained from G by a finite sequence of moves (M1)-(M3), then $\pi = \pi'$.*

Lemma 1.15. [15, 13.6] Any plabic graph G can be transformed by moves (M1)–(M3) and the reduction (R) into a reduced plabic graph.

Definition 1.16. [15, 14.1] Every reduced bipartite plabic graph G can be mapped to a Postnikov diagram D as follows

(i) draw a dot d_e in the middle of every edge e, and a dot d_i at every boundary vertex i.

(ii) for any internal black vertex v, and any edge e that is incident to v, draw an oriented edge from the dot d_e to the dot of the next edge of v in counter-clockwise order.

(iii) for any internal white vertex v, and any edge e that is incident to v, draw an oriented edge from the dot d_e to the dot of the next edge of v in clockwise order.

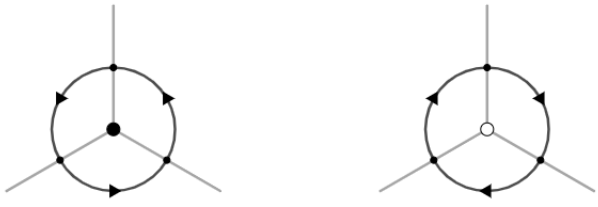

Figure 24

The result is a directed graph $\mathcal{D}$ inside the disk with n boundary vertices of degree 2, and with each internal vertex having degree 4. The strands of the diagram D are the paths of the graph $\mathcal{D}$ between boundary vertices such that all crossings of the paths are transversal.

Example 1.17. The following plabic graph maps into a $\Gamma_{2,5}$-diagram.

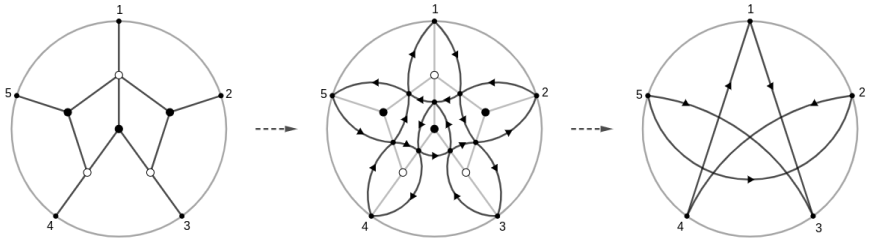

Figure 25

As a result, there is also a correspondence between triangulations and plabic graphs, which we will define explicitly later in the context of bicolored tilings (Definition 3.26). In Remark 3.27 we will see that the square move (M1) corresponds to a quadrilateral flip in the corresponding triangulation.

Proposition 1.18. *[15, 14.2] Let G be a reduced plabic graph, and let D be the corresponding Postnikov diagram as described in Definition 1.16. Let π_G be the decorated (trip) permutation of G and π_D the decorated permutation of D. Then $\pi_G = \pi_D$.*

We will recall the definition of the totally non-negative Grassmannian and its decomposition into positroid cells.

Definition 1.19. [14, p.193] [15, 2.1] The *Grassmannian* $Gr_{k,n}$ of *type* (k, n) is the set of k-dimensional subspaces in an n-dimensional vector space $\mathbb{V}$. Here, $\mathbb{V} = \mathbb{R}^n$.

A point $V \in Gr_{k,n}$ can be described by a full-rank $k \times n$-matrix M, with V being the row-space of M. The row-space of M is invariant under left action by a non-singular $k \times k$-matrix. Thus, we can identify the Grassmannian as

$$Gr_{k,n} = GL_k \backslash Mat_{k \times n}$$

where $Mat_{k \times n}$ is the set of full-rank $k \times n$-matrices. We can embed $Gr_{k,n}$ into the projective space $\mathbb{P}^{\binom{n}{k}-1}$ by setting a coordinate for any k-subset I of $[n] := \{1, \ldots, n\}$

$$\Delta_I = \Delta_I(M)$$

where $\Delta_I(M)$ is the minor of the matrix composed of the column vectors of M enumerated by I. Then the collection $(\Delta_I)_{I \in \binom{[n]}{k}}$ gives us projective coordinates for V. This is called the *Plücker embedding* of $Gr_{k,n}$ [14].

The *totally non-negative Grassmannian* $Gr_{k,n}^{\geq 0}$ is the subset of subspaces in $Gr_{k,n}$ for which all the projective coordinates are all non-negative up to simultaneous scaling with a factor $\lambda \neq 0$.

$Gr_{k,n}^{\geq 0}$ can be decomposed into so-called positroid cells. An in-depth analysis of the stratification of the Grassmannian can be found in [15, 3.2,3.5] and [19, 2.1-2.3]. For our intents and purposes, it is sufficient to define positroid cells as follows.

Definition 1.20. [19, 2.8] A *matroid* $\mathcal{M}$ of type (k, n) is a non-empty collection of k-subsets of $[n]$, i.e. $\mathcal{M} \subset \binom{[n]}{k}$ satisfying the exchange relation:

$$\forall I, J \in \mathcal{M} : \forall i \in I : \exists j \in J : I \setminus \{i\} \cup \{j\} \in \mathcal{M}$$

The elements of $\mathcal{M}$ are called *bases*.

Definition 1.21. [19, 2.2] [15, 3.2] Let $\mathcal{M} \subset \binom{[n]}{k}$ be a matroid. The positroid cell $S_{\mathcal{M}} \subset Gr_{k,n}^{tnn}$ is defined as

$$\begin{aligned} S_{\mathcal{M}} &= \{V \in Gr_{k,n}^{\geq 0} \,|\, \Delta_I(V) \neq 0 \text{ if and only if } I \in \mathcal{M}\} \\ &= \{V \in Gr_{k,n}^{\geq 0} \,|\, \Delta_I(V) > 0 \text{ if and only if } I \in \mathcal{M}\} \end{aligned}$$

If $V \in Gr_{k,n}^{\geq 0}$, and S_V denotes the positroid cell such that $V \in S_V$, then

$$S_V := \{W \in Gr_{k,n}^{\geq 0} \,|\, \forall I \in \binom{[n]}{k} : \Delta_I V = 0 \text{ iff } \Delta_I W = 0\}$$

In other words, V and W are in the same positroid cell, if they share the placing of their zero coordinates. Positroid cells in (k,n) are in bijection with decorated permutations of type (k,n) [15, 17.1]. Thus, if we index positroid cells $S_{\mathcal{M}}$ by their corresponding decorated permutation π, and denote it S_π, this gives us the decomposition of $Gr_{k,n}^{\geq 0}$:

$$Gr_{k,n}^{\geq 0} = \bigsqcup_{\pi \in \mathbb{S}_{k,n}} S_\pi$$

where $\mathbb{S}_{k,n}$ is the set of decorated permutations of type (k,n).

Theorem 1.22. *[15, 3.5] Each positroid cell S_π is homeomorphic to an open ball of some dimension* $\dim S_\pi$.

A more explicit connection between a decorated permutation and its corresponding positroid cell will be explored via bicolored tilings. For now, let us note that plabic graphs can be used to parametrize positroid cells. Two methods are described in [15, 12.7] and [21, 2.17]. We will use the latter method.

Definition 1.23. [21, 2.15] Let G be a bipartite plabic graph such that every boundary vertex is incident to a white vertex. An *almost perfect* matching m of G is a subset of edges of G such that each internal vertex is incident to exactly one edge in m. The *boundary* ∂m of m is the set of boundary vertices that are incident to an edge in m. We recall that boundary vertices of G are labelled $1,\dots,n$, thus

$$\partial m = \{i \in \{1,\dots,n\} \mid i \text{ is incident to an edge of } m\}$$

We denote $\mathcal{M}(G)$ the set of matchings of G.

Remark 1.24. We may define almost perfect matchings for bipartite plabic graphs that have boundary vertices adjacent to black vertices as well. In that case, if W denotes the set of boundary vertices of G adjacent to a white vertex, and B the set of boundary vertices of G adjacent to a black vertex, we would define the boundary of a matching m as

$$\partial m = \{i \in W \mid i \text{ is incident to an edge of } m\} \cup \{i \in B \mid i \text{ is not incident to an edge of } m\}$$

Proposition 1.25. *Let G be a bipartite plabic graph with n boundary vertex such that every boundary vertex is incident to a white vertex. Let $m_1, m_2 \in \mathcal{M}(G)$ be matchings of G. Then $|\partial m_1| = |\partial m_2|$.*

Definition 1.26. Let G be a bipartite plabic graph with n boundary vertices such that every boundary vertex is incident to a white vertex, and such that G has a perfect matching. The *rank* of G is $k = |\partial m|$, where $m \in \mathcal{M}(G)$. We say that G is of *type* (k, n).

Example 1.27. The following plabic graph with 6 boundary vertices has a matching m with $\partial m = \{1, 2, 3, 6\}$, and is thus a graph of type $(4, 6)$.

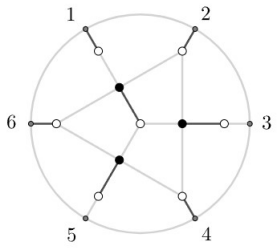

Figure 26

It is the graph obtained by mapping a rhombic tiling (Section 4.3) to its corresponding plabic graph.

Theorem 1.28. *[21, 2.17] Let G be a bipartite plabic graph of type (k, n). Let $\mathcal{E}$ be the set of its edges. Let $w : \mathcal{E} \longrightarrow R_{>0}$ be a weight function on the edges of G. For any $m \in \mathcal{M}(G)$, we set*

$$w(m) = \prod_{e \in m} w(e)$$

Then there is a point $V_w \in Gr_{k,n}$ such that for any k-subset I of $[n]$, we have

$$\Delta_I(V_w) = \sum_{\substack{m \in \mathcal{M}(G) \\ \partial m = I}} w(m)$$

Varying over all such weight functions we get the positroid cell

$$S_G = \{V_w \,|\, w : \mathcal{E} \longrightarrow R_{>0}\}$$

Proposition 1.29. *[15, 12.2] Let G and G' be bipartite plabic graphs of type (k, n) such that G' can be obtained from G by a finite sequence of moves (M1)-(M3) and reduction (R) (as defined in Definition 1.11). Then $S_G = S_{G'}$.*

Proposition 1.30. *[15, 13.4] [21, 2.10] Let G and G' be reduced, bipartite plabic graphs of type (k, n), with decorated permutation π and π', respectively. If $\pi = \pi'$, then $S_G = S_{G'}$.*

Thus we can index positroid cells as described in Theorem 1.28 by the decorated permutation of a graph. Any decorated permutation of type (k, n) gives us a different graph.

Proposition 1.31. *[15, 12.7] Let G be a bipartite plabic graph of type (k, n), $\mathcal{F}$ the set of faces of G, and S_G be the corresponding positroid cell. Them* $\dim S_G = |\mathcal{F}| - 1$.

Remark 1.32. In Definition 1.21 we denoted the positroid cells by indexing them via matroids, vector spaces, and decorated permutations ($S_{\mathcal{M}}$, S_V, and S_π), and via plabic graphs in Theorem 1.28 (S_G). All these notations refer to the same positroid cells, but are just indexed differently. We may use the notations interchangeably, depending on what object we use to infer the corresponding positroid cell. Later in Definition 5.8, we will see how we can index the positroid cells by tilings (S_T).

To sum up, triangulations can be mapped to quivers, $\Gamma_{2,n}$ diagrams, and plabic graphs of type $(2, n)$, with the flip of a diagonal corresponding to the mutation of a vertex, a geometric exchange, and a square move, respectively. Triangulations of an n-gon are linked to the totally non-negative Grassmannian $Gr^{tnn}_{2,n}$. We generalize this connection to objects of any type (k, n) by introducing bicolored tilings.

2 Bicolored tilings

In a first instance, bicolored tilings can be thought of as triangulations where we removed some diagonals and then colored each tile black or white.

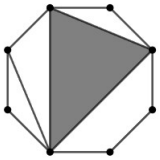

Figure 27

From there, we extend this idea to constructions with internal vertices, loops, and digons. In terms of the Scott map, black tiles will behave similarly to edges,

and as we will see later, some of the propositions count black tiles as edges as well. To this end, we will first define those black tiles as edges between any number of vertices, before we define bicolored tilings as a collection of *compatible* edges in a disk or polygon, similar to how triangulations are a collection of non-crossing chords in a polygon.

Remark 2.1. In [7, 2.3], tilings are defined as a collection of smooth curves with a coloring on the faces that these curves delimit. However, here we adopt the definition of bicolored tilings in the setup of [8, 2.4], as it allows us to restrict bicolored tilings to a smaller collection to avoid odd examples and exceptions.

Definition 2.2. [8, 2.4] Let X be a 2-dimensional connected oriented surface with boundary, with n distinct boundary vertices, enumerated $\{1, \dots, n\}$, and $x_1, \dots, x_m$ internal vertices, for $m \geq 0$. Let V be the set of vertices, both boundary and internal. A *hyperedge* or r-edge $e = (v_1, \dots, v_r)$ is a finite sequence of vertices $v_i \in V$ such that

(i) There are no repetitions of vertices in $v_1, \dots, v_r$, with the exception of boundary vertices which may appear exactly twice in consecutive order (with the convention that v_r and v_1 are consecutive).

(ii) There is a collection of smooth curves $\epsilon_1, \dots, \epsilon_r$ on the surface such that ϵ_i has endpoints v_i and v_{i+1} (with the convention that $v_{r+1} = v_1$), and such that no two curves intersect, other than at the endpoints of any two consecutive curves ϵ_i and ϵ_{i+1}. Furthermore, there are no vertices of V boundary components of X in the interior of the disk with boundary $\bigcup \epsilon_i$.

We call $v_1, \dots, v_r$ the *endpoints* of e. Hyperedges are treated up to cyclical shift of the sequence.

Remark 2.3. We draw an hyperedge with e with boundary $\bigcup \epsilon_i$ by drawing the curves ϵ_i and shading the area between those curves. Hyperedges between 2 distinct vertices can be drawn like regular edges, i.e. as either an arc between the vertices or black digons with the vertices as endpoints (and are considered equivalent), and are also called *(simple) edges*. A hyperedge consisting of a single vertex is drawn as a black 1-gon (a loop whose interior is shaded).

As stated in Definition 2.2(i), we can choose boundary vertices twice as endpoints of a hyperedge. This allows us to create white loops, i.e. white 1-gons, in a tiling, which will map to counter-clockwise loops under the Scott map (Definition 3.1). Conditions (ii) and (iii) ensure that the hyperedge can be embedded in the disk such that each hyperedge is a black $r - gon$ (up to isotopy), and such that no such r-gon contains another vertex inside.

Example 2.4. We consider the disk D_6 with 6 boundary vertices and 3 internal vertices x_1, x_2, x_3.

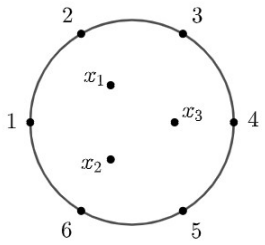

Figure 28

Then for $b_i = (i, i+1)$ (for $i = 1, \ldots, 6$), the following are examples of hyperedges.

- $b_1, \ldots, b_6$, $e_1 = (2, x_1)$, $e_2 = (x_1, x_2, x_3)$, $e_3 = (5, x_3)$
- b_1, b_2, b_3, b_5, b_6, $e_4 = (2, x_1)$, $e_5 = (3, 4, 5, x_1)$
- $b_2, \ldots, b_5$, $e_6 = (1, 2, x_1)$, $e_7 = (1, x_1, 6), e_8 = (x_2)$

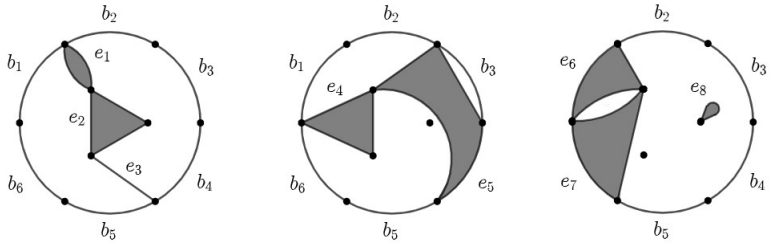

Figure 29

As previously noted, if a boundary vertex i appears twice in the sequence that describes an hyperedge, the curve that has both endpoints i forms a white loop at the boundary, as seen in the second example. If two vertices u, v appear as consecutive vertices in two (or more) hyperedges, this creates (multiple) white digons, as seen in the third example. All three collections of hyperedges are pairwise compatible. We note that in each of the collections, we added hyperedges that serve as boundary components of the construction, namely $b_1, \ldots, b_6$. In the second example, e_5 serves

as a boundary component between boundary vertices 4 and 5. On the other hand, we notice that by having both b_3 and e_5 being hyperedges between the boundary vertices 3 and 4, we create a white digon at the boundary, if we assume the hyperedges to be compatible.

Definition 2.5. Two hyperedges are *compatible* if they can be embedded in the disk such that they do not intersect other than at their shared endpoints.

Definition 2.6. Let X be a 2-dimensional connected oriented surface with boundary, with n distinct boundary vertices, enumerated $\{1, \ldots, n\}$, and $x_1, \ldots, x_m$ internal vertices. We denote the set of these vertices by V. A *bicolored* tiling $T = (X, V, E)$ is the surface X equipped with a finite collection of hyperedges E such that

- the hyperedges are pairwise compatible.
- for any boundary segment between two consecutive boundary vertices u, v, there is exactly one black tile intersecting that whole boundary segment, including the endpoints u, v.

We define tilings up to equivalence given by the following two local transformations

- Hourglass equivalence:

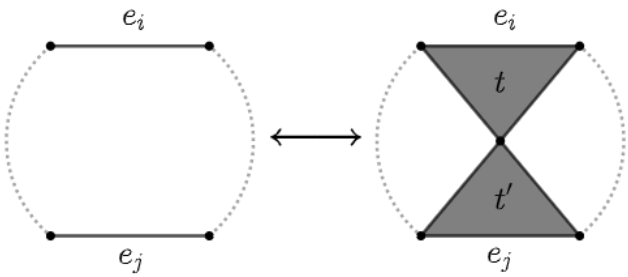

Figure 30

- Digon equivalence:

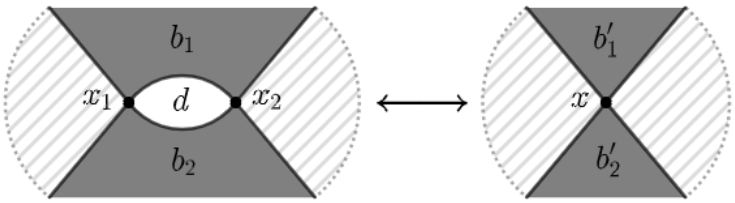

Figure 31

where x_1 and x_2 are not simultaneously boundary vertices.

For the rest of this paper, the surface X will always be a disk, unless otherwise specified. The set of tilings (in a disk) up to tiling equivalence, i.e. hourglass/digon equivalence, is denoted **Til**. The set of tilings with n boundary vertices is denoted $\mathbf{Til}_n$. Furthermore, we define the *mutation/flip* of a simple edge inside a quadrilateral within the tiling, as described in the following figure

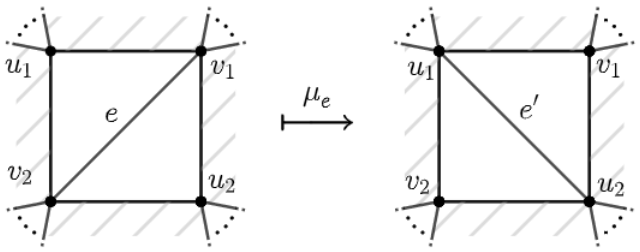

Figure 32

We say that two tilings are flip/mutation-equivalent if one can be obtained from the other by a finite sequence of flips and tiling equivalences. We denote $\overline{\mathbf{Til}}$ the set of flip/mutation-equivalence classes of tilings in **Til**. For simplicity, we will identify T with its flip-equivalence class $\overline{T}$ for the rest of this paper, unless otherwise specified.

Example 2.7. The following is a tiling of D_6, a tiling that is equivalent to it, and a tiling that is flip-equivalent to it.

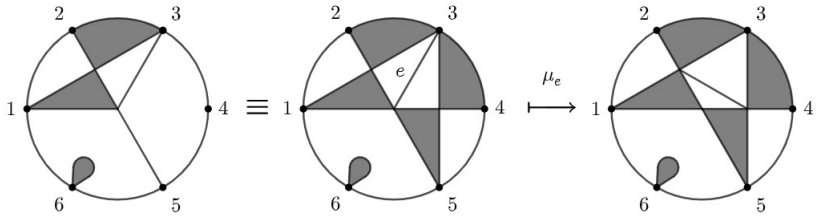

Figure 33

We will usually draw D_n as an $n-gon$, as we work with tilings up to homotopy. This would make our tiling of D_6 look as follows

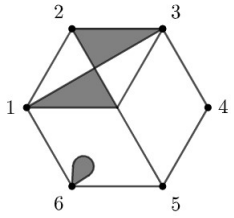

Figure 34

Remark 2.8. The number of internal vertices varies between equivalent tilings. The hourglass equivalence adds or removes the middle vertex when we go right or left in the above depicted transformation, respectively. The digon equivalence contracts two vertices into one from left to right in the depiction above.

A tiling consists of several "ingredients" that we will distinguish in the rest of the paper as follows.

Definition 2.9. Let T be a tiling of a surface X. The set of vertices and hyperedges of T are denoted V and E, respectively. We sometimes refer to the hyperedges of E as *black tiles*.

The *faces* T are the connected components of $X \setminus (\bigcup t_e)$. We also call the faces of a tiling *white tiles*. The set of faces of T is denoted F.

An *angle* α of T is a quadruple $(v, e_1, e_2, f) \in V \times E \times E \times F$, such that e_1 and e_2 are consecutive hyperedges around the face f intersecting in v. Angles are symmetrical with respect to the hyperedges e_1 and e_2. Informally, we choose a vertex around which the angle α lies, and a face inside which α lies. However, this is not

enough in some cases, such as when there is a 1-edge, and thus we need to specify between which two hyperedges α lies. The set of angles of T is denoted A.

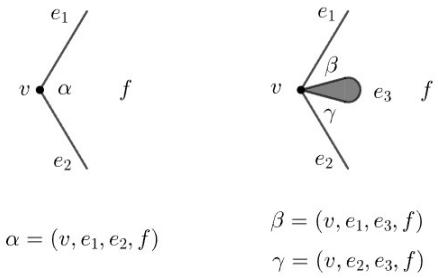

Figure 35

We can use the hourglass equivalence of tilings to flip edges between any two white tiles of size greater than 2. We may do that by adding hourglasses around the edge that we want to flip in order to inscribe it in a white quadrilateral, which may then be flipped.

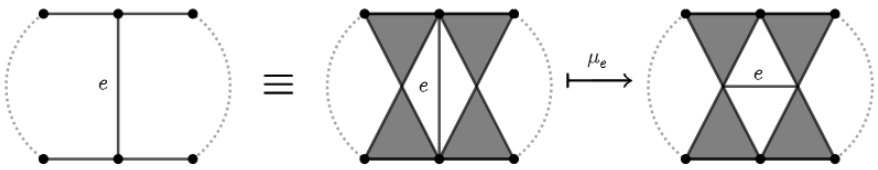

Figure 36

In other words, any edge that acts as the diagonal of a white polygon can be flipped that way.

Example 2.10. We consider the following rhombic tiling (see Section 4.3) with internal edges labeled e_1, e_2, e_3 clockwise, starting with the left one. To mutate the edge e_1, we add two hourglasses inside the adjacent tiles, which then circumscribe the edge inside a quadrilateral, allowing us to flip it. We denote $\mu_i := \mu_{e_i}$.

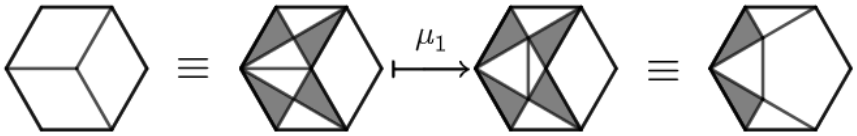

Figure 37

Further flipping the edges e_2, e_3, e_1 in that order indeed returns another rhombic tiling, which is the original tiling to which we applied a Yang-Baxter move. We will see the full mutations in Section 4.3, when discussing rhombic tilings in more detail.

For the rest of this paper, unless otherwise specified, we only consider tilings for the disk $S_n = D_n$ with n boundary vertices, and the boundary vertices are labeled $1, \ldots, n$ in clockwise order.

Finally, we are going to define one more important transformation of tilings, called a *reduction*. This transformation is linked to parallel edge reductions of plabic graphs in [15][12.4, p.43] and will allow us later to describe which tilings map to Postnikov diagrams (Proposition 3.14). Furthermore, reductions on tilings preserve some combinatorial properties of the tilings, such as the positroid cell of the Grassmannian (Definition 5.8) associated to tilings, as we will see in Proposition 5.17.(iii).

Definition 2.11. Let T be a tiling, and let $e \in E$ be a black 1-gon whose only neighboring tile is a white tile. Then the tiling $T' = T - e$ is called a *reduction* of T. We denote this reduction R_e.

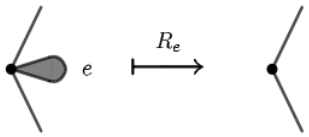

Figure 38

A tiling T is said to be *reduced* if no reduction R_e can be applied to any tiling in its mutation-equivalence class.

It can be hard to see when a tiling is reduced. However, we will see in Proposition 3.14 that reduced tilings map to Postnikov diagrams. Thus, if a tiling does not generate a Postnikov diagram under the Scott map, we know it is not reduced, and try to find a tiling in its mutation-equivalence class to reduce it. We do this until

we obtain a reduced tiling that maps to a Postnikov diagram. Later, we will see that the reduced tiling preserves some combinatorial properties of the initial tiling (particularly in Proposition 5.17).

Definition 2.12. Let T be a reduced tiling. Then the *dimension* of T is $\dim T = |E| - 1$.

We will later see in Proposition 5.23 that the dimension of T is the same as the dimension of the positroid cell associated to T.

Example 2.13. Two special cases of the hourglass equivalence are the following

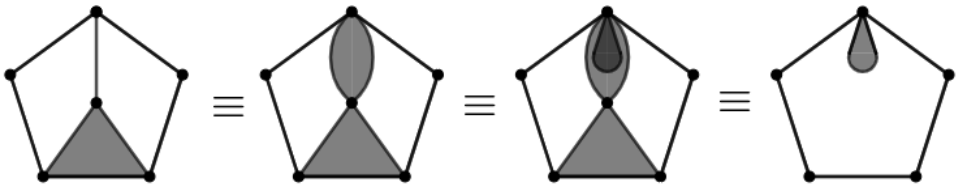

Figure 39

The vertical edge can be viewed as a black 2-gon, which can then be viewed as a black triangle (shaded in a lighter grey) added along the edge of a black 1-gon (shaded in darker grey). With the bottom triangle, this is another hourglass.

Similarly, an internal vertex with two incident edges is another hourglass that can be removed or added.

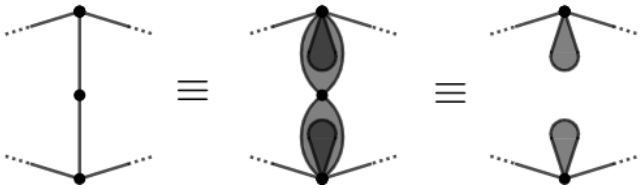

Figure 40

3 Scott map and stellar-replacement map

In this section, we will generalize the Scott map on bicolored tilings. As previously alluded to (p.25), the Scott map will behave the same on white tiles, but will treat

black tiles like edges (i.e. strands will simply go through them and continue along the boundary of the next white tile) (p.17). We also previously noted that not all tilings map to Postnikov diagrams. We will therefore define a more general version of diagrams that allows for closed, oriented cycles, as well as *bad double crossings* (i.e. unoriented lenses created between two strands).

Definition 3.1. Consider a disk with n vertices drawn on its boundary, labeled by the elements in $\{1, \dots, n\}$, in clockwise order. An *(alternating) curve diagram* consists of a finite collection of oriented curves, such that each curve is either a closed cycle or has boundary vertices as endpoints, in which case we call it a strand, with every boundary vertex having exactly one incoming and outgoing strand, and satisfying the following conditions:

(i) A curve does not cross itself in the interior of the disk.

(ii) No three curve cross in one single point.

(iii) All crossings are transversal, i.e. the curves have different tangents on their intersection.

(iv) There are finitely many crossings between curves.

(v) Following any curve in one direction, the curves that intersect it must alternate in orientation.

We define alternating curve diagrams up to the same equivalence as Postnikov diagrams, i.e. twisting and untwisting oriented lenses inside the disk or on the boundary. If two curve diagrams D_1, D_2 are equivalent up to these transformations, we write $D_1 \equiv D_2$. The set of alternating curve diagrams in a disk with n boundary vertices up to equivalence is denoted $\mathbf{Diag_n}$. The set of all alternating curve diagrams is denoted $\mathbf{Diag} = \bigcup \mathbf{Diag_n}$. Furthermore, we treat every diagram up to isotopy with the boundary vertices fixed. When necessary, we denote this equivalence $\sim$. For any $i \in \{1, \dots, n\}$, the strand that starts at the boundary vertex i is denoted γ_i. Any curve diagram has exactly n boundary-to-boundary strands $\gamma_1, \dots, \gamma_n$, and may have closed cycles in the interior of the disk.

In essence, it is the same definition as Definition 1.5 without condition (vi), and where the collection of strands consists of n strands and any finite number of closed, oriented cycles.

Example 3.2. Two examples of alternating curve diagrams with 5 boundary vertices.

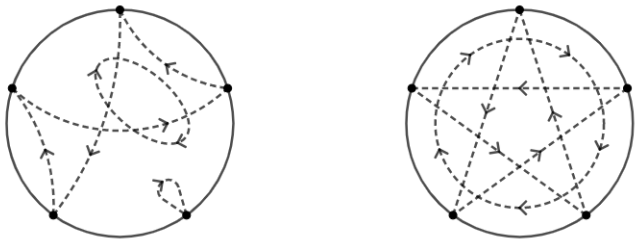

Figure 41

Definition 3.3. [16, p.14-15] [7, 3.1] We define the *Scott map*

$$S : \mathbf{Til_n} \longrightarrow \mathbf{Diag_n}, T \longmapsto D$$

to be the map such that

- any white tile is mapped to a configuration consisting of m curve segments, where m is the size of the tile, following around the border in a counter-clockwise orientation. For example:

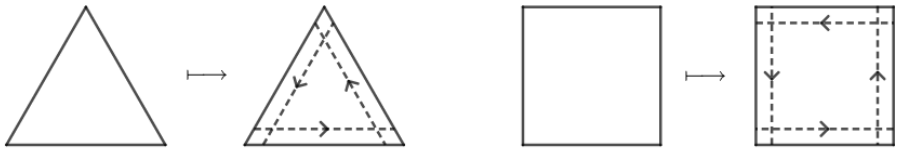

Figure 42

- any black tile is mapped to a configuration consisting of m curve segments, where m is the number of vertices of the tile, such that each curve forms an arc around a vertex inside the tile in a clockwise orientation. For example:

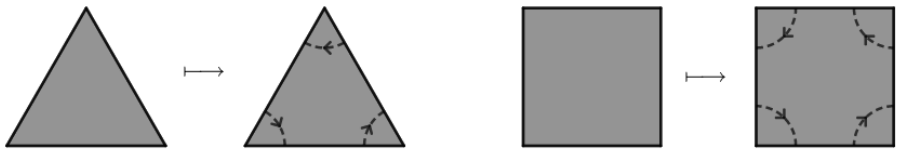

Figure 43

- If two tiles are adjacent, join the pairs of oriented curves segments along their shared boundary. The oriented curves obtained from concatenating all curve segments make up the full curves of the diagram. One can check that these are consistently oriented. Indeed, the only intersections of curves occur in white tiles. Following a single curve, these intersections always come in pairs of two, the first being from left to right, and the second being from right to left. Thus the intersections keep alternating as the curve passes through white tiles.
- The curves join at the boundary, i.e. for any boundary vertex, we take the two curves that intersect the boundary on either side of the vertex closest to it and join them.

Example 3.4. We consider the image of a bicolored tiling of an octagon with one internal vertex under the Scott map. The image is a Postnikov diagram of type $(5, 8)$.

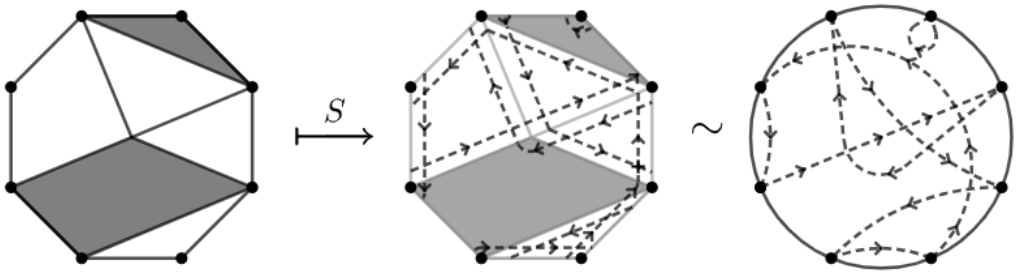

Figure 44

Lemma 3.5. For any tiling T, $S(T)$ is an alternating curve diagram.

Proof. By construction, all intersections of curves are given by the intersections of curves within white tiles. They are trivially pairwise, transversal, and there are

finitely many. It is also easy to see that the endpoints of strands are on the boundary of T. Any endpoints of a strand can only arise as the endpoint of a curve in the configuration if that endpoint is not attached to another curve. However, that is only the case if there is no tile adjacent to the boundary hyperedge of the tile on which that endpoint lies, which means that the endpoint lies on the boundary of T.

Following any strand from its source vertex to its target vertex, any crossings occur only in white tiles and come in pairs of two, always crossing from left to right first (after entering the tile), and from right to left second (before leaving the tile). Thus the alternating property is satisfied for any strand in T. If the curve is a cycle, we choose any point of the cycle that lies on a hyperedge of a white tile and treat it as both source and target vertex, and the same reasoning follows. Thus the alternating property is satisfied everywhere in T.

Thus the resulting construction is an alternating curve diagram. □

Remark 3.6. There is a correspondence between the parts that make up a tiling T and the regions of the diagram $\Gamma = S(T)$. More precisely, if v is a vertex, e an hyperedge, and f a face in T, then

- v maps to a clockwise oriented region in Γ.
- e maps to an alternating region in Γ.
- f maps to a counterclockwise oriented region in Γ.

Proposition 3.7. *Let $T, T' \in$* **Til**. *If $T \equiv T'$ then $S(T) \equiv S(T')$.*

Proof. Since both relations are equivalence relations, it is sufficient to show that if T' is obtained from T by the addition of an hourglass or by digon (de)contraction, then $S(T) \equiv S(T')$. Indeed, adding an hourglass results in locally twisting two paths of the diagram into a clockwise-oriented lens,

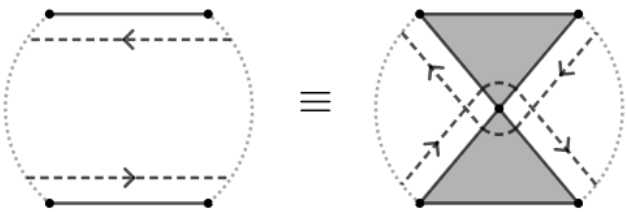

Figure 45

whereas contracting a digon results in locally untwisting two paths of the diagram into a counterclockwise oriented lens.

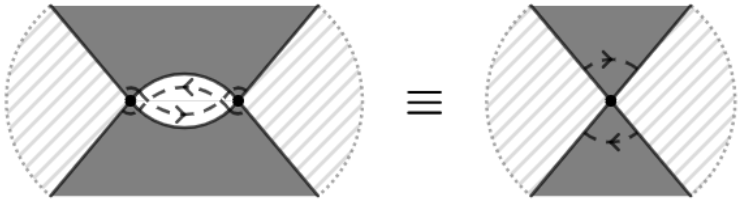

Figure 46

In both cases, $S(T) \equiv S(T')$. □

The following is pointed out in [16, p.16] and still remains true in bicolored tilings.

Proposition 3.8. *The flip of an edge in a quadrilateral corresponds to a geometric exchange in the strand diagram that the tiling maps to, i.e.* $S(\mu_e(T)) \equiv \mu_{S(e)}S(T)$ *for any edge* e *in a tiling* T*.*

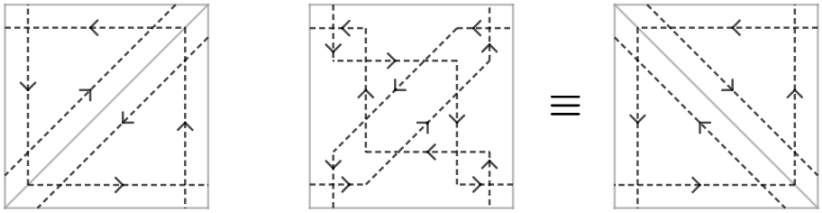

Figure 47

Remark 3.9. As previously stated, Postnikov diagrams map to quivers, which generate cluster algebras, with the vertices of the quiver corresponding to cluster variables. The geometric exchange and consequently the flip of an edge correspond to the mutations of cluster variables, with each tiling corresponding to a cluster.

Definition 3.10. The *rank* k of a tiling T is defined as the rank of the diagram $S(T)$. Similarly, a tiling is of type (k, n) if the diagram $S(T)$ is of type (k, n).

Proposition 3.11. *Let* T *be a tiling of permutation* π*,* e *be a black* 1*-gon, and* $T' = R_e(T)$*. Let* γ_i *and* γ_j *be the strands in* T *that pass through* e *and go around* e*,*

respectively. Then the permutation π' of T' is given by

$$\pi'(l) = \begin{cases} \pi(l), & \text{if } l \neq i, j \\ \pi(j) & \text{if } l = i \\ \pi(i) & \text{if } l = j \end{cases}$$

In other words, $\pi' = (\pi(i)\ \pi(j))\pi$.

Proof. We observe the effect that reductions have from the diagram $S(T)$ to $S(T')$.

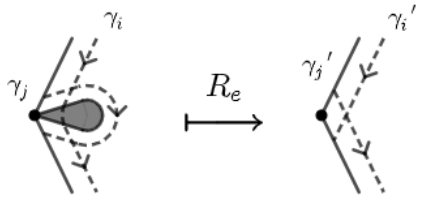

Figure 48

We observe that the strands γ_i and γ_j simply swap target from $S(T)$ to $S(T')$. □

Example 3.12. The following tiling of a hexagon is equivalent (by hourglass equivalence) to a tiling with a black 1-gon e.

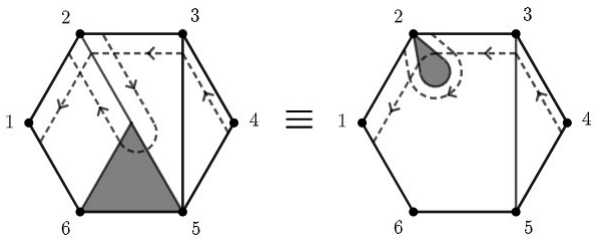

Figure 49

If π is the permutatation of these tilings, we can see that $\pi(2) = 2$ and $\pi(4) = 1$. By applying R_e to the tiling, we obtain a tiling

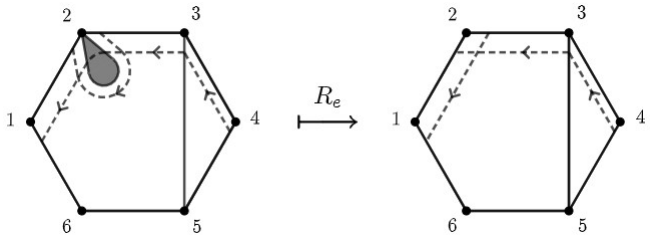

Figure 50

If π' is the permutation of the resulting tiling, then $\pi'(2) = 1$ and $\pi'(3) = 2$. It is easy to verify that for any $i \neq 2, 3$, $\pi(i) = \pi'(i)$.

Proposition 3.13. *Let T be a tiling, e be a black 1-gon, and $T' = R_e(T)$. Then T and T' have the same type.*

Proof. T and T' have the same number of boundary vertices, so it remains to show that T and T' have the same rank. Let γ_i and γ_j be the strands in T that pass through e and go around e, respectively (as shown in the previous figure). Let γ'_i and γ'_j be the strands that intersect at the angle (Definition 2.9) in T' where e was. If π is the permutation of T, then the permutation π' of T' is given by

$$\pi'(l) = \begin{cases} \pi(l), & \text{if } l \neq i, j \\ \pi(j) & \text{if } l = i \\ \pi(i) & \text{if } l = j \end{cases}$$

Then, $s'(i) = s(i) + \pi(j) - \pi(i)$, and $s'(j) = s(j) + \pi(i) - \pi(j)$ Then the rank k' of T' is given by

$$k' = \frac{1}{n}\sum_{l=1}^{n} s'(l) = \frac{1}{n}\sum_{l=1}^{n} s(l) + [\pi(j) - \pi(i) + \pi(i) - \pi(j)] = k$$

□

The following proposition generalizes the result in [4, 3.5] which states that - in the classic setup for tilings - tilings map to Postnikov diagrams under the Scott map. Once we introduce internal vertices and black tiles, this statement does not hold for every tiling anymore. An analogous statement for plabic graphs is given in [15, 14.2].

Proposition 3.14. *T is a reduced tiling if and only if $S(T)$ is a Postnikov diagram.*

Proof. Let T be non-reduced. Then there is $T' \equiv T$ such that T' has a 1-edge e. Then, locally, e maps to a bad double crossing under the Scott map, thus $S(T)$ is not a Postnikov diagram. Hence, if $S(T)$ is a Postnikov diagram, then T is a reduced tiling.

Let T be a reduced tiling, and $G = \Phi(T)$ the corresponding plabic graph as described in Definition 3.26. If $\mathcal{F}$ is the set of faces of G, then $|E| = |\mathcal{F}|$. Assume $S(T)$ is not a Postnikov diagram, then by [15, 14.12], G is not reduced. Then by [15, 12.5], $|\mathcal{F}|$ is not minimal in the movement-reduction class of G. Then $|E|$ is not minimal within the reduction-equivalence class of T, and thus T is not reduced, which is a contradiction. Hence, $S(T)$ is a Postnikov diagram. □

Definition 3.15. A *matching* $m \subset A$ of a tiling T is a choice of angles of T such that.

(i) Each face is matched exactly once, i.e. for any two angles $\alpha, \beta \in m : f(\alpha) \neq f(\beta)$, and for any face f of T, there is $\alpha \in m$ such that $f = f(\alpha)$.

(ii) Each vertex is matched at most once, i.e. for any two $\alpha, \beta \in m : v(\alpha) \neq v(\beta)$.

(iii) Each internal vertex is matched exactly once, i.e. on top of the second condition, for any internal vertex v of T, there is $\alpha \in m$ such that $v = v(\alpha)$.

We denote $\partial m = \{v \in V \mid v \text{ is a boundary vertex and not matched in } m\}$ the *boundary* of m. The set of matchings of a tiling T is denoted $\mathcal{M}(T)$.

The following proposition gives us an easy way to determine the type of a tiling. We will prove this statement later in Proposition 5.7.

Proposition 3.16. *Let T be a tiling with a matching of type (k, n). Then $k = |V| - |F|$.*

By defining an inverse to the Scott map, we can, in particular, construct a tiling for any Postnikov diagram, and as a consequence construct a tiling of any type and permutation as well. This mostly serves the purpose of establishing a bijection between reduced bicolored tilings and Postnikov diagrams, as we will later in Section 4.6 describe a method to directly construct a tiling given any decorated permutation.

Definition 3.17. Let $D \in \mathbf{Diag_n}$ be an alternating path diagram, and let r be a region of D, then the *size* of r is the number of crossings in D which lie on the boundary of r.

Definition 3.18. We define the map

$$\overline{S} : \mathbf{Diag_n} \longrightarrow \mathbf{Til_n}$$

that maps any curve diagram to a tiling of an n-gon such that

- any counterclockwise region of size m is mapped to a white m-gon.
- any clockwise region of size m is mapped to an m-antigon for $m > 1$, while a clockwise region of size 1 (i.e. a clockwise loop) is mapped to a black 1-gon.
- any alternating and any boundary region of size m is mapped to a black m-gon.
- if two regions are hyperedge- or vertex-adjacent, then their images are also hyperedge- or vertex-adjacent, respectively.

Proposition 3.19. *$\overline{S}$ is the inverse of S, i.e. $S\overline{S} = \mathrm{id}_{\mathbf{Diag_n}}$ and $\overline{S}S = \mathrm{id}_{\mathbf{Til_n}}$. We call $S^{-1} = \overline{S}$ the inverse Scott map.*

Proof. Since both maps are defined locally, we can simply look at how applying those maps in succession locally returns the initial construction.

- $S\overline{S} = \mathrm{id}_{\mathbf{Diag_n}}$: We look at the intersection of two curves. The curves divide the region locally into 4 smaller regions, one of which is clockwise oriented. Assume that the clockwise-oriented region is of size $m > 1$, which means that $\overline{S}$ maps it to an m-antigon. We see that applying $\overline{S}$ followed by S returns the same intersecting sections of paths

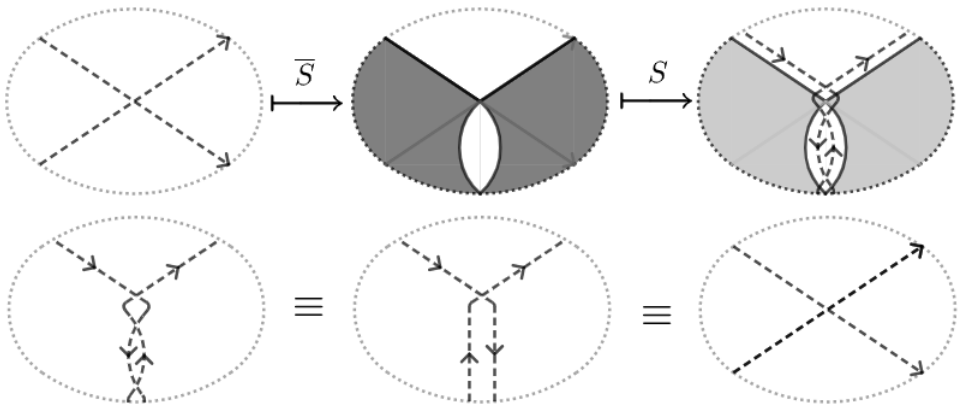

Figure 51

Thus $S\overline{S}$ does not locally change the diagram, and therefore maps the diagram to itself. The case where $m = 1$ is similar.

- $\overline{S}S = \mathrm{id}_{\mathbf{Til_n}}$: Similarly, we look at how $\overline{S}S$ applies locally on a tiling. More precisely, we look at where intersections of the diagram would occur after mapping the tiling by S, which would be at the corner of each white tile. In the illustration below the white tile is adjacent to two black tiles around that corner. However, as seen before, edges can be treated as black 2-gons and drawn as such, hence we do not lose generality with this construction.

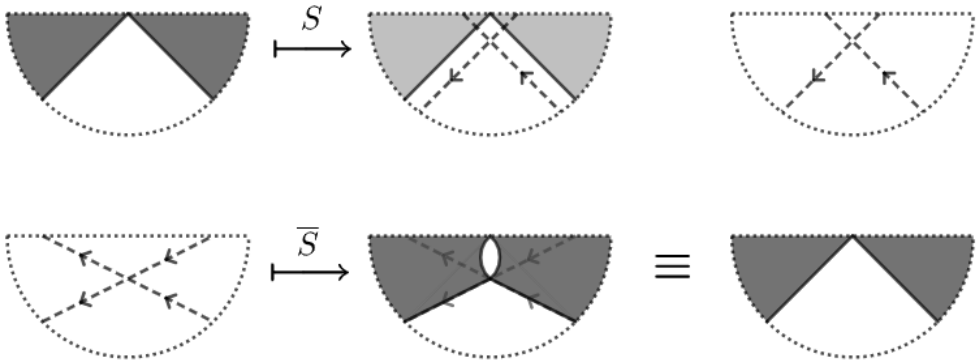

Figure 52

We observe that $\overline{S}S$ does not locally change the diagram, and therefore maps the diagram to itself.

Once again, in the left figure of second line, we assume that $m > 1$, where m is the size of the clockwise oriented region, which maps the region to an antigon under $\overline{S}$. The result is similar if $m = 1$.

Thus we conclude that $\overline{S} = S^{-1}$. □

Example 3.20. We show the effect of S^{-1} on a diagram of type $(3, 6)$

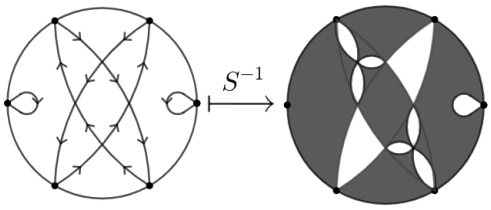

Figure 53

Remark 3.21. The inverse Scott map as defined above helps us determine that every diagram has a corresponding tiling, i.e. a tiling that maps to that diagram. However, the result is not always "clean", in the sense that it contains a lot of digons and hourglasses that we can simplify to obtain a cleaner result.

Example 3.22. Using the equivalences on tilings, we obtain the following tiling for the strand diagram of Example 3.20.

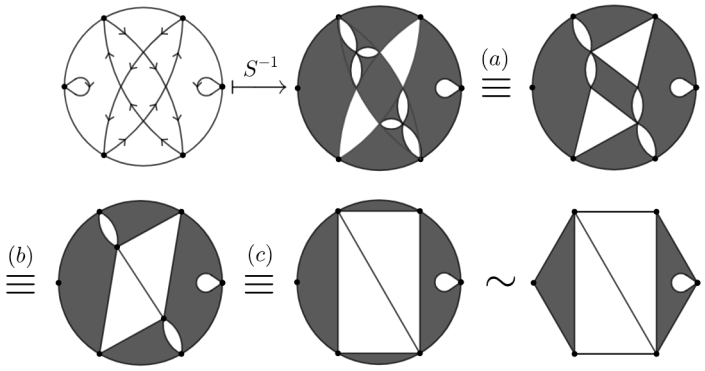

Figure 54

(a) We contract the two horizontal lenses to the left/right of the top-right/bottom-left white triangle, respectively.

(b) We contract the two vertical lenses to the bottom/top of the top-right/bottom-left triangle, respectively.

(c) We contract the two remaining lenses on the boundary.

Theorem 3.23. *[15][14.2, 14.4 -14.7] For any decorated permutation π, there is a Postnikov diagram Γ with permutation π .*

Theorem 3.24. *[7, 4.7] For any decorated permutation π, there is a tiling T whose permutation is π. Alternatively, any Postnikov diagram can be obtained as the image of a bicolored tiling by the Scott map.*

Proof. By Theorem 3.23, there is a Postnikov diagram Γ with permutation π for any decorated permutation π. If $T = S^{-1}(\Gamma)$, then $S(T) = S(S^{-1}(\Gamma)) = \Gamma$. And thus T maps to Γ by the Scott map and, by definition, T has permutation π. □

We will see in later Chapter how to obtain a tiling for a specifically given permutation, specifically one that maps to a Postnikov diagram.

Remark 3.25. We could skip diagrams altogether and define the type and permutation of tilings in the same vein as trips in plabic graphs [15, p.47]. If T is a reduced tiling with boundary vertices $\{1, \ldots, n\}$, we would define the *trip* at boundary vertex i is the oriented path p constructed by the boundaries of the tiles of T as follows.

1. We start at the vertex i. By convention, we consider the boundary segment between $i-1$ and i the last hyperedge traveled by the path, oriented towards i.

2. Any time we reach a vertex v, let e_1 and e_2 be the first and second edges clockwise (around v) from the last hyperedge that p traveled. Let f be the face between the e_1 and e_2. Then we add the boundary of f adjacent to e_2 to the path, oriented from v to the second endpoint u.

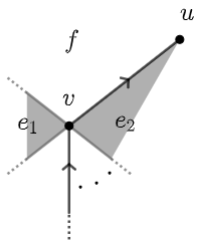

Figure 55

3. Once we reach a boundary vertex after our starting vertex i, the path is complete.

Any *trip* at a boundary vertex i arrives at a boundary vertex j. Then any tiling defines a permutation $\pi : i \longmapsto j$. For instance, the following tiling of type $(5, 8)$ has a trip starting at 1 and ending at 6. Thus its decorated permutation π maps $1 \longmapsto 6$.

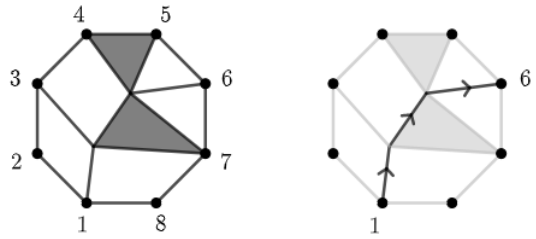

Figure 56

This construction does not give us new insights, and it is clear that a trip is just a strand (or cycle) that is drawn on the hyperedges rather than along the them. However, this can be used to define tilings entirely on their own, and can be used where discussing Postnikov diagrams would only be useful to define the type and permutation of a tiling, as is done in [6].

Now we are going to connect tilings to plabic graphs, which will be useful later. The construction was first introduced in [4, p.48] for the case of unicolored tilings (bicolored tilings whose hyperedges are all simple edges). The map naturally extends to the bicolored set-up.

Definition 3.26. [4, p.48] [8, 2.17] We define the *stellar-replacement map*

$$S : \mathbf{Til_n} \longrightarrow \mathcal{G}_\mathbf{n}, T \longmapsto G$$

such that

- Any vertex v of T is mapped to a white vertex $\Phi(v)$ of G.
- Any face f of T is mapped to a black vertex $\Phi(f)$ of G.
- If $v \in \partial f$, then there is an edge between $\Phi(v)$ and $\Phi(f)$ in G. In other words, any angle $\alpha \in A$ around v and in f is mapped to an edge $\Phi(\alpha)$ in G between $\Phi(v)$ and $\Phi(f)$.

· We draw a circle with n vertices labeled $1'$ to n' in clockwise order. These will be the boundary vertices of G. Then for any boundary vertex i in T, we add an edge from $\Phi(i)$ and i' in G.

Then the resulting construction is the plabic graph $\Phi(T)$.

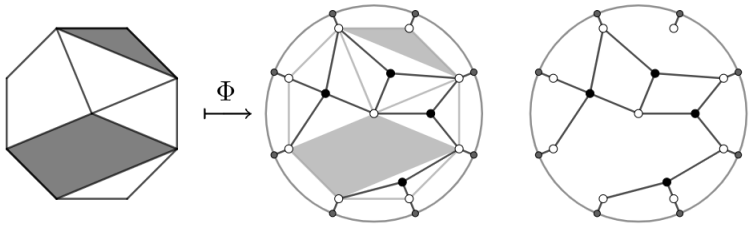

Figure 57

Remark 3.27. If T is a tiling and $G = \Phi(T)$ its corresponding plabic graphic, then mutating an edge in T corresponds to applying a square move (M1) to the plabic graph. A quadrilateral with one diagonal maps to a plabic graph as follows.

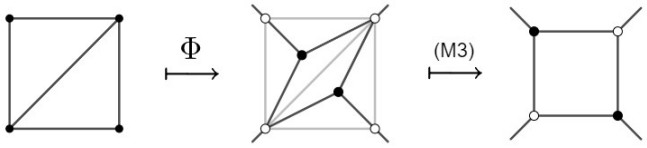

Figure 58

By symmetry, after flipping the diagonal, it maps to

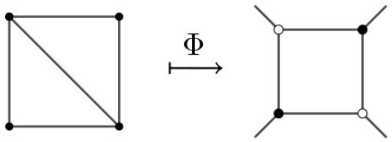

Figure 59

The two resulting plabic graphs are linked my a square move (M1).

After defining triangulations in Definition 1.4, we described how to map a triangulation to a quiver (which then generates the corresponding cluster algebra). We can imitate this process for bicolored tilings, and the same mapping rules apply: If T is a tiling, and Q the corresponding quiver, hyperedges (which includes black tiles) of T map to vertices of Q, and we add an arrow to any two consecutive hyperedges of a tile in T in counter-clockwise order. Boundary hyperedges of T once again map to frozen vertices of Q, and arrows between frozen vertices can be omitted.

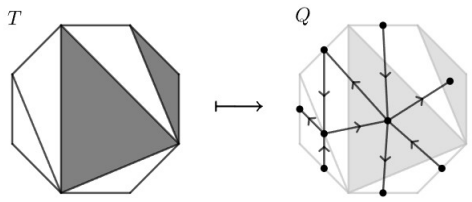

Figure 60

Note that internal m-edges, for $m \geq 2$, have m incoming and m outgoing arrows, alternating in their orientation.

Similarly to the setup of triangulations, flipping a simple edge in T is equivalent to mutating a vertex in Q. In the following example, we mutate the only simple edge on the left of the tiling.

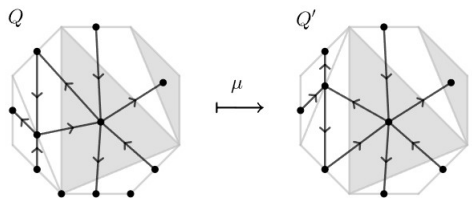

Figure 61

However, one must note that the inverse is not necessarily true. Some vertices in Q are also mapped from non-simple hyperedges in T, as is true for the black triangle in the center of the tiling above. That means that while we can mutate those vertices in Q, we still do not have a corresponding transformation for the black tiles in T. If we mutate the vertex in Q, the resulting quiver is not plane anymore, which means that tilings on their own can not fully describe all clusters of a cluster algebra.

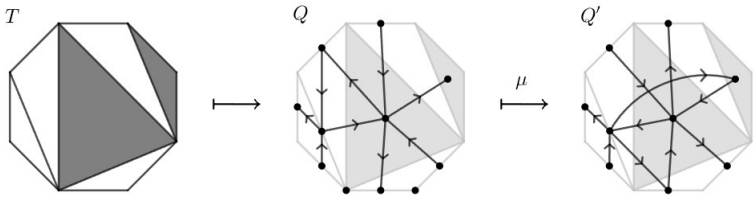

Figure 62

We will write A_T for A_Q, where Q is the quiver of the tiling T.

4 Examples of tilings

In this section, we are going to explore different classes of tilings. Triangulations of the n-gon and diagonal tilings will be the most basic form of reduced tilings, only containing simple edges. Rhombic tilings are a series of $(m+1, 2m)$-tilings that can be defined recursively. Quadrilateral tilings are reduced $\Gamma_{k,n}$-tiling, i.e. tilings of permutation $\pi : i \longmapsto i + k$, but can also be used to derive other tilings of same type (but different permutation). In the end, we will describe a way to generate a reduced tiling for any given permutation.

Before we go into those explicit examples, we first introduce composed tilings.

4.1 Composed tilings

Some tilings behave as if they were two separate tilings, in the sense that they contain two or more subtilings whose edges mutate independently of each other. Consider the following tiling T

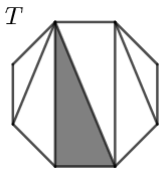

Figure 63

The middle black 3-edge is a boundary hyperedge and thus frozen. Furthermore, it separates T into two triangulations T_L and T_R.

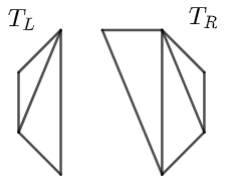

Figure 64

The internal edge of T_L mutates independently of the internal edges of T_R, and vice-versa. We may identify T with those two triangulations instead. More generally, any tilings which is separated by such a boundary 3-edge may be viewed as a *composition* of two smaller tilings.

Definition 4.1. Let T_L, T_R be two tilings. Let a, b be boundary hyperedges of T_L and T_R, respectively. The composition T of T_L and T_R along the boundaries a and b is the tiling obtained by concatenating T_L and T_R to a common 3-edge c along their boundary hyperedges a and b as follows.

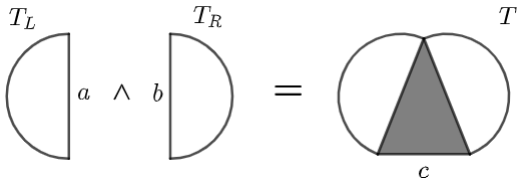

Figure 65

We denote $T = T_L \wedge_{a,b} T_R$, or simply $T = T_L \wedge T_R$ if the context allows it.

Naturally, we ask the question how separating a tiling into two smaller tilings translates into the behavior of the cluster algebras of the three tilings involved. The result is fairly straightforward.

Proposition 4.2. *Let $T = T_L \wedge_{a,b} T_R$. Then*

$$\mathcal{A}_T \cong \mathcal{A}_{T_L} \otimes \mathcal{A}_{T_R} \big/ (a \otimes 1 - 1 \otimes b)$$

Proof. Let c be the 3-edge that joins a and b in T. We label every other hyperedge in T the same as their counterpart in T_L or T_R. Let $x_e = \rho(e)$. Then we construct the map $\phi : T_L \otimes T_R \longrightarrow T, x \longmapsto \varphi(x)$ by setting

- $\varphi(x_e \otimes 1) = x_e$ for $e \neq a$
- $\varphi(1 \otimes x_e) = x_e$ for $e \neq b$
- $\varphi(a \otimes 1) = c$
- $\varphi(1 \otimes b) = c$

and extending φ linearly. Then, $\mathcal{A}_T \cong \mathcal{A}_{T_L} \otimes \mathcal{A}_{T_R} / \ker \varphi$, and $\ker \varphi = (a \otimes 1 - 1 \otimes b)$. □

Remark 4.3. From this point forward, we concern ourselves more with the subtilings that a tiling is composed of, rather than along which boundary edges we attach the subtilings are attached. In accordance with that, we may simplify the notation of composed tilings by omitting the boundaries, i.e. we simply write $T = T_L \wedge T_R$.

For the following two gluing constructions of tilings, we obtain similar results as Proposition 4.2.

1. We denote $T = T_L \,||\, T_R$ the tiling obtained by concatenating T_L and T_R to a common $4-$*edge*.

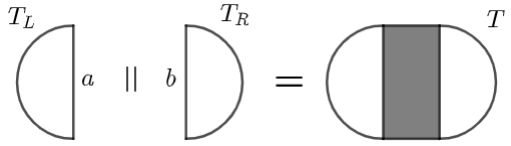

Figure 66

2. We denote $T = T_L \times T_R$ the tiling obtained by concatenating T_L and T_R to two common $3-$*edges* that form an hourglass, this time joining them along two consecutive boundary hyperedges a, c in T_L to two consecutive boundary hyperedges b, d in T_R.

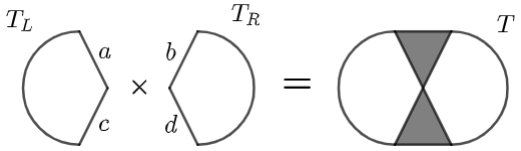

Figure 67

We call all three constructions *compositions* of T_L and T_R. Similarly to before, the two subtilings mutate independently from each other in the composed tilings T. And similarly, the cluster algebra of the composed tiling can be described as the quotient of the product of the two smaller algebras over some ideal.

Proposition 4.4. *Let $T = T_L \,||\, T_R$, along the hyperedges a and b. Then*

$$\mathcal{A}_T \cong \mathcal{A}_{T_L} \otimes \mathcal{A}_{T_R} \big/ (a \otimes 1 - 1 \otimes b)$$

Let $T = T_L \times T_R$, along the pair of hyperedges a, c and b, d. Then

$$\mathcal{A}_T \cong \mathcal{A}_{T_L} \otimes \mathcal{A}_{T_R} \big/ (a \otimes 1 - 1 \otimes b,\ c \otimes 1 - 1 \otimes d)$$

We omit this proof as it is analogous to the proof of Proposition 4.2.

4.2 Triangulations and diagonal tilings

The first class of tilings one considers are triangulations of n-gons, which we already discussed in the introduction. Triangulations are a special class of tilings of type $(2, n)$. Every simple edge is inscribed in a quadrilateral, thus we can mutate every edge throughout the entire mutation-equivalence class. That way, the tilings in the mutation class give us all the clusters of the cluster algebra associated to the tiling. The mutation-equivalence class of a triangulation consists of all the triangulations of that n-gon. We previously defined triangulations as maximal collections of non-crossing chords in a polygon. We may also describe them in the context of tilings.

Definition 4.5. A *triangulation* is a tiling with n boundary vertices and no internal vertices with $n - 2$ simple edges with no parallel edges, i.e. no edges share the same two endpoints. In other words, the tiles of the tiling are all triangles, and the only edges are diagonals.

The following proposition is found in [16, Cor. 2].

Proposition 4.6. *Triangulations are of type $(2, n)$ and of permutation $i \longmapsto i + 2$.*

Definition 4.7. A *diagonal* tiling is a tiling with n boundary vertices and no internal vertices with at most $n - 2$ simple edges with no parallel edges. In other words, all edges are diagonals of the polygon.

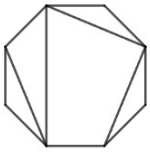

Figure 68

A triangulation is a diagonal tiling with a maximal number of edges. Any other diagonal tiling is obtained by removing diagonals from a triangulation. If a diagonal tiling has d diagonals, it has $d + 1$ faces. Thus the rank of a diagonal tiling is $k = n - d - 1$ by Proposition 5.7 below.

We previously noted that triangulations give us all the clusters of their corresponding cluster algebras. This is not necessarily true for all bicolored tilings. The reason is that we only have a way to mutate simple edges in a tiling, when internal edges between more than 2 vertices also map to non-frozen vertices in the corresponding quiver.

When it comes to diagonal tilings, we have a subset of such tilings that give us all clusters, namely all the diagonal tilings that can be expressed as a composition of triangulations. Consider, for instance, the following diagonal tiling:

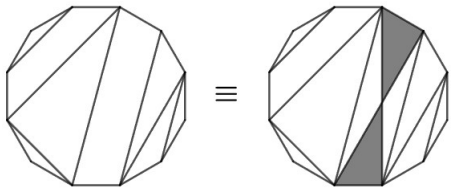

Figure 69

We can see that the left and right parts (from the hourglass) of the figure in the middle act independently of each other, as previously detailed in Section 4.1. Each part is in fact a smaller diagonal tiling. Thus the tiling can be expressed as a composition of two smaller diagonal tilings. By repeating this process, we can describe the diagonal tiling as a composition of smaller triangulations.

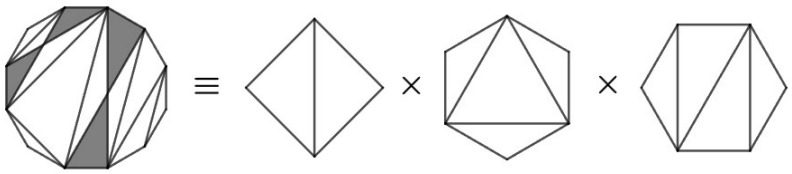

Figure 70

However, this is unfortunately not always possible. If we take the first figure in Definition 4.7, then some of the edges do not mutate independently. Consider the edges e and f as shown below. If we mutate e, f becomes a black triangle, and is thus locked from being mutated in the context of a tiling, while not being frozen when mapped to vertices in the corresponding quiver.

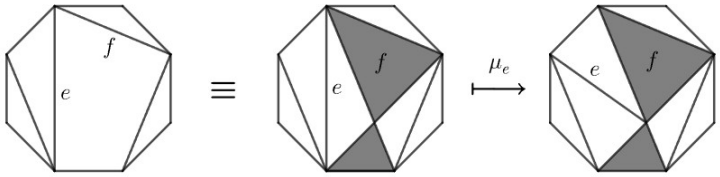

Figure 71

We insert an hourglass into the quadrilateral to flip edge e. But now f is black 3-edge, and cannot therefore not be flipped. However f is an internal edge, and maps to a non-frozen vertex in the corresponding quiver.

Thus, this tiling cannot be decomposed into triangulations. Generally, we can describe a diagonal tiling as a composition of two smaller diagonal tilings if one of the tiles has two non-adjacent boundary edges that are also boundary edges of the tiling (in other words, the tile has two non-consecutive frozen edges). In that case, we can inscribe an hourglass into that tile that divides the tiling into two parts. If we can repeat this process, the tiling can be described as a composition of triangulations, and its flip-equivalence class gives us all the clusters of the corresponding cluster algebra.

If on the other hand, a tiling has a tile of size 3 or more, and that tile has 2 consecutive boundary edges e, f that are interior edges of the tiling (in other words, 2 consecutive mutable boundary edges), then mutating e requires inscribing an hourglass into the tile that transforms f into a black triangle, and thus does not allow it to be mutated. In that case, the tiling cannot be described as a composition

of triangulations, and its flip-equivalence class does not give us all the clusters of the corresponding cluster algebra.

4.3 Rhombic tilings

Rhombic tilings are a class of tilings of type $(m+1, 2m)$ for $m > 1$ that can be defined recursively. Rhombic tilings have the property that certain sequences of mutations generate a local transformation that resembles that of a Yang-Baxter move. To define rhombic tilings we start with the base case.

Definition 4.8. The *rhombic tiling* of type $(3, 4)$ is the diagonal tiling of type $(3, 4)$ with no diagonals, i.e. a square with no internal vertices or hyperedges.

Definition 4.9. Let T be a rhombic tiling of type $(m+1, 2m)$. We define a rhombic tiling T' of type $(m + 2, 2(m + 1))$ as follows:

- Rotate and redraw T such that the boundary vertices 1 and $m+1$ are positioned at the top and bottom respectively.
- Draw a copy of the boundary of T between 1 and $m + 1$ outside the boundary disk of T parallel to the original boundary segment, and label the copied vertices $1'$ to $(m + 1)'$.
- For each $1 \leq i \leq m + 1$, connect the vertices i and i'.
- The resulting tiling has $2m + 2$ boundary vertices. Finally, relabel the new boundary vertices $1, \ldots, 2m + 2$.

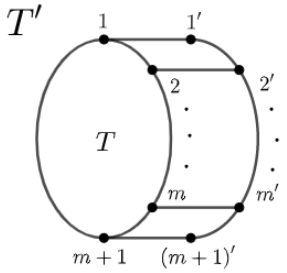

Figure 72

Then the resulting tiling is the rhombic tiling T' of type $(m + 2, 2(m + 2))$.

Remark 4.10. We denote $\tilde{R}_m$ the constructed rhombic tiling of type $(m+1, 2m)$.

Example 4.11. The rhombic tilings $\tilde{R}_2$, $\tilde{R}_3$, $\tilde{R}_4$ are as follows.

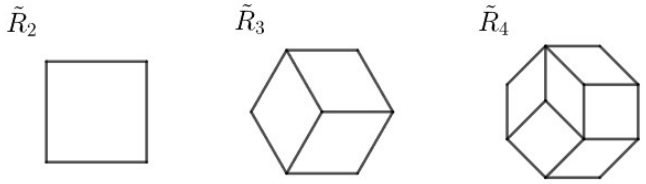

Figure 73

Lemma 4.12. The rhombic tiling $\tilde{R}_m$ has a matching (Definition 5.1).

Proof. We prove this by induction on m. The tiling $\tilde{R}_2$ has a trivial matching given by the choice of any of its four angles. Let $\tilde{R}_m$ be a rhombic tiling with matching x. When constructing $\tilde{R}_{m+1}$, we add exactly m faces $f_1, \ldots, f_m$ such that each top left vertex of f_i is the boundary vertex i of $\tilde{R}_m$, and the top right vertex of f_i is the new parallel vertex i'. We construct a matching x' of $\tilde{R}_{m+1}$ as follows

- If i is matched in x, then i is matched to the same face in x'.
- If i is not matched in x, then i is matched to f_i in x'.
- For any remaining f_i that is not matched yet, match f_i to i' in x'.

Then x' is a matching of $\tilde{R}_{m+1}$. Thus, by induction, all rhombic tilings $\tilde{R}_m$ have a matching. □

Example 4.13. If we start with a matching of $\tilde{R}_3$, we obtain a matching of $\tilde{R}_4$ as follows.

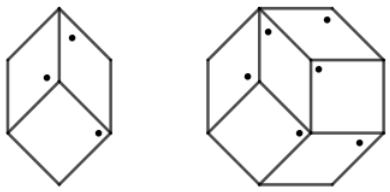

Figure 74

Proposition 4.14. *The rhombic tiling $\tilde{R}_m$ is indeed a tiling of type $(m+1, 2m)$.*

Proof. R_2 is of type $(3, 4)$. Assume that $\tilde{R}_m$ is of type $(m+1, 2m)$. While constructing $\tilde{R}_{m+1}$, we add $m+1$ new boundary vertices $1', \ldots, (m+1)'$. At the same time the $m-1$ vertices $2, \ldots, m$ become internal vertices in $\tilde{R}_{m+1}$. Thus the total number of boundary vertices of $\tilde{R}_{m+1}$ is $2m + (m+1) - (m-1) = 2(m+1)$.

Meanwhile, when going from $\tilde{R}_m$ to $\tilde{R}_{m+1}$ we add m faces and $m+1$ vertices. Since $\tilde{R}_{m+1}$ has a matching by Lemma 4.12, the rank of $\tilde{R}_{m+1}$ is the difference between vertices and faces, which goes up by 1 compared to the difference in $\tilde{R}_m$. Thus the rank is $m+1+1 = m+2$.

Thus $\tilde{R}_{m+1}$ if of type $(m+2, 2(m+1))$. The result follows by induction. □

Example 4.15. We consider the rhombic tiling $\tilde{R}_3$ and label its internal edges e_1, e_2, e_3.

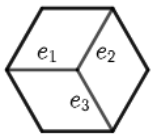

Figure 75

We denote the mutation $\mu_i := \mu_{e_i}$ for any i. Then mutating the edges e_1, e_2, e_3, e_1 in succession in that order applies a transformation to the initial tiling that resembles a Yang-Baxter move. We can do this by inserting hourglasses when necessary to flip an edge as we now show step by step.

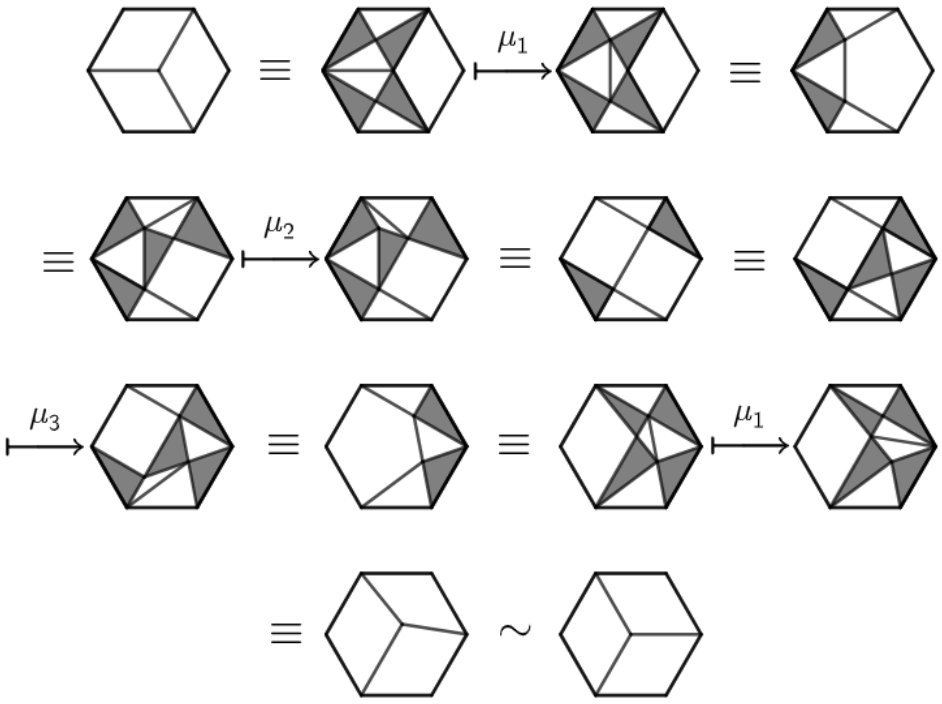

Figure 76

We can do the same procedure as in Example 4.15 to any such subtiling $\tilde{R}_3$ of a rhombic tiling $\tilde{R}_m$, i.e. whenever we have three rhombi sitting together at an internal vertex, we can rotate them inside the hexagon they span. This also means that the orientation of a tiling $\tilde{R}_m$ does not matter when using it to construct the next tiling $\tilde{R}_{m+1}$ since we treat the tilings up to mutation-equivalence. The class of rhombic tilings of type $(m+1, 2m)$ up to a Yang-Baxter move is denoted R_m.

Remark 4.16. This is not the only sequence of mutations that generates this transformation. The second tiling in the mutation sequence above $(\mu_2 \circ \mu_1)$ is an example of a quadrilateral tiling (up to isotopy) (Section 4.4).

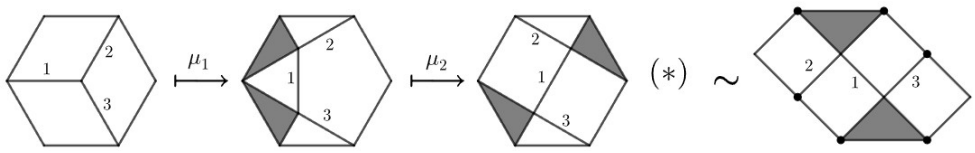

Figure 77

Using Remark 4.21, we can mutate that tiling $(*)$ such that it rotates or mirrors itself. Then we can mutate it back into the original form of a rhombic tiling. Doing so in different ways gives us different sequences of mutations that result in a Yang-Baxter move the identity. The difference between the different sequences is how edge individually evolves within the tiling.

For instance, in the first example above ($\mu_1 \circ \mu_3 \circ \mu_2 \circ \mu_1$), the edges move inside the tiling as follows.

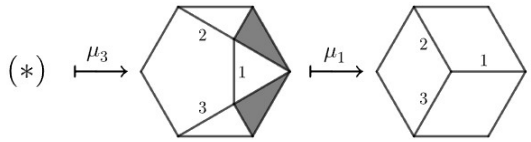

Figure 78

Whereas if we take the the sequence $\mu_{e_1} \circ \mu_{e_3} \circ \mu_{e_1} \circ \mu_{e_2} \circ \mu_{e_1}$, we obtain the same final transformation, but the edges within the tiling move to different locations.

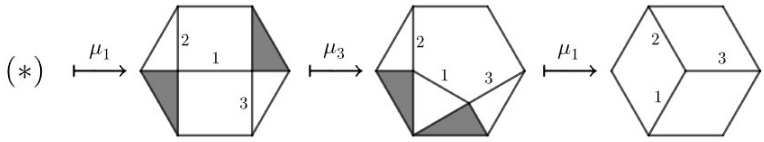

Figure 79

On the other hand, we can also find sequences that result shuffle around the mutable edges, such $\mu_1 \circ \mu_2 \circ \mu_1 \circ \mu_2 \circ \mu_1 = \mathrm{id}$.

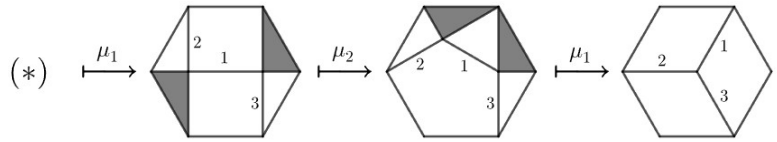

Figure 80

4.4 Quadrilateral tilings

The quadrilateral arrangements in [16, p.17-20] are Postnikov diagrams defined recursively, by starting with the base case of a $(2, n)$-diagram and adding rows of strands to increase n. We define a similar construction for tilings. We could use the same recursive procedure, but we can also directly obtain the maximal quadrilateral tiling for a given type (k, n), i.e. a tiling made out of quadrilaterals (almost) with maximum dimension for that type (and corresponding to the positroid cell in $Gr_{k,n}$ of highest dimension (Proposition 5.23)). We explain this now. Consider the following mesh in $\mathbb{R}^2$.

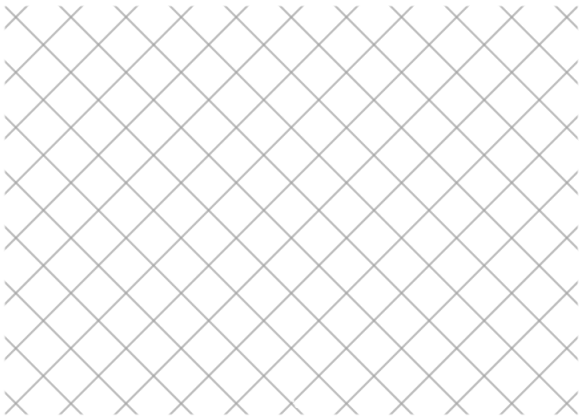

Figure 81

The mesh cuts the plane into squares, which can be divided into columns, with each column consisting of a square and all the squares that lie exactly above or below it (left figure shades one such column). Similarly we define the rows of the mesh (right figure).

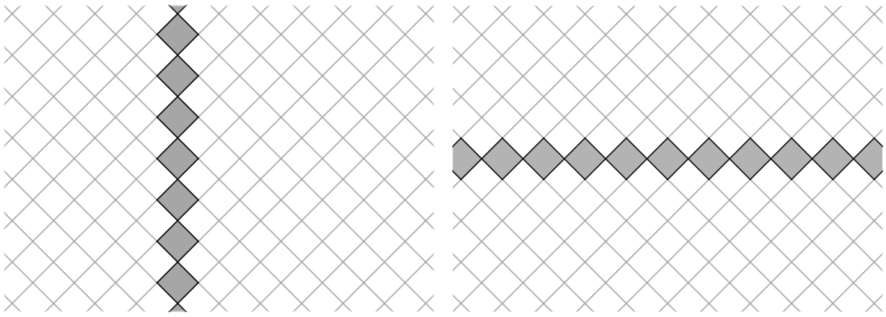

Figure 82

Let $k, n \in \mathbb{N}$, with $1 < k < n$. We cut out a rectangle of size $k \times (n-k)$ from the mesh, with k being the number of columns delimited by the rectangle, and $n-k$ being the number of rows. The bottom left corner of the rectangle sits in the center of one of the squares.

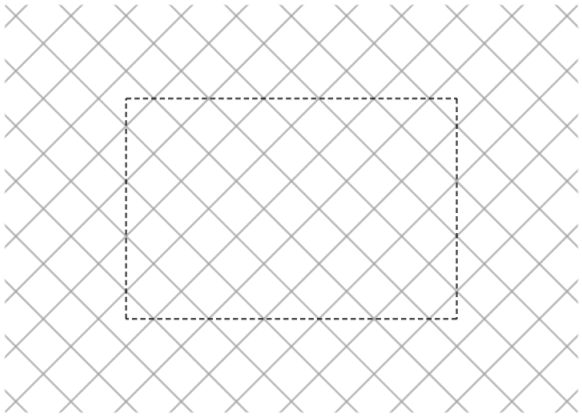

Figure 83

The mesh now prescribes the tiles we get from the rectangle. Any square that is entirely within the rectangle is a tile. Any half of a square of the mesh that is on the top or bottom border of the rectangle is a 3-edge between the three vertices of that triangle. The remaining half-squares on the side borders are ignored. We set the vertices of the tiling to be the minimum set of vertices required such that the resulting object is a tiling, i.e. anywhere where more than 3 hyperedges coincide. This construction defines a tiling $T_{k,n}$ for any $k, n \in \mathbb{N}$ with $1 < k < n$, called the

maximal quadrilateral tiling for (k, n). In our example, we obtain the tiling $T_{11,18}$. Later we will define *quadrilateral tilings* more generally in Definition 4.24.

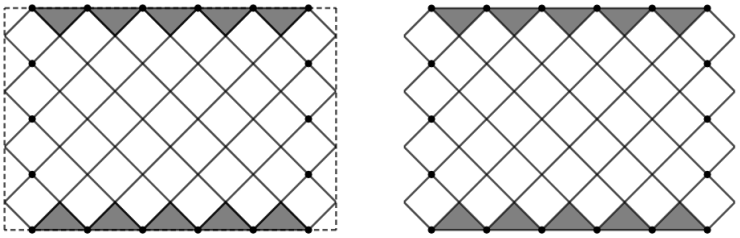

Figure 84

Remark 4.17. Instead of fixing the bottom left corner to be in the center of one of the squares, we can also choose it to be on a corner/crossing of the mesh. This produces a different quadrilateral tiling with the same number of columns and rows. We denote this tiling $T'_{k,n}$.

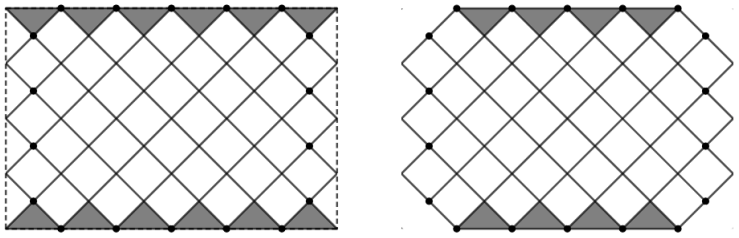

Figure 85

We will prove a list of properties for $T_{k,n}$ and $T'_{k,n}$. The proofs detail the case for $T_{k,n}$, but similar reasoning applies to $T'_{k,n}$.

Lemma 4.18. For any (k, n) with $1 < k < n$, $T_{k,n}$ and $T'_{k,n}$ have a matching.

Proof. In any quadrilateral $T_{k,n}$, choose the bottom angle. Then any face is matched, and any vertex is matched other than the boundary vertices that are adjacent to 3-edges on the half-row of the figure. Thus $T_{k,n}$ has a matching. □

Proposition 4.19. *For any* (k, n) *with* $1 < k < n$, $T_{k,n}$ *and* $T'_{k,n}$ *are of type* (k, n).

Proof. In the matching mentioned in Lemma 4.18, the only vertices not matched are the boundary vertices on the top half-row of $T_{k,n}$ adjacent to the black 3-edges of $T_{k,n}$. There are exactly as many such vertices as there are columns in $T_{k,n}$, i.e. k such vertices. Hence, the rank of the tiling is $|V| - |F| = k$. □

Proposition 4.20. *For any (k, n) with $1 < k < n$, $S(T_{k,n})$ and $S(T'_{k,n})$ are $\Gamma_{k,n}$-diagrams, i.e. the corresponding permutation is $i \mapsto i + k$.*

Proof. □

Let us consider the quadrilateral tiling $T = T_{4,8}$. The internal edges of T can be partitioned into two sets E^+ and E^-, with the edges in each set being parallel to one another in our embedding of T. We choose E^+ to be the internal edges that go from the top left to the bottom right, and E^- the internal edges that go from the bottom left to the top right.

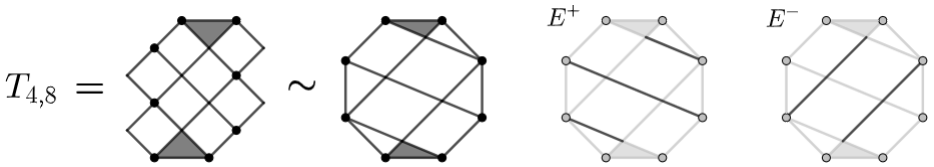

Figure 86

The edges in E^+ mutate independently of each other, and so do the edges in E^-. We can therefore mutate all edges in E^+ in any order, in other words, the mutations μ_e for $e \in E^+$ commute. The same goes for E^-. Let μ_{E^+} and μ_{E^-} be the sequences of mutations $\prod_{e \in E^+} e$ and $\prod_{e \in E^-} e$, respectively. Then the mutations μ_{E^+} and μ_{E^-} lead to the following transformations

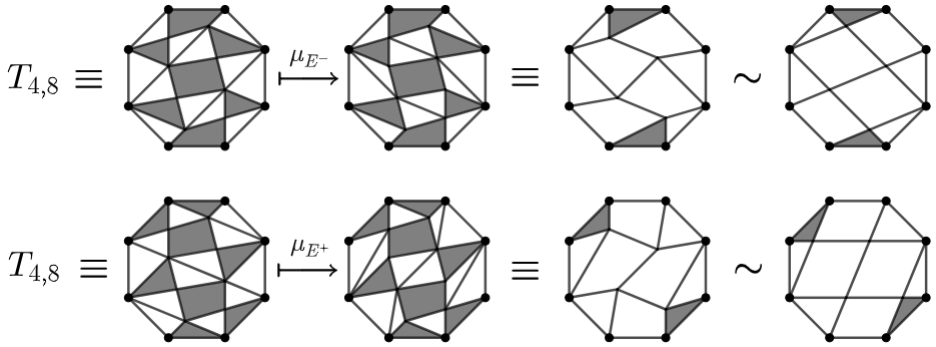

Figure 87

It seems like T flips along a different axis. If we take a look at $T_{3,6}$, we see a slightly different transformation.

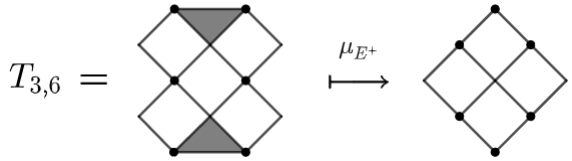

Figure 88

Instead of flipping the tiling, it seems as if we obtained version $T'_{3,6}$ (a rotated version, if we labeled the boundary vertices). This suggests that we may obtain the transformed tiling by moving the initial tiling horizontally in the mesh that we previously used to defined it on.

Let's consider the same mesh, but remove the parts above and below the mesh, only focusing on the horizontal strip in which the tiling lies. Let us label the vertices on the bottom line by cycling through $\{1, \ldots, n\}$ in a descending order, starting with 1 as the bottom left vertex of the tiling. For our example, $T = T_{5,8}$.

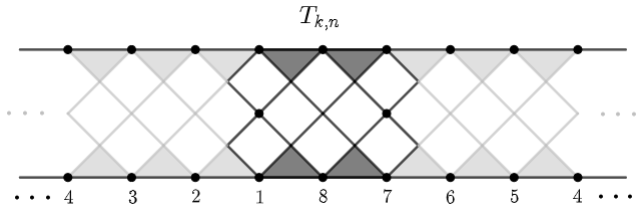

Figure 89

Then $\mu_{E^+}(T)$ is the tiling obtained by shifting T by one column to the right, and $\mu_{E^-}(T)$ is the tiling obtained by shifting T by one column to the left, and labeling the vertices $\{1, \ldots, n\}$ in a clockwise orientation, starting with the vertices on the bottom lattice of the tiling as given by the labels on the bottom of the mesh.

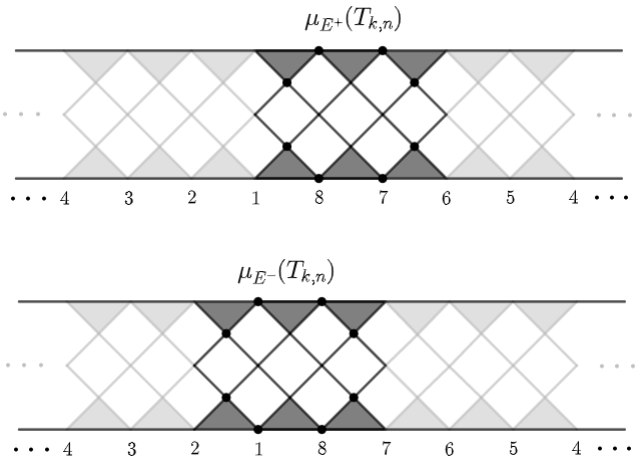

Figure 90

Remark 4.21. If (k, n) are both even, e.g. $(4, 8)$, this will then look like mirroring the tiling (if we disregard the labels). And mutating any quadrilateral tiling in the same direction twice yields a rotation of the tiling.

Using this, we may obtain the different sequences of Remark 4.16. First we mutate the tiling to its quadrilateral form by mutating the edges e_1 and e_2 (any two distinct edges would work and would return either $T_{4,6}$ or $T'_{4,6}$ up to rotation of its boundary vertices).

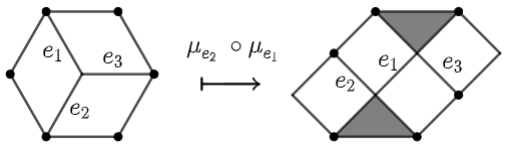

Figure 91

Now we rotate, or mirror the tiling as often as we want. And finally, we mutate the tiling back to its rhombic appearance. By experimenting with possible combinations to obtain a Yang-Baxter move that way, we get the sequences of mutations described in Remark 4.16.

The tiling $T_{k,n}$ gives us the tiling of type (k, n) whose permutation is $\pi : i \longmapsto i+k$ mod n. It is associated to the positroid cell of maximum dimension in $Gr_{k,n}^{\geq 0}$, with its dimension being $k(n-k)$. In [8, 5.3-5.7] we described a way to find tilings of lower dimension. From the quadrilateral tiling $T_{k,n}$, we can derive several tilings of the type (k, n) of lower dimension. Consider the tiling $T = T_{7,12}$

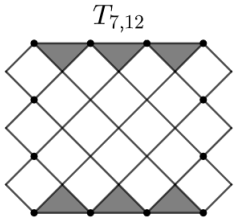

Figure 92

We construct two new tilings T_1, T_2, and T_3 by cutting one or more full diagonal lines of quadrilaterals on the boundary of T, such that the number of columns and row does not change.

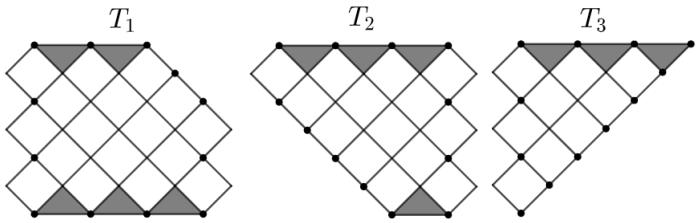

Figure 93

Then T_1 and T_2 are of type $(7, 12)$ as well, but of different permutation and of lower dimension. We do not necessarily need to cut off an entire diagonal. Instead, we can "fold" a boundary tile over itself or "collapse" its boundary vertex onto its opposite vertex and obtain a new tiling of the same type, but lower dimension.

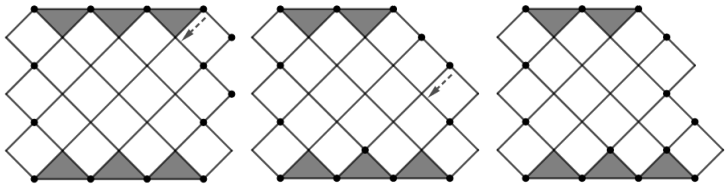

Figure 94

Cutting off a diagonal line of quadrilaterals can be achieved by removing individual tiles in succession. More generally, we describe the following transformations

(D1) If we have three boundary vertices in a quadrilateral, with one vertex v being of degree 2 (vertex on top in the figure below), and the vertex opposing v is not on the boundary of the tiling, then we remove the quadrilateral by removing the two edges incident to v. In doing so, the vertex opposite to v becomes a boundary vertex

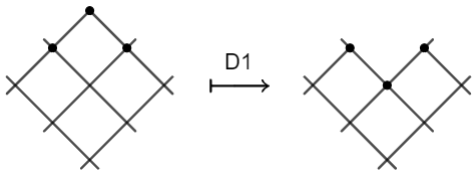

Figure 95

(D2) Same as (D1), except the tile adjacent to the removed quadrilateral is a 3-edge.

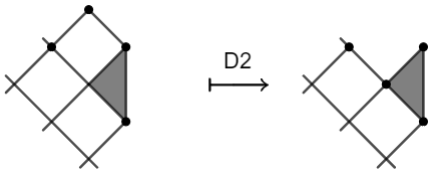

Figure 96

(D3) Similar to (D1), but the quadrilateral is a tile of size 3, and we also remove one of the boundary vertices.

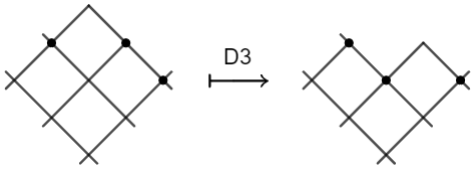

Figure 97

(D4) Same as (D3), except the tile adjacent to the removed quadrilateral is a 3-edge.

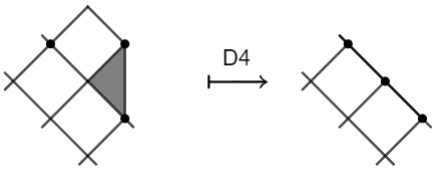

Figure 98

Lemma 4.22. Let T be a tiling obtained by applying a finite sequence of transformations (D1)−(D4) on $T_{k,n}$. Then T has a matching.

Proof. The result is straightforward. We shall give the reasoning for the case of D1, the remaining cases are similar. Let T be the tiling obtained from $T_{k,n}$ after D1. Let m be a matching of $T_{k,n}$. Let u be the internal vertex in $T_{k,n}$ that becomes a

boundary vertex after D1, f be the face we remove with D1, and α the angle in f around u. If f is matched to u in m, i.e. $\alpha \in m$, then $m \setminus \alpha$ is a matching of T, as u is now a boundary vertex and does not need to be matched. If f is not matched to u in m, then there is some other angle $\beta \neq \alpha$ in f such that $\beta \in m$, with β being around one of the three boundary vertices on the boundary of f. Then $m \setminus \beta$ is a matching of T. Thus, either way, T has a matching.

A similar reasoning applies to D1-D4. Then, the reasoning applies recursively to a finite sequence of transformations D1-D4. □

Lemma 4.23. Let $T = T_{k,n}$. The transformations (D1)−(D4) return a new tiling T' of type (k, n) with $\dim T' < \dim T$.

Proof. By Lemma 4.22, T' has a matching. In (D1)−(D4), the number of vertices removed is 1, and the number of faces removed is 1, thus the rank remain constant. The number of boundary vertices also remains constant. Thus the type remains constant. The number of hyperedges are reduced in all cases, thus the dimension of the associated positroid cell is reduced as well. □

We can define quadrilateral tilings recursively, by starting with the tilings $T_{k,n}$ of maximum dimension defined at the beginning of this section and generating more tilings by either mutating already existing quadrilateral with μ_{E^+} or μ_{E^-}, or with the transformations (D1)−(D4).

Definition 4.24. A tiling T is *quadrilateral* if it satisfies either of the following conditions

(i) $T = T_{k,n}$ for some $1 < k < n$.

(ii) $T = \mu_{E^+}(T')$ or $T = \mu_{E^-}(T')$ for some quadrilateral tiling T' of maximal dimension.

(iii) T is obtained by applying a transformation among (D1)−(D4) to another quadrilateral.

Example 4.25. If we take $T_{4,7}$ and apply some of the above transformations, we obtain some of the quadrilateral tilings of type $(4, 7)$ as follows.

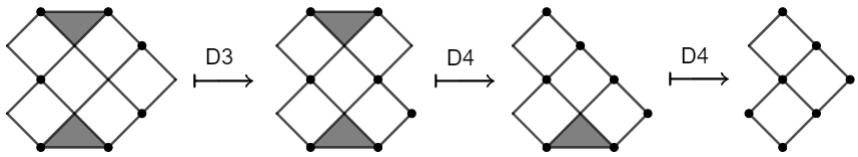

Figure 99

4.5 Loops, shifts, and other useful tilings

Until now, we have mostly ignored permutations of tilings in this section. We now want to explore ways to generate tilings for several permutations. To so, we need to construct tilings whose permutations and diagrams have fixed points and loops, respectively, as well as tilings with permutation $i \longmapsto i+1$. We first note that a simple n-gon with no internal hyperedges gives us the permutation $i \longmapsto i-1 \mod n$ for all i.

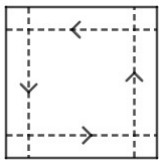

Figure 100

We obtain the dual version of that as follows.

Definition 4.26. The n-antigon is the tiling with n boundary vertices $\{1, \ldots, n\}$, one internal vertex v, and hyperedges $(i, v, i+1)$ for each i (with the convention that $n+1 = 1$). In other words, we align n tiles of size 2 around v, such that the other endpoint of each such tile is a different boundary vertex. We denote the n-antigon by P_n^*.

Example 4.27. The 4-antigon P_4^* looks as follows.

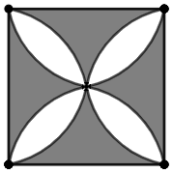

Figure 101

Proposition 4.28. *The n-antigon is a tiling of type $(1, n)$ with permutation $i \longmapsto i+1$.*

Proof. A matching of P_n^* is given by choosing any one of the n faces and matching it to internal vertex, then matching the remaining faces to the boundary vertex

they are adjacent to. P_n^* has $n+1$ vertices and n faces, hence the rank of P_n^* is $k = n+1-n = 1$, and the type is $(1, n)$. It is easy to verify that each strand originating in i ends in $i+1$, thus the permutation is $i \longmapsto i+1$. □

Next, we are looking at fixed points of decorated permutations, which in terms of strands appear in two forms: clockwise loops and counter-clockwise loops.

Definition 4.29. We say that a tiling T has a *loop* at its boundary vertex i if there is a hyperedge e such that (i, i) is a subsequence of e. In other words, there is a tile of size 1 at the boundary vertex i. We say that T has a *co-loop* at v if there is a hyperedge e such containing the subsequence $(i-1, i, i+1)$. In other words, the vertex i is not adjacent to any face.

Example 4.30. The following tiling of type $(3, 6)$ has a loop at the boundary vertex 6 and a co-loop at 3.

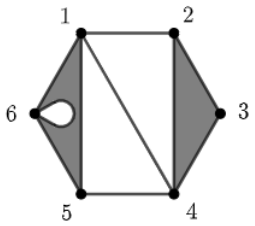

Figure 102

Proposition 4.31. *If T has a loop or co-loop at i, then in the permutation π of T, we have $i \longmapsto i$, with its strand being a counter-clockwise or clockwise loop, respectively.*

Example 4.32. Using this, we can construct all the tilings of type $(2, 4)$ and their permutations (up to rotation). We list them here grouped by the dimension of the corresponding positroid cell (Definition 2.12).

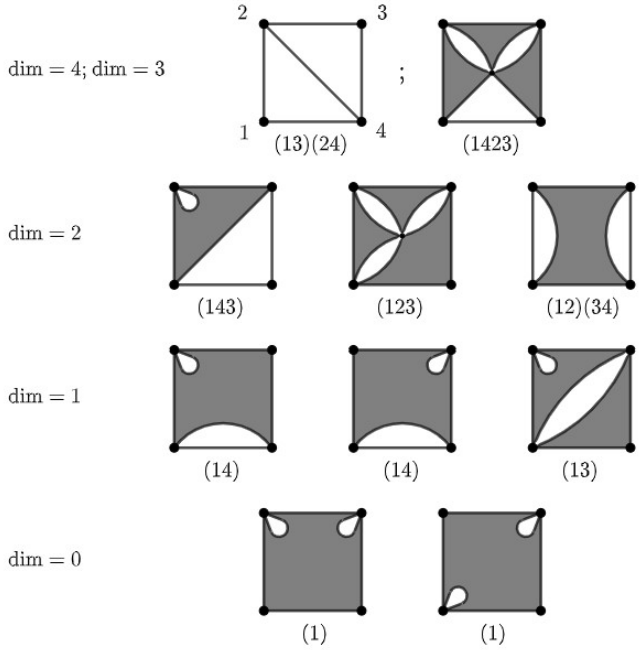

Figure 103

4.6 Tilings of any type and permutation

In this last part, we will finally introduce a way to generate tilings for any permutations. For simplicity, we are going to omit the decoration of the permutation, i.e. we are going to ignore the coloring of the fixed points of the permutation. Given that the difference between either coloration is the addition or removal of a loop (a white 1-gon) on the boundary of the corresponding fixed point, the procedure to generate decorated permutations is the same, with the addition of adding loops to some of the boundary vertices that correspond to fixed points of the permutation.

We take a look at the following tiling T and its corresponding Postnikov diagram $\Gamma = S(T)$, or permutation $\pi = (13524)$.

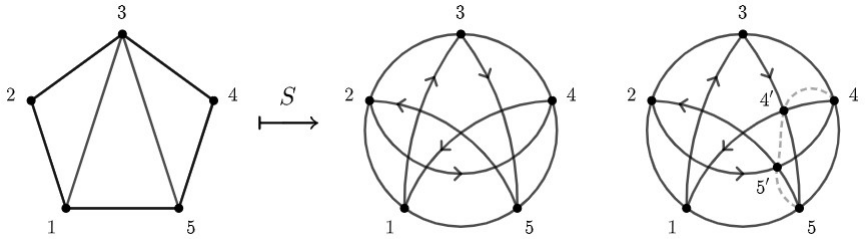

Figure 104

The diagram can be divided into two parts, indicated by the dotted line. The dotted line goes through two intersection points of the strands of the diagram that we label $4'$ and $5'$. Then we may see the left part as a diagram with 5 boundary vertices $1, 2, 3, 4', 5'$. If we drop the dashes on $4'$ and $5'$, permutation of that diagram is $\sigma = (134)(25)$. The corresponding diagram would be

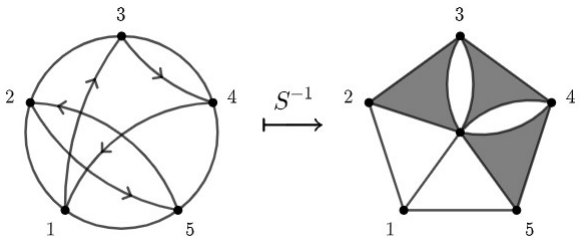

Figure 105

And we have $\pi = (45)\sigma$. For the part of the diagram to the right of the dotted line, we have the tiling with boundary vertices $4, 5, 5', 4'$ as follows.

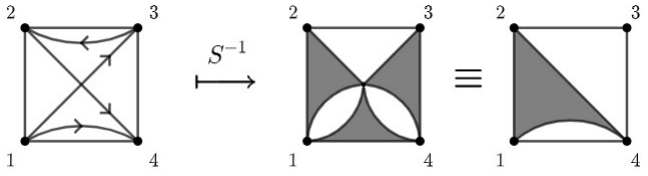

Figure 106

We can connect the two tilings into a tiling of a pentagon, by gluing them together along the border between vertices $4'$ and $5'$, and completing the areas between $3, 4, 4'$ and $1, 5, 5'$ with a black triangle each. The resulting tiling is equivalent to the initial triangulation.

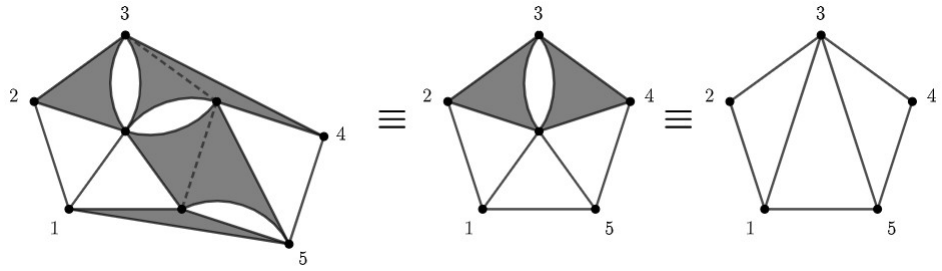

Figure 107

With this in mind, we can develop a general method to describe a tiling for any permutation by first writing the permutation of transpositions between adjacent vertices, i.e. transpositions of the form $(i \;\; i+1) \mod n$.

We describe a transformation of a tiling with T with n boundary vertices $1, \ldots, n$ as follows.

(i) We start with an empty n-gon with vertices labeled $1, \ldots, n$.

(ii) We add an internal vertex i', preferably drawn near the boundary vertex i (given that we treat tilings up to isotopy, the exact position of i' does not matter).

(iii) We add an edge between i' and $i+1$, and replace the boundary edge $[i-1, i]$ with a boundary hyperedge between $i-1, i, i'$. In other words, we will have a black triangle with endpoints $i-1, i, i'$, and a white triangle with endpoints $i', i, i+1$.

(iv) We fill the n-gon with boundary vertices $1, \ldots, i-1, i, i+1, \ldots, n$ with the tiling T, gluing the boundary segments $[l, l+1]$ of T with the boundary segments of the n-gon labeled the same way (treating i' as if it was the vertex i of that n-gon).

Then the denote the resulting tiling $\tau_i(T)$.

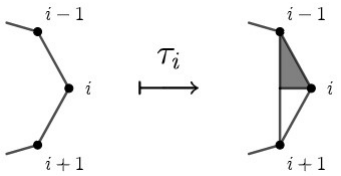

Figure 108

The following proposition is easy to verify by applying the Scott map locally on the boundary between T and the double triangle we constructed.

Proposition 4.33. *If a tiling T is of permutation π, then $\tau_i(T)$ is of permutation $(i\ \ i+1)\,\pi$.*

If we write a permutation in the form $\pi = \tau_{i_1} \cdot \cdots \cdot \tau_{i_m}$, we can use the above construction m times to generate a tiling with permutation π.

Example 4.34. Let $\pi = (14)(356) = (34)(45)\sigma$ with $\sigma = (134)(56)$. Then a tiling with permutation σ is

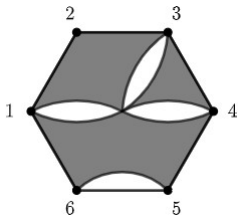

Figure 109

Then we use the above steps for τ_3 and τ_4 inwards in that order:

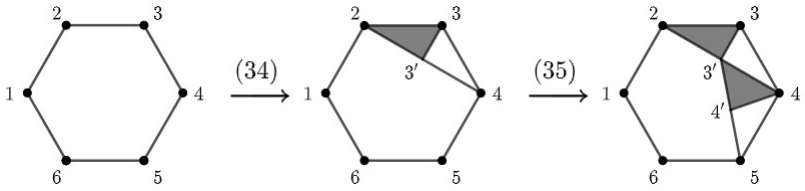

Figure 110

And finally we fill the remaining space with the tiling T' for σ, returning the tiling $T = \tau_3(\tau_4(T'))$ with permutation $\pi = \tau_3\tau_4\sigma$:

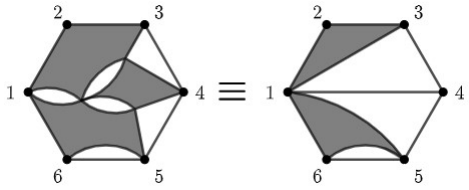

Figure 111

Furthermore, T is reduced.

Next, we want to find a way to write the permutation as a product of adjacent transpositions. Ideally, we want to generate only reduced tilings. To facilitate this, we define two reductions given by the figures below

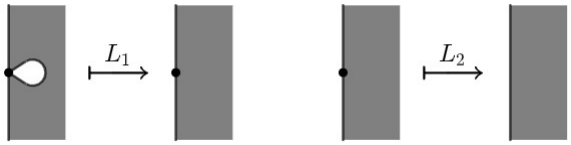

Figure 112

These will come in handy in cases where the new vertex i' does not attach to any other hyperedge, as well as when the tiling with permutation σ has a white 1-gon. In Example 4.34, we gave the permutation written in the form that we needed it. But depending on how we write the permutation, we may obtain a tiling with the right permutation, but that is not reduced.

Example 4.35. We write $\pi = (16)(34)(56)(16)\sigma'$ with $\sigma' = (13)(456)$. Then the above procedure returns the non-reduced tiling and corresponding diagram as follows:

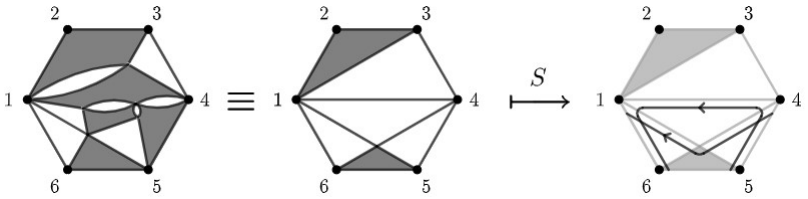

Figure 113

To understand why we obtain this, we can look at the *permutation diagram* of π and how it evolves during the process.

Definition 4.36. Let π be a decorated permutation of $\{1, \ldots, n\}$. Let D_n be the disk with distinct boundary vertices $1, \ldots, n$ in clockwise order. Then the permutation diagram of π is the collection of n arrows γ_i that have i as tail and $\pi(i)$ as head. If i is a fixed point, γ_i is a loop.

Example 4.37. The permutation diagram of $\pi = (14)(356)$ is

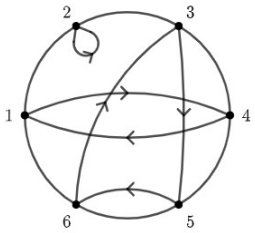

Figure 114

When we perform a transpositions π_i, what happens is that the arrows whose target vertices are i and $i+1$ swap those targets. Let us call these arrows α_a and α_b, so $\pi(a) = i$ and $\pi(b) = i+1$. Then when we cross/uncross α_a and α_b, the corresponding strands in the strand diagram γ_a and γ_b intersect. Thus, if two such arrows cross/uncross multiple times, this will lead to a bad double crossing in the strand diagram, making the tiling not reduced. Equally, if we cross two arrows, and those two arrows remain crossed in the final permutation σ as part of the same cycle, then there will be at least two intersection between the corresponding strands in the same direction, thus, again, creating a double crossing. In Example 4.35, two arrows behave that way, namely α_4 and α_5 (the dashed and dotted arrows, respectively).

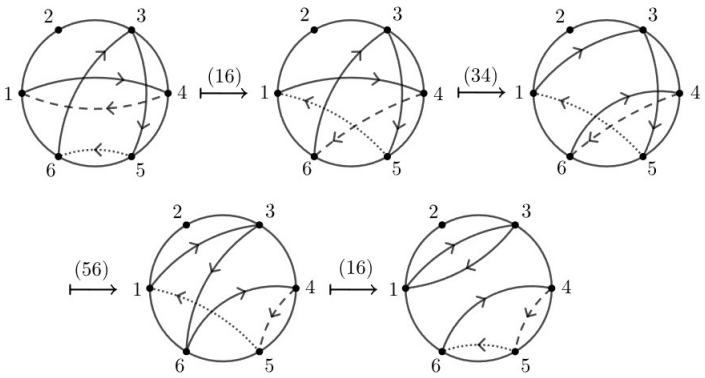

Figure 115

Thus, to write a permutation as $\pi = \tau_{i_1} \cdots \tau_{i_m} \sigma$ such that using the above procedure returns a reduced tiling, we may use the permutation diagram of π and uncross arrows with neighboring target vertices $i, i+1$, avoiding creating new crossings.

Example 4.38. Let $\pi = (14)(356)$. Then we can use the permutation diagram to uncross arrows until we obtain a permutation whose tiling we can easily derive.

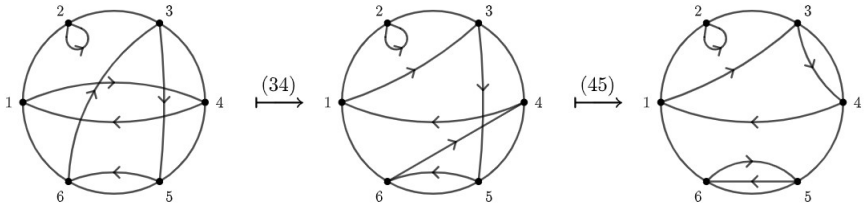

Figure 116

We write $\pi = (34)(45)\sigma$, with $\sigma = (134)$. This gives us the correct way of writing this permutation as shown in Example 4.34.

Remark 4.39. When we uncross the permutation diagram, it is sufficient to do so until no arrows cross other than on the boundary of the disk. In other words, the collection of arrows is made up of isolated cycles. Then the tiling for those cycles is easy to derive; the tiling for clockwise oriented cycles is given in Definition 4.26, while the tiling for a counterclockwise cycle with m vertices is an empty m-gon.

Alternatively, we can uncross arrows until all arrows are loop, leaving us with the identity as the tiling to fit into the center of our construction. The tiling for the

identity with m boundary vertices (ignoring the orientation of the fixed points) is a black m-gon. For $m = 4$ we have

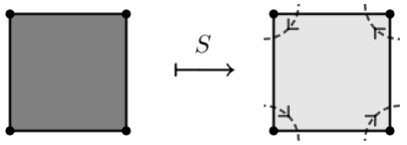

Figure 117

The method described so far assumes that we can always find neighboring arrows that cross while uncrossing the permutation diagram. That is, however, not always given. For instance, the permutation diagram of $\pi = (15)(37)$ with 8 vertices looks as follows

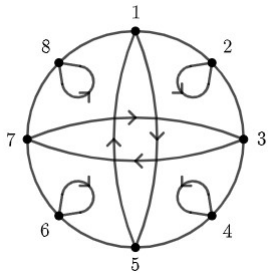

Figure 118

This permutation diagram has no two crossing arrows with targets i,$i+1$ for any i. However, we also see that the diagram is composed of five different components: four loops, and one subdiagram with boundary vertices $1, 3, 5, 7$. In that subdiagram, the arrows with target vertices 1 and 3 do cross, and are neighbors within that subdiagram. We could apply our method on that component by uncrossing 1 and 3, while still avoiding to add any new crossing. It would be therefore sufficient to check that any permutation either has neighboring vertices or is disconnected to show that we can always rely on our method. In the former case, we can apply a transposition to uncross those arrows, and in the latter, we divide the diagram into its connected components and apply the same process on those components.

Definition 4.40. A permutation is *disconnected* if there is an embedding of the permutation diagram in the disk such that the collection of arrows are disconnected,

i.e. we can write the collection of arrows as a disjoint union $A \cup B$ where for any arrow $\alpha \in A$ and any arrow $\beta \in B$, α and β do not cross.

Remark 4.41. Some notation is required for the proof that follows. For two distinct boundary vertices i and j, we denote (i, j) the set of boundary vertices stricly between i and j in a clockwise order. For instance, if $n = 9$, then $(3, 7) = \{4, 5, 6\}$, and $(8, 3) = \{9, 1, 2\}$. Furthermore, $j - i$ is the number of vertices counted from i to j clockwise including j, i.e. $j - i = |(i, j)| + 1$. Finally, if $x \in \{0, \ldots, n - 1$, then $j - x$ is the x^{th} vertex counted counter-clockwise from j, i.e. if $i = j - x$, then $(i, j) = \{i + 1, \ldots, i + (x - 1)\}$.

Proposition 4.42. *Any permutation π is either disconnected or has crossing neighbors.*

Proof. If π has a fixed point, it is trivially disconnected. Suppose that π has no fixed point. Then we have two cases to check

(i) $\exists i : \pi(i) = i + 1$. In that case, let $a = \pi^{-1}(i)$ Then the arrows α_i and α_a cross and have endpoints i and $i + 1$ respectively, hence π has crossing neighbors.

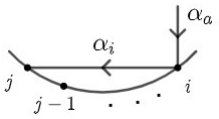

Figure 119

(ii) $\forall i : \pi(i) > i+1$. In that case, we will look for the arrows that travels minimally from one vertex to the other. For that, we define $s(i) \in \{0, \ldots, n-1\}$ such that $\pi(i) = i + s(i)$. In other words, $s(i)$ is how many vertices arrow α_i "jumps" ahead from its source to its target. Let $m := \min\{s(i) : i \in [n]\}$, which is the smallest such jump. Let $i \in [n]$ such that $\pi(i) = i + m =: j$. Since $m > 1$, $j - 1 \in (i, j)$.

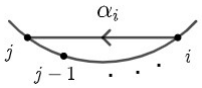

Figure 120

Let $a := \pi^{-1}(j-1)$. Then $j-1 = a + m'$ for some $m' \geq m$. Then

$$a = j - 1 - m' \leq j - 1 - m = (j-m) - 1 = i - 1 \Longrightarrow a \leq i - 1$$

Thus π has crossing neighbors $i \mapsto j$ and $a \mapsto j-1$.

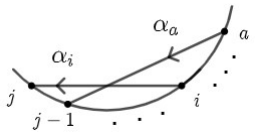

Figure 121

□

Example 4.43. Let $\pi = (15)(37)$ with 8 boundary vertices. We apply the transpositions on π as follows

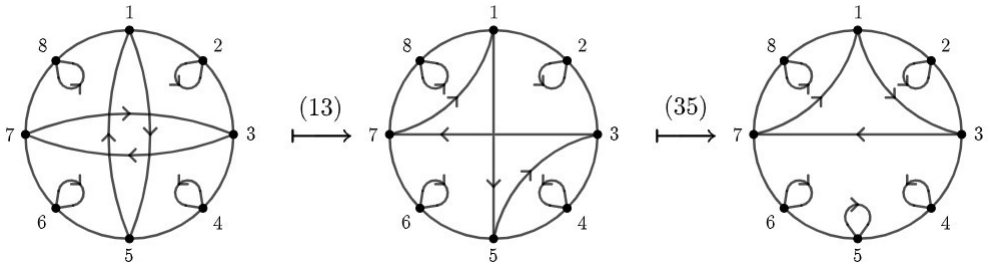

Figure 122

Then $\pi = (13)(35)\sigma$ with $\sigma = (137)$. The tiling for $\sigma = (137)$ restricted to the boundary vertices $1, 3, 5, 7$ is

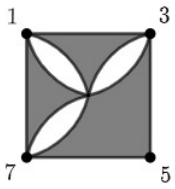

Figure 123

Since $2, 4, 6, 8$ are fixed points of π, we add black triangles at these vertices in the tiling and apply our method within the quadrilateral with boundary vertices $1, 3, 5, 7$. First we apply the transformations for the transpositions (13) and (34)

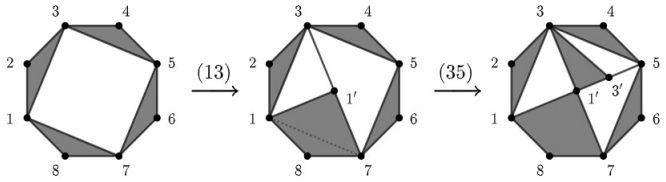

Figure 124

Then, we inscribe the tiling for σ inside the quadrilateral with vertices $1', 3', 5, 7$, and obtain the tiling up to equivalence.

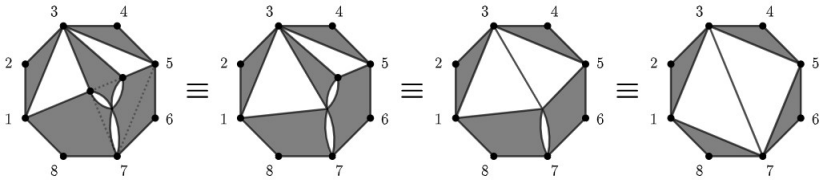

Figure 125

Example 4.44. Let $\pi = (1479)(28)(35\,10\,6)$. Then

$$\pi = (45)(67)(56)(89)(9\,10)(1\,10)(12)(78)(9\,10)(1\,10)(13)\sigma$$

for $\sigma = (16)(345)(8\,10)$.

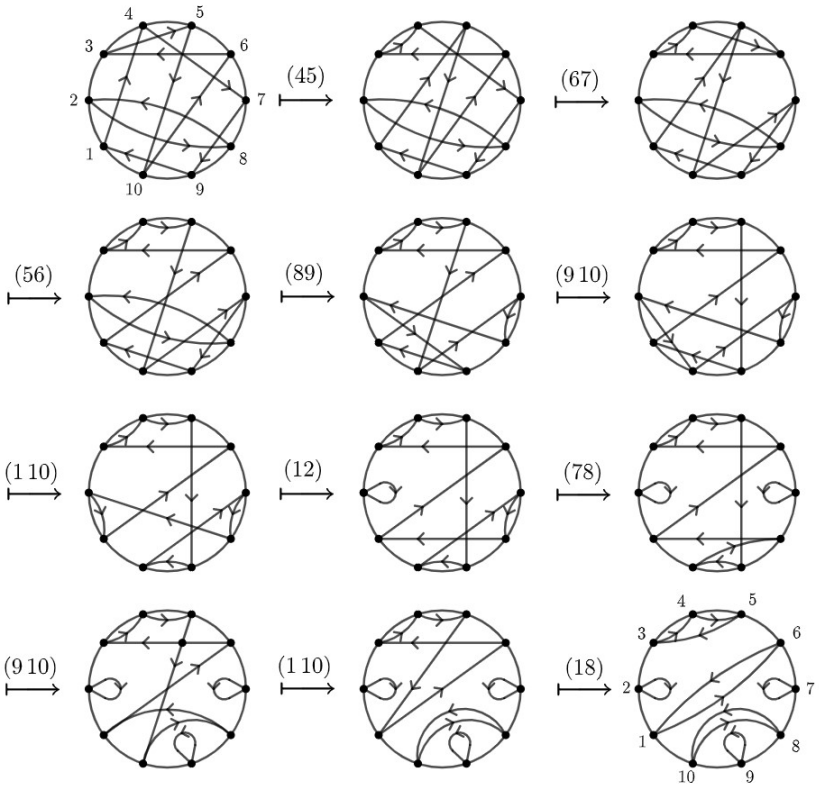

Figure 126

Then we apply the transpositions to the empty decagon, fill in σ, and simplify the tiling by equivalence.

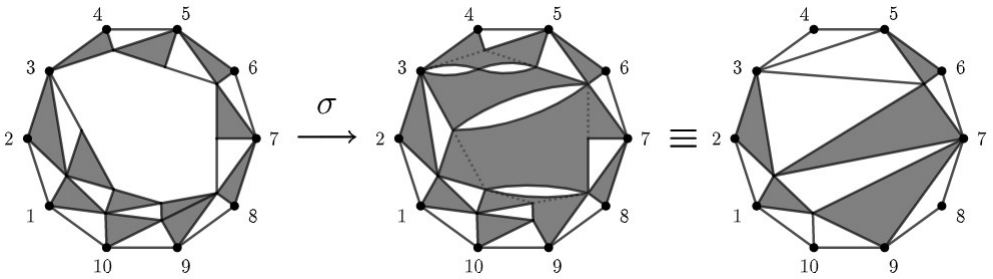

Figure 127

5 The totally non-negative Grassmannian through the lens of bicolored tilings

In this section, we will introduce a method to parametrize the positroid cells defined in Definition 1.21 using bicolored tilings. This method will mirror the method used in [21, 2.17] described in Theorem 1.28. We will demonstrate that this parametrization is invariant under equivalence, mutation, and reduction of tilings. This gives us a decomposition of the Grassmannian that is indexed by the mutation-reduction-equivalence classes of tilings.

From there, we introduce the notion of *degenerations of tilings*. Positroid cells admit a partial order defined by the inclusion of the closure of the cells. We can observe this partial order in tilings as well.

5.1 Parametrizing positroid cells in the totally non-negative Grassmannian

We recall that the Grassmannian $Gr_{k,n}$ is the set of k-dimensional vector spaces in an n-dimensional space (in our case, that is $\mathbb{R}^n$). A point $V \in Gr_{k,n}$ can be expressed as a full rank $k \times n$ matrix M, where V is the row-space of M. Since the row-space of M is invariant under left action by a non-singular $k \times k$-matrix, we can identify the Grassmannian as

$$Gr_{k,n} = GL_k \backslash Mat_{k \times n}$$

We can also describe V in projective coordinates by taking the collection of all maximal minors of M. The totally non-negative Grassmannian $Gr_{k,n}^{\geq 0}$ is the subset of $Gr_{k,n}$ consisting of all the points for which all projective coordinates are non-negative (up to simultaneous scaling with a factor $\lambda > 0$). We can decompose $Gr_{k,n}^{\geq 0}$ as follows

$$Gr_{k,n}^{\geq 0} = \bigsqcup_{\pi \in \mathbb{S}_{k,n}} S_\pi$$

where $\mathbb{S}_{k,n}$ is the set of all decorated permutations of $[n]$. We will now introduce a way to parametrize these cells using bicolored tilings.

We recall the definition of matchings of tilings. For the rest of this paper, unless otherwise specified, the set of vertices, hyperedges, faces, and angles of T will be denoted V, E, F, and A, respectively. If we have a second tiling T', we use V',E',F', and A', respectively. We denote the angle near $v \in V$ inside the face f by α_f^v. In that case, we also denote $v = v(\alpha)$ and $f = f(\alpha)$.

Definition 5.1. A *matching* $m \subset A$ of a tiling T is a choice of angles of T such that.

(i) Each face is matched exactly once, i.e. for any two angles $\alpha, \beta \in m : f(\alpha) \neq f(\beta)$, and for any face f of T, there is $\alpha \in m$ such that $f = f(\alpha)$.

(ii) Each vertex is matched at most once, i.e. for any two $\alpha, \beta \in m : v(\alpha) \neq v(\beta)$.

(iii) Each internal vertex is matched exactly once, i.e. on top of the second condition, for any internal vertex v of T, there is $\alpha \in m$ such that $v = v(\alpha)$.

We denote $\partial m = \{v \in V \mid v \text{ is a boundary vertex and not matched in } m\}$ the *boundary* of m. The set of matchings of a tiling T is denoted $\mathcal{M}(T)$.

Example 5.2. Consider the following tiling T of type $(4, 6)$ with one internal vertex and 12 angles.

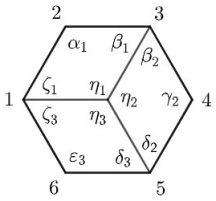

Figure 128

Then three examples of matchings of T would be

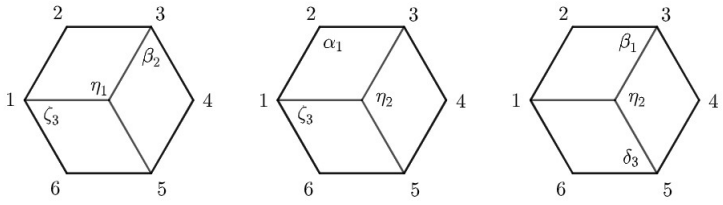

Figure 129

For simplification, we often denote the k-subsets I simply by concatenating their elements, that is $\partial m_1 = 2456$, $\partial m_2 = 3456$, and $\partial m_3 = 1246$.

Definition 5.3. Let G be a plabic graph. A *perfect orientation* of G is a choice of an orientation of its edges such that each black vertex has exactly one outgoing arrow, and each white vertex has exactly one incoming arrow.

We recall that an almost perfect matching of G is a subset of edges of G such that each internal vertex of G is adjacent to exactly one edge in that subset of edges. We also recall that if T has n boundary vertices, then $G = \Phi(T)$ has n boundary vertices too, which are all of degree 1 and incident to a single boundary edge.

Remark 5.4. Let T be a tiling, and $G = \Phi(T)$ the corresponding plabic graph (Definition 3.26). Any matching m of T gives rise to an almost perfect matching of G and a perfect orientation of G. This works as follows:

Any angle α of T maps to a unique edge e_α of G: Let $m = \{\alpha_i \,|\, i \in \mathcal{I}\}$ be a matching of T. Let $\tilde{E}$ be the set of boundary edges in G that are adjacent to white vertices in G whose pre-image under Φ is in ∂m, i.e. they are not matched in m. Then $\mathfrak{m} = \{e_{\alpha_i} \,|\, i \in \mathcal{I}\} \cup \tilde{E}$ is an almost perfect matching of G.

At the same time, an almost perfect matching results in a perfect orientation of G by orienting all edges in $\mathfrak{m}$ from the black vertex to the white vertex, and all other edges that are not in $\mathfrak{m}$ the other way around.

Example 5.5. Consider the tiling T from Example 5.2, and the matching $m = \{\alpha_1, \gamma_2, \eta_3\}$. For simplicity, we will label $a = \alpha_1$, $b = \gamma_2$, and $c = \eta_3$.

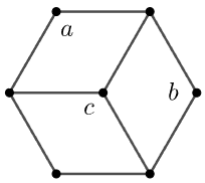

Figure 130

Let $G = \Phi(T)$ be the corresponding plabic graph.

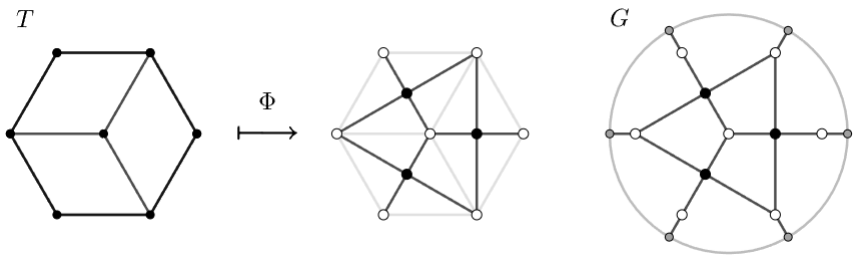

Figure 131

Then the corresponding almost perfect matching of G and perfect orientation of G are

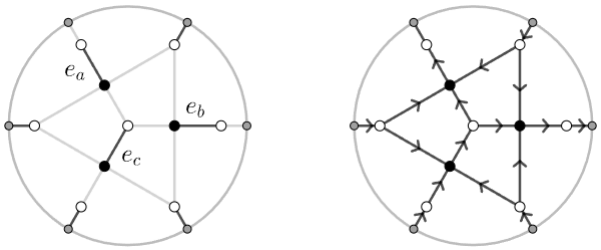

Figure 132

This also gives us the following proposition.

Proposition 5.6. *If T is a tiling of type (k, n) with a matching m, then $|\partial m| = k$.*

Proof. Let $G = \Phi(T)$ be the bipartite plabic graph associated to T. Let $\mathfrak{m} = \Phi(m)$ be the almost perfect matching of G described in Remark 5.4. Then $i \in \partial m$ if and only if i is not matched in m. Any boundary vertex i maps to a white vertex w in G that is exactly adjacent to the boundary vertex i in G and one internal black vertex b. Since i is not matched in m, the edge between w and b is not in $\mathfrak{m}$ either. This means that the edge between w and i in G is in $\mathfrak{m}$. Thus if a vertex i of T is not matched in m, the corresponding boundary vertex i of G is matched in $\mathfrak{m}$. Hence $\partial m = \partial \mathfrak{m}$. Since G is of type (k, n), $|\partial m| = |\partial \mathfrak{m}| = k$. □

Proposition 5.7. *Let T be a tiling with a matching of type (k, n). Then $k = |V| - |F|$.*

Proof. If m is a matching of T, then every face is matched to exactly one vertex. Then, $k = |\partial m|$ is given by the number of boundary vertices that are not matched, which is the number of total vertices minus the number of faces of the tiling. □

We will now parametrize positroid cells using bicolored tilings.

Definition 5.8. We consider any matching m of T as a monomial given by the product of its elements. Then for any k-subset I of $[n]$, we set

$$\Delta_I = \sum_{\substack{m \in \mathcal{M}(T) \\ \partial m = I}} m$$

where $M(T)$ is the set of all matchings of T. The *positroid cell* S_T *associated to* T is given by all the points $(\Delta_I)_{I \in \binom{[n]}{k}}$ for which the parameters $\alpha \in A$ are all positive, i.e.

$$S_T = \{(\Delta_I)_I \,|\, \alpha \in \mathbb{R}_{>0} \ \ \forall \alpha \in A\}$$

We call $P_T = (\Delta_I)_I$ the parametrization, and Δ_I the *Plücker coordinates* of T and S_T. The closure $\overline{S_T}$ of a positroid cell S_T is given by

$$\overline{S_T} = \{(\Delta_I) \mid \alpha \in \mathbb{R}_{\geq 0} \ \ \forall \alpha \in A\}$$

The closure of one cell S_T is nested in another cell $S_{T'}$ if the zero coordinates of $S_{T'}$ are also zero coordinates of S_T. An in-depth view of this partial order can be found in [15, Ch.17]. We will later explore this partial order through the lense of bicolored tilings. For our purposes, it is sufficient to know that $\overline{S_T} = \overline{S_{T'}} \implies S_T = S_{T'}$, since positroid cells are homeomorphic to open balls as given in Theorem 1.22 (the converse is evidently true as well). Thus if we wanted to show that two positroid cells are the same, we may instead prove that their closures are the same (e.g. Lemma 5.15).

Example 5.9. We consider the tiling T of type $(4, 6)$ from the previous example. Let $I = 2456$. Then the matchings m with $\partial m = I$ are

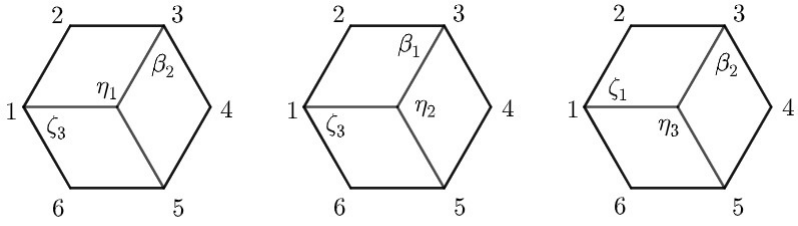

Figure 133

Then $\Delta_{2456} = \beta_2\zeta_3\eta_1 + \beta_1\zeta_3\eta_2 + \beta_2\zeta_1\eta_3$. Doing this for every k-subset I of $[n]$, we obtain

$$\begin{aligned} P_T = (&\Delta_{1234}, \Delta_{1235}, \Delta_{1236}, \Delta_{1245}, \Delta_{1246}, \Delta_{1256}, \Delta_{1345}, \\ &\Delta_{1346}, \Delta_{1356}, \Delta_{1456}, \Delta_{2345}, \Delta_{2346}, \Delta_{2356}, \Delta_{2456}, \Delta_{3456}) \end{aligned}$$

with

$$\begin{aligned} \Delta_{1234} &= \delta_2\varepsilon_3\eta_1 \\ \Delta_{1235} &= \gamma_2\varepsilon_3\eta_1 \\ \Delta_{1236} &= \gamma_2\delta_3\eta_1 \\ \Delta_{1245} &= \beta_1\varepsilon_3\eta_2 + \beta_2\varepsilon_3\eta_1 \\ \Delta_{1246} &= \beta_1\delta_2\eta_3 + \beta_1\delta_3\eta_2 + \beta_2\delta_3\eta_1 \\ \Delta_{1256} &= \beta_1\gamma_2 + \eta_3 \\ \Delta_{1345} &= \alpha_1\varepsilon_3\eta_2 \\ \Delta_{1346} &= \alpha_1\delta_2\eta_3 + \alpha_1\delta_3\eta_2 \\ \Delta_{1356} &= \alpha_1\gamma_2\eta_3 \\ \Delta_{1456} &= \alpha_1\beta_2\eta_3 \\ \Delta_{2345} &= \varepsilon_3\zeta_1\eta_2 \\ \Delta_{2346} &= \delta_2\zeta_1\eta_3 + \delta_2\zeta_3\eta_1 + \delta_3\zeta_1\eta_2 \\ \Delta_{2356} &= \gamma_2\zeta_1\eta_3 + \gamma_2\zeta_3\eta_1 \\ \Delta_{2456} &= \beta_2\zeta_3\eta_1 + \beta_1\zeta_3\eta_2 + \beta_2\zeta_1\eta_3 \\ \Delta_{3456} &= \alpha_1\zeta_3\eta_2 \end{aligned}$$

And finally, $S_T = \{P_T \,|\, \alpha_1, \beta_1, \beta_2, \gamma_2, \delta_2, \delta_3, \varepsilon_3, \zeta_1, \zeta_3, \eta_1, \eta_2, \eta_3 > 0\}$.

Using the allocation of matchings of tilings to almost perfect matching of plabic graphs described in Remark 5.4, it follows that the parametrization described in Definition 5.8 aligns with the parametrization described in Theorem 1.28. We make this more explicit in Proposition 5.21.

Before we do that, we want to prove that equivalences, mutations, and reductions of a tiling preserve the corresponding positroid cell. To do so, we first define *subtilings* of tilings, which are simply the result of "cutting out" a piece of the tiling along the boundaries of its hyperedges, with the rest of the tiling being referred to as the *remainder*. This allows us to explore how local changes of a tiling change the positroid cell of the whole tiling. We also introduce the union of tilings, since "cutting out" a subtiling from a tiling might result in the remainder not being connected.

Definition 5.10. Let $\mathcal{C} = X_1 \cup \cdots \cup X_r$ be a finite union of 2-dimensional connected oriented surfaces X_i with $n_1, \ldots, n_r$ boundary vertices, such that the intersection of any two surfaces X_i and X_j is either empty or a common boundary vertex. Then a *tiling* $\mathcal{T}$ of $\mathcal{C}$ is the union of tilings $T_1 \cup \cdots \cup T_r$ such that $T_i = (X_i, V_i, E_i)$ is a tiling of X_i, where $T_i \cup T_j = (X_i \cup X_j, V_i \cup V_j, E_i \cup E_j)$.

Definition 5.11. Let T be a tiling of a surface X with vertex set V and hyperedge set E. Let $v_1, \ldots, v_m$ be vertices of T such that for any $i \in [m]$, there is a curve γ_i with endpoints v_i, v_{i+1} (with $v_{m+1} = v_1$), as described in Definition 2.2. Let $X' \subset X$ be a surface with boundary $\bigcup \gamma_i$ and boundary vertices $v_1, \ldots, v_m$. Then we define a tiling T' of X' as follows

- hyperedge set $E' = \{e \cap X' \,|\, e \in E \text{ and } e \cap X' \neq \emptyset\}$,
- vertex set $V' = V \cap X'$,
- boundary vertices $\partial V' = \{v_1, \ldots, v_m\} \cup (\partial V \cap \partial X)$.

We say that T' is a *subtiling* of T under X'. Let $\tilde{X} = X \setminus \mathrm{int}(X') \subset X$ be the surface with boundary $\partial \tilde{X} = \overline{\partial X \cup \partial X' \setminus (\partial X \cap \partial X')}$. Then we call the subtiling $\tilde{T}$ under $\tilde{S}$ the *remainder* of T under X'. We also denote $\tilde{T} = T \setminus T'$.

Remark 5.12. Let T be a tiling of type (k, n) of a disk D_n. Let T' be a subtiling of T under a disk $D_m \subset D_n$ as in Definition 5.11, and $\tilde{T} = T \setminus T'$. We can extend the definition of *matchings* to tilings of surfaces other than disks, such as $\tilde{T}$, i.e. we choose angles in $\tilde{T}$ satisfying the conditions (i)-(iii) in Definition 5.1.

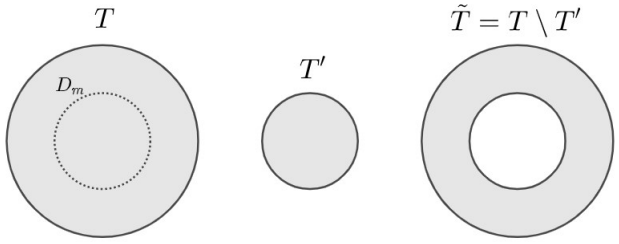

Figure 134

We partition the boundary of a matching of $\tilde{T}$. If $\tilde{m}$ is a matching of $\tilde{T}$, we will denote $\partial_1 \tilde{m}$ the set of boundary vertices of $\tilde{T}$ on the boundary of T that *are not*

matched in $\tilde{m}$, and we will denote $\partial_2\tilde{m}$ the boundary vertices of $\tilde{T}$ on the boundary of T' that *are* matched in $\tilde{m}$. Then, similarly, we define the I-th coordinate of $\tilde{T}$ as

$$\tilde{\Delta}_I = \sum_{\substack{\tilde{m}\in\mathcal{M}(\tilde{T}) \\ \partial_1\tilde{m}=I}} \tilde{m}$$

If m is a matching of T, we will write m° for the angles of m inside T', and $\tilde{m}$ for the angles of m inside $\tilde{T}$, i.e. $m^\circ = m|_{T'}$ and $\tilde{m} = m|_{\tilde{T}}$. Note that in that case, $m = m^\circ \sqcup \tilde{m}$, and we have $\partial_1\tilde{m} = \partial m$ and $\partial_2\tilde{m} = \partial m^\circ$.

Example 5.13. Here is an example of a tiling T of type $(8, 13)$ and a matching $m \in \mathcal{M}(T)$.

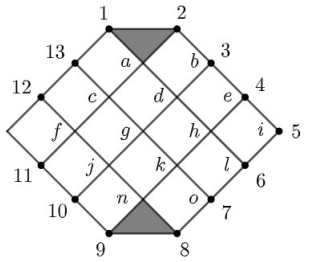

$m = \{a, b, c, \ldots, l, n, o\} \in \mathcal{M}(T)$
$\partial m = \{1, 2, 8, 9, 10, 11\}$

Figure 135

Then we can "cut out" the subtiling T' consisting of the four white tiles in the center of T. The remainder is the tiling $\tilde{T}$.

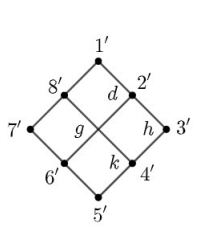

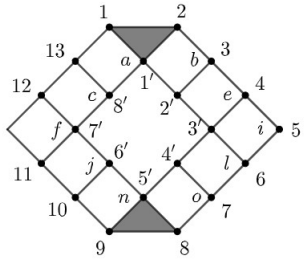

$m^\circ = \{d, g, h, k\} \in \mathcal{M}(T')$
$\partial m^\circ = \{1', 5', 6', 7', 8'\}$

$\tilde{m} = \{a, b, c, e, f, i, k, l, n, o\} = m \setminus m^\circ \in \mathcal{M}(\tilde{T})$
$\partial_1\tilde{m} = \{1, 2, 8, 9, 10, 11\} = \partial m$
$\partial_2\tilde{m} = \{1', 5', 6', 7', 8'\} = \partial m^\circ$

Figure 136

The following lemma separates the variables in the coordinates Δ_I in the parametrization of a tiling into variables that come from angles inside a subtiling and outside of it. This allows us to prove Lemma 5.15 and Corollary 5.16, which state that if a local transformation on a tiling does not change the positroid cell of the subtiling it was applied on, then it does not change the positroid cell of the full tiling.

Lemma 5.14. Let T be a tiling of type (k, n). Let T' be a subtiling of T, and $\tilde{T} = T \setminus T'$. Then for any k-subset I of $[n]$, the I-th coordinate of the positroid cell S_T is given by

$$\Delta_I = \sum_{\substack{\tilde{m} \in \mathcal{M}(\tilde{T}) \\ \partial_1 \tilde{m} = I}} \Delta^\circ_{\partial_2 \tilde{m}} \cdot \tilde{m}$$

where Δ°_J denotes the J-th coordinate of the positroid cell $S_{T'}$.

Proof. Let $m \in \mathcal{M}(T)$ be a matching of T with $\partial m = I$. We write $m = m^\circ \sqcup \tilde{m}$, where m° denotes the angles of m that are inside T', and $\tilde{m}$ the angles outside T' (that is, they are in $\tilde{T}$). Then m° is a matching of T' and $\tilde{m}$ is a matching of $\tilde{T}$.

Let $J = \partial m^\circ$. Then for any matching m' of T' with $\partial m' = J$, $m' \sqcup \tilde{m}$ is a matching of T with $\partial(m' \sqcup \tilde{m}) = I$. In other words, all the matchings m of T with $\partial m = I$ are given as a combination of a matching $\tilde{m}$ of $\tilde{T}$ with $\partial_1 \tilde{m} = I$ and a matching m° of T' with $\partial m^\circ = \partial_2 \tilde{m}$. By summing them as monomials, we obtain the I-th coordinate

$$\Delta_I = \sum_{\substack{\tilde{m} \in \mathcal{M}(\tilde{T}) \\ \partial_1 \tilde{m} = I}} \tilde{m} \cdot \left(\sum_{\substack{m^\circ \in \mathcal{M}(t) \\ \partial m^\circ = \partial_2 \tilde{m}}} m^\circ \right)$$

where the second sum is the coordinate $\Delta^\circ_{\partial_2 \tilde{m}}$ of the positroid cell $S_{T'}$. Thus,

$$\Delta_I = \sum_{\substack{\tilde{m} \in \mathcal{M}(\tilde{T}) \\ \partial_1 \tilde{m} = I}} \tilde{m} \cdot \Delta^\circ_{\partial_2 \tilde{m}}$$

□

We remind that if the closures of two positroid cells are the same, then the cells themselves are as well, i.e. $\overline{S_{T_1}} = \overline{S_{T_2}} \Longrightarrow S_{T_1} = S_{T_2}$ (p.88). Thus, in the following three statements (Lemma 5.15, Corollary 5.16, Proposition 5.17), we will work with the closures of the cells, as they also give us ways to describe inclusions (which the positroid cells themselves don't give, as they are disjoint). Any equalities of the closures also give us the equalities of the cells themselves.

Lemma 5.15. Let T_1 be a tiling with subtiling A. Let T_2 be the tiling obtained by replacing A in T_1 with a new subtiling B of same type as A such that $\overline{S_A} \subset \overline{S_B}$. Then $\overline{S_{T_1}} \subset \overline{S_{T_2}}$.

Proof. Let $\alpha_1, \ldots, \alpha_r$ and $\alpha_{r+1}, \ldots, \alpha_R$ be the angles in A and $\tilde{T} = T_1 \setminus A$, respectively. Let $\beta_1, \ldots, \beta_s$ be the angles in B.

Consider a point $x = P_{T_1}(x_1, \ldots, x_r, x_{r+1}, \ldots, x_R) \in \overline{S_{T_1}}$, with $x_i \geq 0$. We want to express x as a point in $\overline{S_{T_2}}$, parametrized by P_{T_2}. We know that $x^\circ = P_A(x_1, \ldots, x_r)$ is a point in $\overline{S_A}$. Since $\overline{S_A} \subset \overline{S_B}$, there are $y_1, \ldots, y_s \geq 0$ such that $x = P_B(y_1, \ldots, y_s) \in \overline{S_B}$.

In other words, if Δ_J^A and Δ_J^B are the J-th coordinate in P_A and P_B, respectively, then there is a $\lambda \in \mathbb{R}_{>0}$ such that

$$\Delta_J^A(x_1, \ldots, x_r) = \lambda \Delta_J^B(y_1, \ldots, y_s) \qquad (*)$$

Then for any k-subset I of $[n]$, if $\Delta_I^{(1)}$ and $\Delta_I^{(2)}$ are the I-th coordinate in P_{T_1} and P_{T_2}, we have by Lemma 5.14

$$\begin{aligned}
&\Delta_I^{(1)}(x_1, \ldots, x_r, x_{r+1}, \ldots, x_R) \\
&= \sum_{\substack{\tilde{m} \in \mathcal{M}(\tilde{T}) \\ \partial \tilde{m} = I}} \Delta^A_{\partial_2 \tilde{m}}(x_1, \ldots, x_r) \cdot \tilde{m}(x_{r+1}, \ldots, x_R) && \text{by Lemma 5.14} \\
&= \sum_{\substack{\tilde{m} \in \mathcal{M}(\tilde{T}) \\ \partial \tilde{m} = I}} \lambda \cdot \Delta^B_{\partial_2 \tilde{m}}(y_1, \ldots, y_s) \cdot \tilde{m}(x_{r+1}, \ldots, x_R) && \text{using } (*) \\
&= \lambda \cdot \sum_{\substack{\tilde{m} \in \mathcal{M}(\tilde{T}) \\ \partial \tilde{m} = I}} \Delta^B_{\partial_2 \tilde{m}}(y_1, \ldots, y_s) \cdot \tilde{m}(x_{r+1}, \ldots, x_R) \\
&= \lambda \Delta_I^{(2)}(y_1, \ldots, y_r, x_{r+1}, \ldots, x_R) && \text{by Lemma 5.14}
\end{aligned}$$

Thus $x = (\Delta_I^{(2)}(y_1, \ldots, y_s, x_{r+1}, \ldots, x_R))_{I \in \binom{[n]}{k}} \in \overline{S_{T_2}}$. Hence $\overline{S_{T_1}} \subset \overline{S_{T_2}}$, which concludes the proof. □

Corollary 5.16. Let T_1 be a tiling with subtiling A, and T_2 the tiling obtained by replacing A in T_1 with a new subtiling B with $\overline{S_A} = \overline{S_B}$. Then $\overline{S_{T_1}} = \overline{S_{T_2}}$. Equivalently, if $S_A = S_B$, then $S_{T_1} = S_{T_2}$.

Proposition 5.17. *The positroid cell associated to T is invariant under*

(*i*) *mutation of a tiling.*

(*ii*) *tiling equivalence.*

(*iii*) *reductions of a tiling.*

Proof. For all three parts of the proof we will pick a point in the open cell S_{T_1} of a tiling T_1 and show that that point can be expressed as a point in the closed cell $\overline{S_{T_2}}$ where T_2 is the tiling obtained after transforming T_1 as described in (*i*),(*ii*), and (*iii*), respectively, thus showing that $S_T \subset \overline{S_{T'}}$. It is crucial that we use the open positroid cell of T', to avoid division by 0 in some of the calculations. Since $S_T \subset \overline{S_{T'}} \implies \overline{S_T} \subset \overline{S_{T'}}$, we still obtain the desired result.

Moreover, by Corollary 5.16 it is sufficient to show that these transformations preserve the positroid cell locally.

(*i*) Consider the two triangulations T_1 and T_2 of a quadrilateral and their parametrizations as described in Definition 5.8.

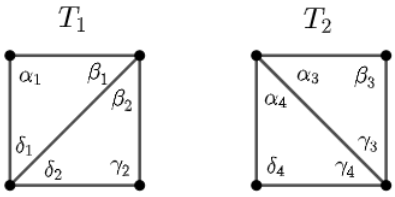

Figure 137

$$P_{T_1} = (a_1\beta_1, \alpha_1\gamma_2, \alpha_1\delta_2, \beta_1\gamma_2, \beta_1\delta_2 + \beta_2\delta_1, \gamma_2\delta_1)$$
$$P_{T_2} = (\alpha_4\beta_3, \alpha_3\gamma_4 + \alpha_4\gamma_3, \alpha_3\delta_4, \beta_3\gamma_4, \beta_3\delta_4, \gamma_3\delta_4)$$

Let $x \in S_{T_1}$ given by the fixed parameters $a_1, b_1, b_2, c_2, d_1, d_2 > 0$, i.e.

$$x = (a_1b_1, a_1c_2, a_1d_2, b_1c_2, b_1d_2 + b_2d_1, c_2d_1)$$

Then let $y \in \overline{S_{T_2}}$ be the point given by the fixed, non-negative parameters

$$\beta_3 = a_1 \qquad \delta_4 = \frac{b_1d_2 + b_2d_1}{a_1}$$
$$\alpha_4 = b_2 \qquad \alpha_3 = \frac{a_1d_2}{\delta_4}$$
$$\gamma_4 = \frac{b_1c_2}{a_1} \qquad \gamma_3 = \frac{c_2d_1}{\delta_4}$$

Then $y = (a_1b_1, a_1c_2, a_1d_2, b_1c_2, b_1d_2 + d_2d_1, c_2d_1) = x$, thus $x \in \overline{S_{T_1}}$. Hence $S_{T_1} \subset \overline{S_{T_2}}$. Then we also have $S_{T_2} \subset \overline{S_{\mu_e(T_2)}} = \overline{S_{T_1}}$, and thus $S_{T_1} = S_{T_2}$.

(*ii*) (*a*) (Hourglass equivalence) Consider the tiling T_1 that is an empty n-gon, and T_2 that is obtained by adding an hourglass inside T_1.

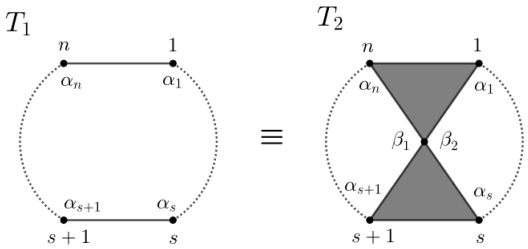

Figure 138

We call α_i the angle at the boundary vertex i in both tilings, and β_1 and β_2 the angles around the internal vertex in T_2. The parametrizations of these tilings are

$$P_{T_1} = (\alpha_n, \ldots, \alpha_1)$$

$$P_{T_2} = (\alpha_n\beta_2, \ldots, \alpha_{s+1}\beta_2, \alpha_s\beta_1, \ldots, \alpha_1\beta_1)$$

- Let $x = (a_n, \ldots, a_1) \in S_{T_1}$ with $a_i > 0$ for any $i = 1, \ldots, n$. We construct $y \in \overline{S_{T_2}}$, with parameters $\alpha_i = a_i \geq 0$ and $\beta_1 = \beta_2 = 1$. Then
$$y = (a_n \cdot 1, \ldots, a_1 \cdot 1) = x,$$
thus $x \in \overline{S_{T_2}}$. Thus, $S_{T_1} \subset \overline{S_{T_2}}$.
- Let $y \in S_{T_2}$ with parameters a_i, $b_j > 0$, that is
$$y = (a_nb_2, \ldots, a_{s+1}b_2, a_sb_1, \ldots, a_1b_1).$$
We construct $x \in \overline{S_{T_1}}$ with parameters
$$\alpha_i = \begin{cases} a_ib_2, & \text{if } i = 1, \ldots, s \\ a_ib_1, & \text{if } i = s+1, \ldots, n. \end{cases} \in \mathbb{R}_{\geq 0}$$
Then $x = y$, and $y \in \overline{S_{T_1}}$. Thus, $S_{T_2} \subset \overline{S_{T_1}}$.

We conclude that $S_{T_1} = S_{T_2}$.

(b) Consider the tiling T and one of its boundary vertices i. Let T' be the tiling obtained by decontracting at i, i.e.

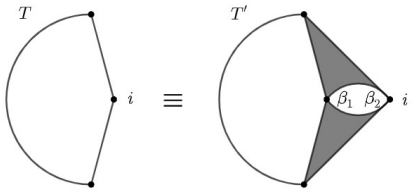

Figure 139

We call $\alpha_1, \ldots, \alpha_r$ the angles in the angles in T, with $\alpha_1, \ldots, \alpha_s$ being the angles around vertex i in T. We call β_1, β_2 the angles in the digon. Let I be a k-subset of $[n]$. Let Δ_I be the I-th coordinate of P_T, and Δ'_I be the I-th coordinate of $P_{T'}$.

- If $i \in I$, then for all matchings m of T with $\partial m = I$, $m' = m \sqcup \beta_1$ is a matching of T', with $\partial m' = I$.
- If $i \notin I$, then for all matchings m of T with $\partial m = I$, $m' = m \sqcup \beta_2$ is a matching of T', with $\partial m' = I$.

Thus by defining

$$\lambda_I(\beta_1, \beta_2) = \begin{cases} \beta_1 \text{ if } i \in I \\ \beta_2 \text{ if } i \notin I \end{cases}$$

we get that for matching m of T, $m' = m \sqcup \lambda_{\partial m}$ is a matching of T', and for any I, $\Delta'_I = \lambda_I \Delta_I$.

- Let $x = P_T(a_1, \ldots, a_r) \in S_T$. In other words, the I-th coordinate of x is $\Delta_I(a_1, \ldots, a_r)$. Then we construct $y \in \overline{S_{T'}}$ with parameters $\alpha_i = a_i$ and $\beta_i = 1$. Then the I-th coordinate of y is

  $$\Delta'_I(a_1, \ldots, a_r, 1, 1) = \lambda_I(1, 1)\Delta_I(a_1, \ldots, a_r) = \Delta_I(a_1, \ldots, a_r)$$

  Thus $y = x$, and thus $x \in \overline{S_{T'}}$. Hence, $S_T \subset \overline{S_{T'}}$.
- Let $y = P_{T'}(a_1, \ldots, a_r, b_1, b_2) \in S_{T'}$. In other words, the I-th coordinate of y is $\Delta'_I(a_1, \ldots, a_r, b_1, b_2)$. We recall that monomials appearing in any coordinate have the same length p (i.e. the number of angles/variables in the monomial which equals the number

of faces of the tiling). We denote $q = p^{-1}$. Then we construct $x = P_T(a_1\mu, \ldots, a_s\mu, a_{s+1}\nu, \ldots, a_r\nu) \in \overline{S_T}$, where $\mu = b_2 b_1^{-q(p-1)}$ and $\nu = b_1^q$. Then

$$\Delta_I(a_1\mu, \ldots, a_s\mu, a_{s+1}\nu, \ldots, a_r\nu) = \sum_{\partial m = I} m(a_1\mu, \ldots, a_s\mu, a_{s+1}\nu, \ldots, a_r\nu)$$

Evaluating a monomial on the parameters equates to multiplying p of the parameters (corresponding to the angles in the matching). We distinguish two cases

- $i \in I$. Then $\alpha_1, \ldots, \alpha_s \notin m$. Thus the monomial is completely independent of those first s parameters and is a product of p of the remaining parameters. We can then write

$$\begin{aligned} m(a_1\mu, \ldots, a_s\mu, a_{s+1}\nu, \ldots, a_r\nu) &= \nu^p m(a_1, \ldots, a_s, a_{s+1}, \ldots, a_r) \\ &= b_1 m(a_1, \ldots, a_r) \end{aligned}$$

  Thus

$$\begin{aligned} \Delta_I(a_1\mu, \ldots, a_s\mu, a_{s+1}\nu, \ldots, a_r\nu) &= b_1 \sum_{\partial m = I} m(a_1, \ldots, a_r) \\ &= \lambda_I(b_1, b_2)\Delta_I(a_1, \ldots, a_r) \\ &= \Delta'_I(a_1, \ldots, a_r, b_1, b_2) \end{aligned}$$

- $i \notin I$. Then there is exactly one $j \in \{1, \ldots, s\}$ such that $\alpha_j \in m$, which means exactly one copy of μ appears. The remaining $\{\alpha_1, \ldots, \alpha_s\} \setminus \{\alpha_j\}$ do not appear in the monomial m, and instead $p-1$ of the angles $\alpha_{s+1}, \ldots, \alpha_r$ do. Thus

$$\begin{aligned} m(a_1\mu, \ldots, a_s\mu, a_{s+1}\nu, \ldots, a_r\nu) &= \mu\nu^{p-1} m(a_1, \ldots, a_s, a_{s+1}, \ldots, a_r) \\ &= b_2 m(a_1, \ldots, a_r) \end{aligned}$$

  Thus

$$\begin{aligned} \Delta_I(a_1\mu, \ldots, a_s\mu, a_{s+1}\nu, \ldots, a_r\nu) &= b_2 \sum_{\partial m = I} m(a_1, \ldots, a_r) \\ &= \lambda_I(b_1, b_2)\Delta_I(a_1, \ldots, a_r) \\ &= \Delta'_I(a_1, \ldots, a_r, b_1, b_2) \end{aligned}$$

Thus for any k-subset I of $[n]$, $\Delta'(a_1\mu, \ldots, a_s\mu, a_{s+1}\nu, \ldots, a_r\nu) = \Delta'_I(a_1, \ldots, a_r, b_1, b_2)$, thus $x = y$, and thus $y \in \overline{S_T}$. Hence $S_{T'} \subset \overline{S_T}$.

We conclude that $S_T = S_{T'}$.

(*iii*) Consider the tiling T_1 that is an n-gon with one 1-edge e (w.l.o.g at boundary vertex n). Let $T_2 = R_e(T_1)$, i.e. T_2 is an empty n-gon.

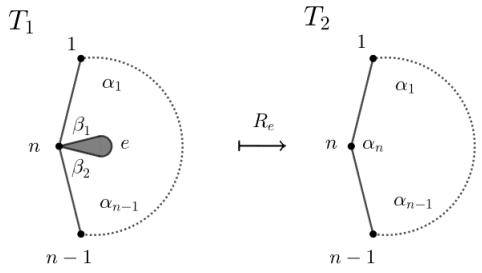

Figure 140

We call α_i the angle at the boundary vertex i in both tilings, except for the angles at the vertex n in T_1 which we call β_1 and β_2. The parametrizations of these tilings are

$$P_{T_1} = (\beta_1 + \beta_2, \alpha_{n-1}, \ldots, \alpha_1)$$
$$P_{T_2} = (\alpha_n, \ldots, \alpha_1)$$

· Let $x \in S_{T_1}$ with parameters $\alpha_i = a_i$, $\beta_j = b_j > 0$, that is

$$x = (b_1 + b_2, a_{n-1}, \ldots, a_1)$$

We construct $y \in \overline{S_{T_2}}$ with parameters $\alpha_n = b_1 + b_2 \geq 0$, and $\alpha_i = a_i \geq 0$ for $i = 1, \ldots, n-1$. Then $y = x$, and $x \in \overline{S_{T_2}}$. Thus, $S_{T_1} \subset \overline{S_{T_2}}$.

· Let $y = (a_n, \ldots, a_1) \in S_{T_2}$ with parameters $a_i > 0$. We construct $x \in \overline{S_{T_1}}$ with parameters

$$\begin{cases} \alpha_i = a_i, & \text{for } i = 1, \ldots, s-1 \\ \beta_1 = \beta_2 = \frac{1}{2}a_n \end{cases} \in \mathbb{R}_{\geq 0}$$

Then $x = y$, and $y \in \overline{S_{T_1}}$. Thus $S_{T_2} \subset \overline{S_{T_1}}$.

Hence, $S_{T_1} = S_{T_2}$.

□

In order to prove Proposition 5.21, we introduce the following construction.

Definition 5.18. Let T be a tiling of type (k, n). We construct a tiling T' of type (k, n), called the expansion of T, as follows.

(i) Draw a disk D_n with n boundary vertices $1', \ldots, n'$.

(ii) Draw the tiling T inside the disk D.

(iii) Between each pair of vertices i and i', draw two curves that form a digon with endpoints i and i'.

(iv) The area between any two digons is black.

Example 5.19. An example of a tiling T of type $(3, 5)$ and its expansion T' is

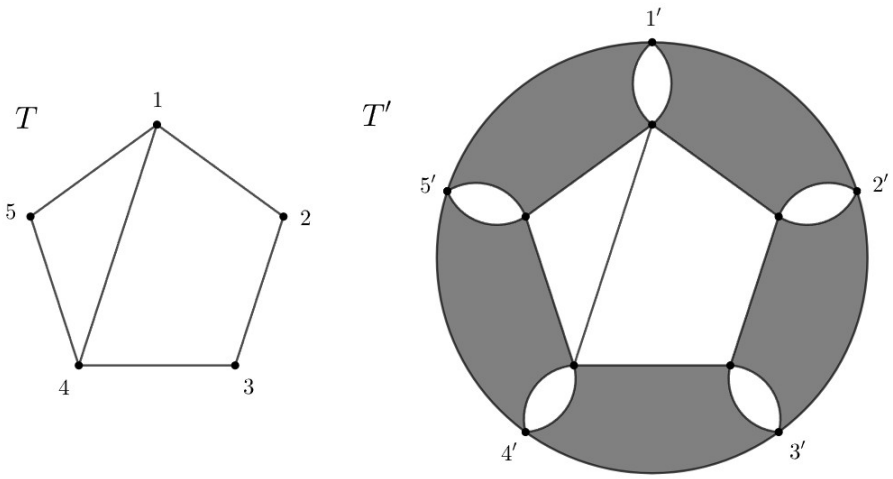

Figure 141

Remark 5.20. By Proposition 5.17.(ii).b, $S_T = S_{T'}$. Any matching m of T induces a matching m' of T' by choosing one of the angles of each digon, which depends on which boundary vertex i of T was matched and which was not. The boundary vertex i' of T' is matched in m' exactly when the boundary vertex i of T is matched in m. Otherwise, the other vertex of the digon is matched.

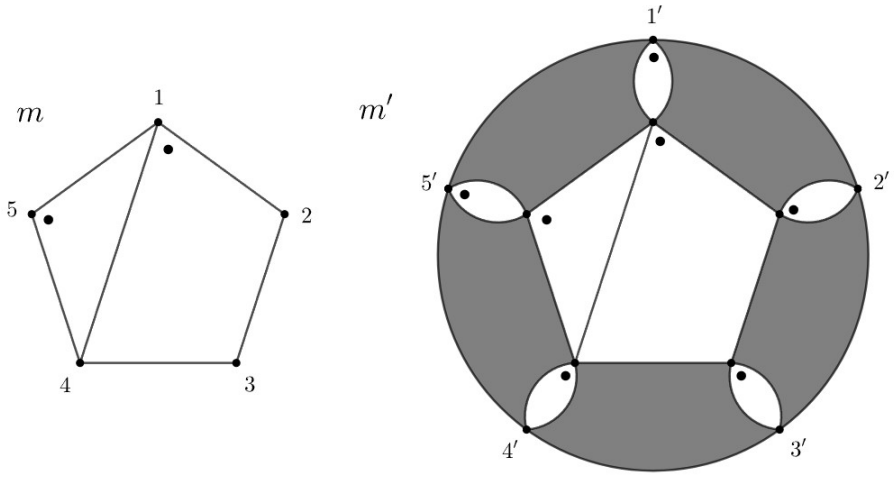

Figure 142

Let us take a look at the corresponding plabic graphs $G = \Phi(T)$ and $G' = \Phi(T')$ and their corresponding almost perfect matchings $\mathfrak{m}$ and $\mathfrak{m}'$ as described in Remark 5.4.

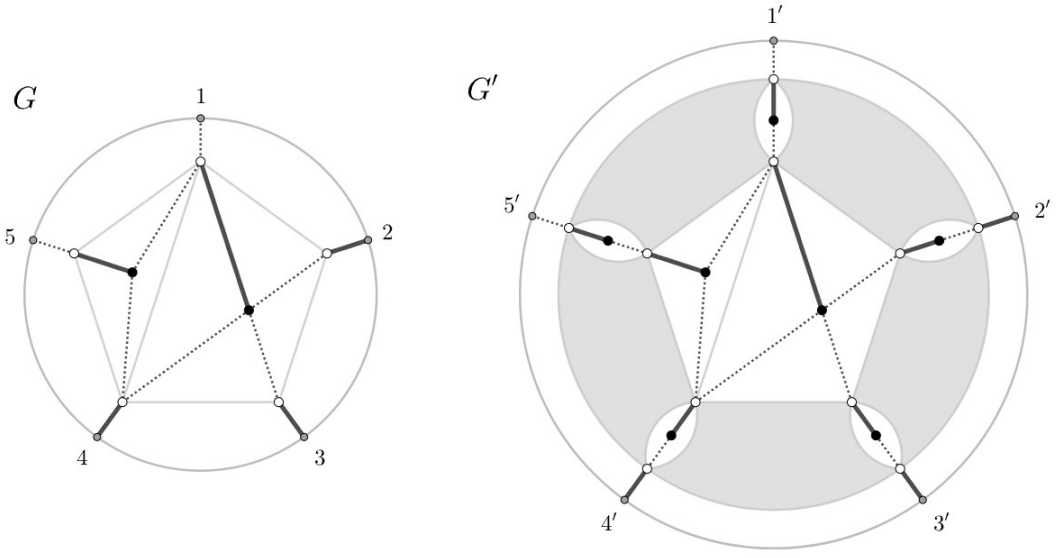

Figure 143

As described in Remark 5.4, G has some extra edges compared to angles in T that appear on the boundary and that we labeled $\tilde{E}$. This means that any matching m of T translate into an almost perfect matching $\mathfrak{m}$ of G with some extra elements, which translates into extra variables in the parametrization of S_G. This makes it easy to describe a point of S_T as a point in S_G. The same is true for $S_{T'}$ and $S_{G'}$. However T' has some extra angles compared to edges of G as well. We denote $\tilde{A} = \{\alpha_i \,|\, i \in \tilde{\mathcal{I}}\}$ the boundary angles of T'. Any almost perfect matching $\mathfrak{m}$ of G thus translates into a matching m' of T' with some extra elements, which, again, translate into extra variables in the parametrization of $S_{T'}$, namely the angles found in A'. This allows us to describe a point in S_G as a point in $S_{T'}$, as we will do in Proposition 5.21.

We are now ready to prove that the parametrization of positroid cells using bicolored tilings described in Definition 5.8 aligns with the one using plabic graphs described in Theorem 1.28, also found in [21, 2.17].

Proposition 5.21. *Let T be a tiling and $G = \Phi(T)$. Then $S_T = S_G$.*

Proof. Let m be a matching of T and $\mathfrak{m} = \{e_{\alpha_i} \,|\, i \in \mathcal{I}\} \cup \tilde{E}$ the corresponding almost perfect matching of G as described in Remark 5.4. We recall that a point $x \in S_G$ is given by a weight function $w : \mathcal{E} \longrightarrow \mathbb{R}_{>0}$, and each coordinate is given by

$$\Delta_I(x) = \sum_{\substack{\mathfrak{m} \in \mathcal{M}(G) \\ \partial \mathfrak{m} = I}} w(\mathfrak{m}), \quad \text{where} \quad w(\mathfrak{m}) = \prod_{e \in \mathfrak{m}} w(e)$$

Let $x \in S_T$, i.e. $x = P_T((a_i)_{i \in \mathcal{I}})$ for some values $a_i > 0$. We construct $y \in S_G$ by choosing the weight function w_y such that

$$w_y(e) = \begin{cases} a_i, & \text{if } e = e_{\alpha_i} \\ 1, & \text{if } e \in \tilde{E}. \end{cases}$$

Then for any matching m and $\mathfrak{m} = \Phi(m)$

$$w_y(m) = \prod_{e \in \mathfrak{m}} w_x(e) = \prod_{\substack{e_{\alpha_i} \in \mathfrak{m} \\ e = e_{\alpha_i}}} a_i = \prod_{\alpha_i \in m} a_i$$

which is just the matching m identified as the product of its members evaluated at $\alpha_i = a_i$, as explained in Definition 5.8. Hence, the $I - th$ coordinate Δ_I of y is given by

$$\Delta_I(y) = \sum_{\substack{m \in \mathcal{M}(T) \\ \partial m = I}} m((a_i)_{i \in \mathcal{I}}) = \Delta_I(x)$$

and thus $y = x$, and $x \in S_G$. Thus, $S_T \subset S_G$.

Let T' be the expansion of T as described in Definition 5.18. Let $x \in S_G$ given by some weight function $w_x : \mathcal{E} \longrightarrow \mathbb{R}_{>0}$. We construct the point $y = P_{T'}((b_i)_{i \in \mathcal{I}'}) \in S_{T'}$ given by

$$b_i = \begin{cases} w_x(e_{\beta_i}), & \text{if } i \in \mathcal{I} \\ 1, & \text{if } i \in \tilde{\mathcal{I}} = \mathcal{I}' \setminus \mathcal{I}. \end{cases}$$

Then for any matching m' of T' and corresponding matching $\mathfrak{m}$ of G, we have

$$\prod_{\alpha_i \in m'} b_i = \prod_{\substack{e_{\alpha_i} \in \mathfrak{m} \\ i \in \mathcal{I}}} b_i = \prod_{\substack{e_{\alpha_i} \in \mathfrak{m} \\ i \in \mathcal{I}}} w_x(e_{\beta_i}) = \prod_{e \in \mathfrak{m}} w_x(e) = w_x(\mathfrak{m})$$

Then $y = x$, and thus $x \in S_{T'}$. And since $S_T = S_{T'}$ by Proposition 5.17.(ii).b, $S_G \subset S_T$.

We conclude that $S_T = S_G$.

□

Now that we defined bicolored tilings, as well as described how they map onto positroid cells, we can state the main result of this paper.

Theorem 5.22. *Reduced (bicolored) tilings of type (k, n) up to tiling equivalence are in bijection with positroid cells of the totally non-negative Grassmannian $Gr_{k,n}^{\geq 0}$.*

Proof. This follows from the fact that positroid cells are in bijection with Postnikov diagrams [15, 14.2,14.7] up to geometric exchange, which are in bijection with reduced tilings up to tiling equivalence. More explicitly, any reduced tiling T is in bijection with the Postnikov diagram $\Gamma = S(T)$ as described in Definition 3.1, and with the positroid cell S_T as described in Definition 5.8. □

Proposition 5.23. *Let T be a tiling and S_T its corresponding positroid cell. Then* $\dim T = \dim S_T$.

Proof. If $\mathcal{F}$ is the set of faces of G, then $\dim S_T = |\mathcal{F}| - 1$ by [15, 12.7]. Since hyperedges of T map to faces of G, we have $\dim T = |E| - 1 = |\mathcal{F}| - 1 = \dim S_T$. □

5.2 Degenerations of tilings

We recall from Definition 5.8 that the closure of a positroid cell is given by

$$\overline{S_T} = \{(\Delta_I) \mid \alpha \geq 0 \ \ \forall \alpha \in A\}$$

We can describe this order in terms of tilings by defining the degeneration of tilings.

Definition 5.24. We define a partial order on **Til** by

$$T < T' \iff S_T \subset \overline{S_{T'}} \iff \overline{S_T} \subset \overline{S_{T'}}$$

Degenerations of a tiling happen with respect to angles of that tiling. In order to get consistent results, we distinguish between two types of angles as follows.

Definition 5.25. An angle α of a tiling T is said to be *essential* if for any matching $m \in \mathcal{M}(T)$, we have $\alpha \in m$. Similarly, α is said to be *non-essential* if there is a matching $m \in \mathcal{M}(T)$ such that $\alpha \notin m$.

Definition 5.26. Let T be a tiling, and $\alpha \in A$ a non-essential angle of T. Let $v = v(\alpha)$ be the vertex at α, and $f = f(\alpha)$ the face in which α lies. Let e_1 and e_2 be the two hyperedges adjacent to α, and let v_1 and v_2 be the second endpoints of e_1 and e_2, respectively. Let T' be the tiling obtained by constructing a black triangle with endpoints v,v_1, and v_2 inside f, such that the hyperedges e_1, e_2 of T merge with the black triangle.

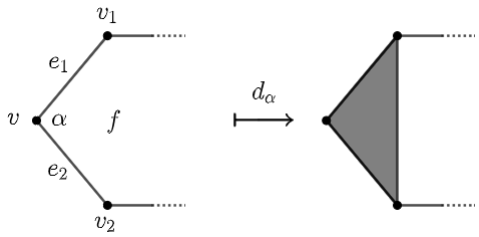

Figure 144

Then T' is called the *degeneration of T with respect to α*, and is denoted $d_\alpha T$.

Proposition 5.27. *The type of a tiling T is invariant under degeneration.*

Proof. Let T be a tiling of type (k, n) and α an angle of T. Let $T' = d_\alpha T$. Let m be a matching of T such that $\alpha \notin m$. Then m is a matching of T'. Thus T' has rank $\partial m = k$. Since the number of boundary vertices are not changed when degenerating, the type of T' is (k, n). □

If T is a tiling with diagram $S(T)$, then any intersection between two strands in $S(T)$ determines an angle. This follows from the definition of the Scott map (see Definition 3.1). If two strands γ_i and γ_j intersect and determine the angle α, we denote $\alpha = \gamma_i \wedge \gamma_j$. Since strands may intersect more than once, we choose α to be the last intersection between γ_i and γ_j when following the orientation of γ_i.

Proposition 5.28. *Let T be a tiling of permutation π, and γ_i, γ_j be two distinct, intersecting strands of $S(T)$. Let $\alpha = \gamma_i \wedge \gamma_j$ be a non-essential angle of T. Let π' be the permutation of $T' = d_\alpha T$. Then $\pi' = (\pi(i)\,\pi(j)) \circ \pi$.*

Proof. This result is immediate if we observe how degenerations affect the diagram locally from T to T'.

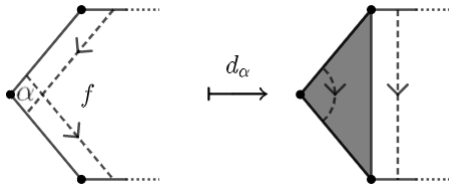

Figure 145

□

Proposition 5.29. *Let T be a tiling with angles $\alpha_1, \ldots, \alpha_r$. Let $P_T = P_T(\alpha_1, \ldots, \alpha_r)$. Let $T' = d_{\alpha_i} T$ for some non-essential angle $\alpha_i \in A$. Then the parametrization of $S_{T'}$ is*

$$P_{T'} = P_{T'}(\alpha_1, \ldots, \alpha_{i-1}, \alpha_{i+1}, \ldots, \alpha_r) = P_T|_{\alpha_i=0} = P_T(\alpha_1, \ldots, \alpha_{i-1}, 0, \alpha_{i+1}, \ldots, \alpha_r)$$

Proof. Let m be a matching of T with $\alpha_i \notin m$. Then m is also a matching of T'. Conversely, if m' is a matching of T', then m' is a matching of T as well, with $\alpha_i \notin m'$. In other words, the matchings of T' are exactly the matchings of T that do not contain α_i. Thus, if Δ_I and Δ'_I denote the I-th coordinate of T and T', respectively, we get

$$\Delta'_I = \sum_{\substack{m \in \mathcal{M}(T') \\ \partial m = I}} m = \sum_{\substack{m \in \mathcal{M}(T) \\ \partial m = I \\ \alpha_i \notin m}} m = \sum_{\substack{m \in \mathcal{M}(T) \\ \partial m = I}} m|_{\alpha_i=0} = \left(\sum_{\substack{m \in \mathcal{M}(T) \\ \partial m = I}} m \right) |_{\alpha_i=0} = \Delta_I|_{\alpha_i=0}$$

Hence

$$P_{T'} = (\Delta'_I) = (\Delta_I|_{\alpha_i=0}) = P_T|_{\alpha_i=0}$$

which concludes the proof. □

Corollary 5.30. If $T' = d_\alpha T$, then $T' < T$.

Proof. This follows directly from Proposition 5.29, as $\overline{S_{T'}} \subset \overline{S_T}$. □

The number of hyperedges is reduced by exactly 1 after degenerating a tiling, as two hyperedges are merged together into one by adding a black triangle. From Definition 2.12 the following immediately follows.

Corollary 5.31. Let $T' = d_\alpha(T)$ be the degeneration of a tiling T with respect to the angle α. Then $\dim S_{T'} \leq \dim S_T - 1$.

Remark 5.32. The reason why we do not have an equality $\dim S_{T'} = \dim S_T - 1$ is that the equality $\dim S_T = E - 1$, where E is the set of hyperedges of T, is only true if T is reduced. After degenerating, the resulting tiling is not necessarily reduced.

Example 5.33. The following reduced tiling T of type $(3, 6)$ and of dimension 7 can be degenerated at α. The resulting tiling T' is not reduced. After reducing T' to a tiling T'', we see that the dimension of the corresponding positroid cell is $\dim S_{T''} = 5$.

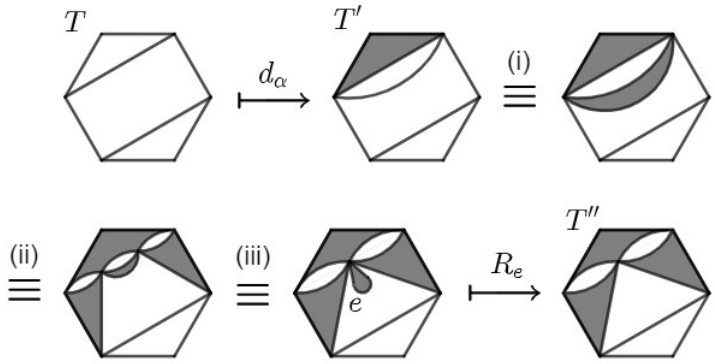

Figure 146

The steps applied to the degenerated tiling T' are as follows

(i) Any simple edge is also a black digon/2-hyperedge.

(ii) We decontract two white digons. It may be easier to see the transformation from right to left, by contracting the two digons that are adjacent to the boundary.

(iii) We contract the central digon. This transforms the black digon into a 1-gon that can be reduced to arrive at T''.

We summarize the main results of this section.

Theorem 5.34. *Let T be a tiling of type (k, n) with permutation π, and let $\alpha \in A$ such that $\exists$ distinct $i, j \in [n]$ with $\gamma_i \wedge \gamma_j = \alpha$. Let $T' := d_\alpha(T)$ be the degeneration of T at α, and let $P = P(\alpha)_{\alpha \in A}$ be the parametrization of T. Then*

- *T' is of type (k, n).*
- *T' has decorated permutation $\pi' = (\pi(i)\ \pi(j)) \circ \pi$.*
- *T' parametrizes the positroid cell $S_{\pi'}$ by $P|_{\alpha=0}$.*
- *$T < T'$ and $\dim S_T < \dim S_{T'}$.*

Example 5.35. Consider the Grassmannian of type $(1, 3)$, i.e. the set of lines through the origin in the 3-dimensional real space. We may represent this as a projective space in a half-sphere model, where each point of the half-sphere represents a line (more precisely the line going through that point and the origin), identifying antipodal points in the plane $0xy$, i.e. $[x : y : 0] = [-x : -y : 0]$.

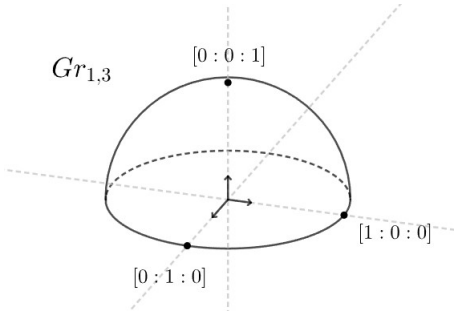

Figure 147

If we divide this dome into four quadrants, divided by the planes $0xz$ and $0yz$, the totally non-negative Grassmannian $Gr_{1,3}^{\geq 0}$ is then given by the points in the quadrant facing towards us in the figure above.

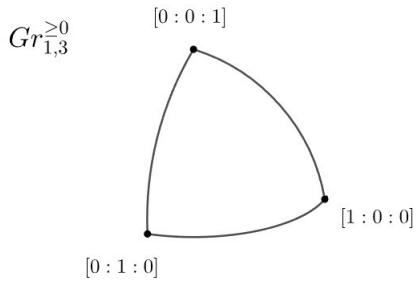

Figure 148

Let us now find the positroid cells of $Gr_{1,3}^{\geq 0}$. There are a total of 7 reduced tilings of type $(1, 3)$, namely

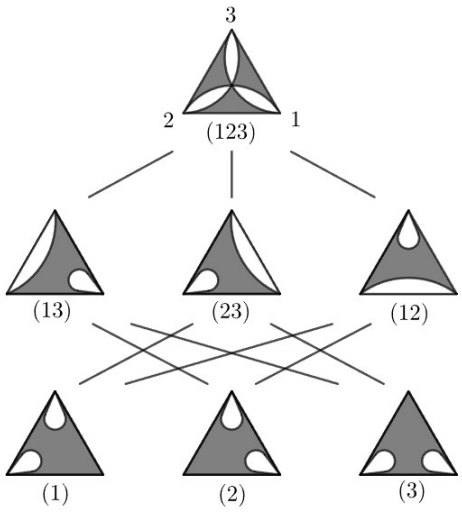

Figure 149

In this chart, if two tilings are connected by a line, the upper tiling degenerates into the lower tiling with respect to one of its non-essential angles. In other words, it is the Hasse diagram for the partial order on tilings of type $(1, 3)$ defined in Definition 5.24. The first tiling parametrizes the positroid cell of maximal dimension, $\dim = 2$, as follows

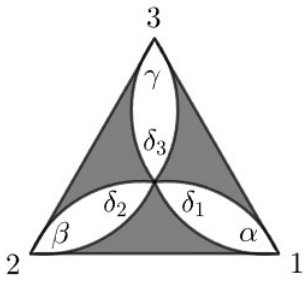

$$\Delta_1 = \beta\gamma\delta_1$$
$$\Delta_2 = \alpha\gamma\delta_2$$
$$\Delta_3 = \alpha\beta\gamma_3$$

Figure 150

Since the coordinates are projective, we may divide each parameter by $\alpha\beta\gamma > 0$ simultaenously, which gives us the parametrization

$$P_T = (\beta\gamma\delta_1, \alpha\gamma\delta_2, \alpha\beta\delta_3) = (\frac{\delta_1}{\alpha}, \frac{\delta_2}{\beta}, \frac{\delta_3}{\gamma}) = (a, b, c)$$

after a change of variables $a = \frac{\delta_1}{\alpha}$, $b = \frac{\delta_2}{\beta}$, $c = \frac{\delta_3}{\gamma}$. We see that the open cell it parametrizes is simply the quadrant without its boundary. Two of the other cells are parametrized as follows.

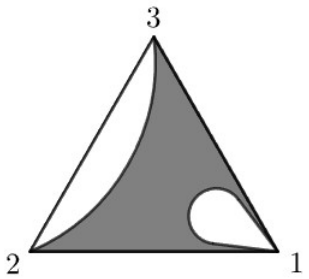

$$\Delta_1 = 0$$
$$\Delta_2 = \alpha\gamma$$
$$\Delta_3 = \alpha\beta$$

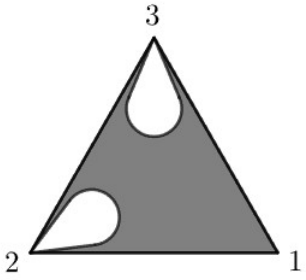

$$\Delta_1 = \beta\gamma$$
$$\Delta_2 = 0$$
$$\Delta_3 = 0$$

Figure 151

giving us parametrizations

$$P_{T_2} = (0, b, c), \quad P_{T_3} = (a, 0, 0)$$

with the other 4 cells parametrizing the same cells, up to rotation of the coordinates. We see that the three 1-dimensional tilings parametrize the three open segments that

are part of the boundary of the quadrant, while the three 0- dimensional tilings gives us the three points that are the boundaries of those segments.

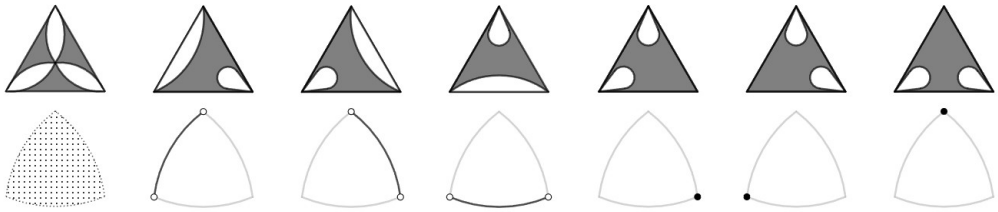

Figure 152

We further notice that the degenerations of the maximal tiling T are its three open boundary segments. While any boundary segment degenerates into both its boundary points. If we take the closure of each cell, we can see how each of the positroid cells is nested inside the other, as explained in Definition 5.8. This correlates with the partial order we defined in Definition 5.24.

In terms of the corresponding decorated permutations, this order is called the *circular Bruhat order* [15, 17.5], which is given by $\pi \leq \sigma \iff \overline{S_\pi} \leq \overline{S_\sigma}$. The top element of this ordering in any Grassmannian $Gr_{k,n}^{\geq 0}$ is the permutation $i \longmapsto i + k \mod n$, whose positroid cell is of dimension $k(n-k)$. The minimal elements are all the $\binom{n}{k}$ decorated identities $i \longmapsto i \mod n$, with each choice of k white-colored fixed points (p.13) corresponding to a different positroid cell of dimension 0 [15, 17.6].

6 Closing thoughts

We summarize what we achieved in this paper. We defined bicolored tilings as the collection of compatible hyperedges in a surface (in our case a disk) with a finite number of marked points, where hyperedges act as a generalization of edges between any positive number of vertices. We then extended the Scott map to map bicolored tilings to alternating curve diagrams, and discovered which bicolored tilings map to Postnikov diagrams in particular.

This gave us a reduction-flip-equivalence class of tilings that is in bijection with Postnikov diagrams up to geometric exchange. Consequently, bicolored tilings (up to equivalence) are in bijection with a variety of objects, such as plabic graphs, or positroid cells. We described the mapping to plabic graphs via the stellar-replacement map, and we parametrized positroid cells using bicolored tilings. Finally,

we introduced a partial ordering on bicolored tilings that aligns with the partial order of the corresponding positroid cells, and described how to obtain lower-dimensional tilings via degenerations.

One future point of interest would be to describe the connection between bicolored tilings and cluster algebras more explicitly and more comprehensively. As previously seen (p.48), tilings naturally map to quivers with frozen vertices, which means every tiling represents a cluster in a cluster algebra. This mapping aligns with the mapping of Postnikov diagrams to quivers seen in [3, 2.5] and the mapping to seeds found in [16, Thm.2 p.24].

It would be interesting to explore what information about the corresponding cluster algebra can be read off the tiling. When is the cluster algebra of finite or infinite type? Which cluster variables can be obtained within the flip-equivalence class of a tiling? One obstacle lies in generalising the mutation of hyperedges. In this paper we described how to mutate any simple edge, but non-boundary hyperedges map to mutable cluster variables in quivers as well. Bicolored tilings in their current form are not sufficient to describe this mutation in a "nice" geometrical way.

More beginner-friendly approaches could include the search for more easily identifiable classes of tilings and patterns that emerge from their mutations. Triangulations give us the maximum-dimensional tiling of type $(2, n)$ with their flip-equivalences class giving us all cluster variables of the corresponding cluster algebra. Rhombic tilings give us the maximum-dimensional tiling of type $(m + 1, 2m)$ in a format where certain sequences of mutations perform a Yang-Baxter move on the tiling. Quadrilateral tilings generalise this a little bit, giving us all (k, n)-tilings of maximal dimension, where certain sequences of mutations shift the tiling in the mesh we used to create it. Exploring more such patterns could serve as an introduction to bicolored tilings.

References

[1] Alexey Balitskiy and Julian Wellman. Flip cycles in plabic graphs. Selecta Mathematica, 26(1):15, Feb 2020.

[2] Karin Baur. Grassmannians and cluster structures. Bull. Iranian Math. Soc., 47(suppl. 1):S5–S33, 2021.

[3] Karin Baur, Alastair D. King, and Bethany R. Marsh. Dimer models and cluster categories of Grassmannians. Proceedings of the London Mathematical Society, 113(2):213–260, 07 2016.

[4] Karin Baur and Paul P. Martin. The fibres of the Scott map on polygon tilings are the flip equivalence classes. Monatsh. Math., 187(3):385–424, 2018.

[5] Arkady Berenstein, Sergey Fomin, and Andrei Zelevinsky. Cluster algebras iii: Upper bounds and double bruhat cells. Duke Mathematical Journal, 126:1–52, 2003.

[6] Joel Costa. Example of bicolored tilings. work in progress.

[7] Joel Costa. Bicolored tilings and the Scott map. arXiv:2112.08007, 2021.

[8] Joel Costa. Parametrizing positroid cells using bicolored tilings. arXiv:2304.02483, 2023.

[9] Sergey Fomin and Andrei Zelevinsky. Cluster algebras I: Foundations. Journal of the American Mathematical Society, 15, 05 2001.

[10] Sergey Fomin and Andrei Zelevinsky. Cluster algebras ii: Finite type classification. Inventiones mathematicae, 154(1):63–121, Oct 2003.

[11] Pavel Galashin and Thomas Lam. Positroid varieties and cluster algebras. Annales Scientifiques de l École Normale Supérieure, 2019.

[12] Bethany R. Marsh. Lecture notes on cluster algebras. Zurich Lectures in Advanced Mathematics. European Mathematical Society (EMS), Zürich, 2013.

[13] Fatemeh Mohammadi and Francesca Zaffalon. Computing positroid cells in the grassmannian of lines, their boundaries and their intersections. arXiv:2206.14001, 2022.

[14] Joseph Harris Phillip Griffiths. Complex Algebraic Varieties, chapter 1, pages 128–211. John Wiley I& Sons, Ltd, 1994.

[15] Alexander Postnikov. Total positivity, Grassmannians, and networks. arXiv:math/0609764, 2006.

[16] Jeanne Scott. Grassmannians and cluster algebras. Proceedings of the London Mathematical Society, 92(2):345–380, 2006.

[17] K. Serhiyenko, M. Sherman-Bennett, and L. Williams. Cluster structures in schubert varieties in the grassmannian. Proceedings of the London Mathematical Society, 119(6):1694–1744, jul 2019.

[18] K. Talaska. A formula for plucker coordinates associated with a planar network. International Mathematics Research Notices, jul 2010.

[19] Kelli Talaska and Lauren Williams. Network parametrizations for the Grassmannian. Algebra & Number Theory, 7(9):2275 – 2311, 2013.

[20] Dylan P. Thurston. From dominoes to hexagons. arXiv:math/0405482, 2016.

[21] Lauren K. Williams. The positive Grassmannian, the amplituhedron, and cluster algebras. arXiv:2110.10856, 2021. To appear in the Proceedings of the 2022 ICM.

School of Mathematics, University of Leeds, Leeds LS2 9JT, UK
E-mail address: mm17jcdr@leeds.ac.uk, joelcosta94i@gmail.com